

https://dspace.org/

Diabetic skeletopathy of the Sprague-Dawley rat mandible in a chronic alcohol intake and antiretroviral therapy: An immunohistochemical and microfocus X-ray computed tomography study

Eguavoen, Idemudia

2025

University of the Witwatersrand, Johannesburg

https://hdl.handle.net/10539/48440

Eguavoen, Idemudia . (2025). Diabetic skeletopathy of the Sprague-Dawley rat mandible in a chronic alcohol intake and antiretroviral therapy: An immunohistochemical and microfocus X-ray computed tomography study [PhD thesis, University of the Witwatersrand, Johannesburg]. https://hdl.handle.net/10539/48440

Downloaded from a DSpace repository. https://dspace.org/

DIABETIC SKELETOPATHY OF THE SPRAGUE-DAWLEY RAT MANDIBLE IN CHRONIC ALCOHOL INTAKE AND ANTIRETROVIRAL THERAPY: AN IMMUNOHISTOCHEMICAL AND MICRO-FOCUS X-RAY COMPUTED TOMOGRAPHY STUDY

Idemudia Eguavoen

Student number: 0616737M

A thesis submitted to the Faculty of Health Sciences, University of the Witwatersrand, Johannesburg, in fulfilment of the requirements for the degree of Doctor of Philosophy in Anatomy

Johannesburg, April 2025

DECLARATION

I, Idemudia Eguavoen declare that this dissertation entitled “Diabetic skeletopathy of the Sprague- Dawley rat mandible in chronic alcohol intake and antiretroviral therapy: An immunohistochemical and micro-focus X-ray computed tomography study” is my own work. It is being submitted for the Degree of Doctor of Philosophy at the University of the Witwatersrand, Johannesburg. It has not been submitted before for any degree or examination at any other University.



_____

Dr Idemudia Eguavoen

7 April 2025

Date

CONFERENCE PRESENTATION

I. Eguavoen, V. Perry, D Pillay, E.F. Mbajiorgu, R. Ndou. **Alcohol aggravates skeletopathy in the diabetic male Sprague Daley rat mandible.** XXVIII International Symposium on Morphological Sciences (ISMS) 5th to 8th August 2023

PUBLISHED ARTICLE

I Eguavoen, EF Mbajiorgu, V Perry, D Pillay and R Ndou. 2024.**Mandibular trabecular morphometry and tensile strength assessment in the diabetic Sprague Dawley rat consuming alcohol**, *International Journal of Morphology*. 42(6):1706-1712

DEDICATION

In memory of my uncle

Montacute Bamidele Davies

1954 – 2019

ACKNOWLEDGMENTS

- All thanks be to Almighty God for providing the resources for this research and making it a success.
- I sincerely thank my supervisors, Professor R Ndou and Professor E.F Mbajiorgu, for suggesting the research problems to me.
- I also express my gratitude to my co-worker, Mr. Vaughan Perry.
- I sincerely thank Dr. Diana Pillay of the Department of Anatomy and Histology, School of Medicine, Sefako Makgatho University of Health Sciences (SMU) for her immense contribution to this work. Thank you to Drs. Nkosi Xhakaza Khuthazelani and Isaac Ayoola Jegede for giving me valuable advice and assistance.I am grateful to Mrs. Hasena Alli of the School of Anatomy, University of the Witwatersrand, Faculty of Health Sciences, University of the Witwatersrand (Wits), and Mrs. Katlego Mphaga of the Department of Human Anatomy and Histology, School of Medicine, Sefako Makgatho University (SMU) for the technical and laboratory supports they provided during this research.
- I also appreciate the entire staff of the Anatomy Department of both Schools.
- My appreciation goes to Professors T. Augustine and E. Hutchinson for providing valuable advice on immunohistochemistry and MicroCT. Special appreciation to Drs. J. Davimes and B. Billings for assisting with the photographs of the hemimandibles, and to Dr. A. Ngwenya for providing valuable advice and assistance.
- I am also grateful to the staff of the Central Animal Services (CAS) of the University of the Witwatersrand for assisting with animal housing, welfare, and the procedures carried out at the CAS facility.

- A profound appreciation to Mr. Robert Nshimirimana, Mr. J. Hoffman, Dr. Lunga Bam, and other staff members at Microfocus X-ray Radiography and tomography (MIXRAD) facility of the South African Nuclear Energy Co-operation (Necsa) for helping with three-dimension computed tomography scanning and analysis.
- My profound appreciation to my family, loved ones, and students at both Wits and SMU universities, especially Mr. Ronald Ndabenzinle, Miss Tlou Mokonyama, Miss Naledi Thobane, and Mr. Gcinokuhle Mamba.
- Finally, my appreciation goes to the Faculty Research Committee (FRC) Individual Research Grant for providing a Grant to partially support this work (grant no 001.254.8421101 7th segment 5254).

ABSTRACT

The prevalence of non-communicable diseases such as diabetes mellitus is increasing worldwide with Type 2 diabetes mellitus accounting for 90 to 95 per cent of all diabetes cases. Type 2 diabetes mellitus, excessive alcohol consumption, and co-infection with the Human Immunodeficiency Virus (HIV) are some of the most common chronic health and socioeconomic problems in South Africa. Individuals infected with HIV are enrolled in combination antiretroviral therapy (cART), adding further difficulty to the country's health system.

As type 2 diabetes is characterized by hyperglycemia and insulin resistance, chronic alcohol abuse increases caloric intake and leads to obesity, and later, to type 2 diabetes. Alcohol abuse also affects the ability to make good behavioural choices, increasing the likelihood of HIV infection and subsequent enrolment in a cART programme. Although cART is effective, it is associated with metabolic dysregulation with insulin resistance. These metabolic disorders exacerbate type 2 diabetes mellitus and increase the risk of osteoporosis and bone fractures.

Type 2 diabetes mellitus is among the causes of osteoporosis and an increased risk of bone fractures. Research studies link type 2 diabetes, excessive alcohol consumption and the use of cART, independently, to osteoporosis and an increase in the risk of bone fracture. Transforming growth factors (TGF-β1) and bone morphogenetic proteins 3 (BMP-3) are notable cytokines that promote bone remodeling, proliferation, and differentiation of mesenchyme bone forming cells (osteogenesis). Alcohol, type 2 diabetes mellitus, and cART individually or together may have

detrimental effects on these cytokines. While the singular effects of alcohol, type 2 diabetes mellitus or cART have been reported, their combined effect is unknown. This is despite the high prevalence of coexistence of diabetes, alcohol abuse and cART among individuals.

The present study aimed to determine the impact of the interaction of alcohol and combination antiretroviral treatment (cART) on the diabetic Sprague Dawley male rat mandible. The rats were randomly distributed into 10 groups consisting of 3 control groups, 3 non-diabetic groups and 4 diabetic groups. The animals were placed in the following groups: (i) Untreated control group which received no treatment (n=8); (ii) Citrate buffer controls (CB), received a once of injection of citrate buffer (n=6); (iii) Gelatine group (GEL), received gelatine (n=8); (iv) Alcohol (ALC), consumed alcohol (n=8); (v) received combination antiretroviral treatment (cART) (n=8); (vi) ALC+cART, received alcohol and cART (n=7); (vii) DBT, diabetic group (n=7). The study included additional diabetic groups that received alcohol or cART or both as follows; (viii) diabetic animals that received alcohol (DBT+ALC) (n=6); (ix) diabetic animals received cART (DBT+cART) (n=7); and (x) diabetic animals that received both alcohol and cART (DBT+ALC+cART) (n=6). Gelatine was used as a mode of administration of the treatment cART treatment. Diabetes was induced by a diet enriched with 20% fructose a a once off sing STZ (40mg/kg.bw, ip) dose.

The study begins by inducing and confirming induction of type 2 diabetes mellitus in the appropriate rat groups (DBT, DBT+ALC, DBT+cART and DBT+ALC+cART). Confirmation of diabetes was achieved by monitoring the fasting blood glucose levels, oral glucose tolerance tests (OGTT)

and serum insulin levels. Serum levels of hormones that regulate bone health were then assessed. Afterwards, mandibular osteometry measurements were made. The trabecular microstructure parameters were assessed from microfocus X-ray computed tomography (Micro CT) to measure thickness (TbTh), spacing (TbSp), and number (TbN). The bones were tested for strength with a universal tensile tester and histologically evaluated for normal morphology. The expression of osteocytes, transforming growth factor beta-1 (TGF-1), and bone morphogenic protein-3 (BMP-3) was evaluated by immunohistochemistry.

Diabetes was successfully induced as confirmed by, hyperglycemia, poor oral glucose tolerance and hypoinsulinemia in the groups that had diabetes (DBT, DBT+cART and DBT+ALC+cART). Serum parathyroid hormone and calcitonin concentrations were low in rats that were diabetic and taking and cART (DBT+cART) or diabetic rats taking both alcohol and cART (DBT+ALC+cART). Significantly higher levels of serum sclerostin were detected in rats subjected to various combinations of alcohol, CART or diabetes (ALC+cART, DBT+cART and DBT+ALC). However, the diabetic rats that received both alcohol and cART (DBT+ALC+cART) had normal sclerostin levels. Serum osteocalcin and catenin levels were also unaffected in this group. Diabetic rats on cART, with or without alcohol, showed decreased parathyroid hormone and calcitonin, but normal sclerostin, osteocalcin, and catenin. This suggests a specific disruption of parathyroid hormone and calcitonin regulation, while other compensatory mechanisms might maintain the levels of the other hormones.

Diabetes adversely affected mandibular dimensions and was worsened by concurrent alcohol and cART. While the DBT+cART+ALC group had the highest stiffness, it was characterised by lower values for maximum force and break force, less displacement, and time to fracture, indicating stiff and brittle bones. This finding supports the hypothesis that concomitant cART and alcohol use in diabetes may result in weaker bones. The high BV/TV and TbN in the DBT, DBT+cART and DBT+cART+ALC did not translate to stronger bones, therefore, the bone was of lower quality.

Diabetes (DBT), alcohol (ALC), diabetes with alcohol (DBT+ALC) or diabetics consuming alcohol and antiretroviral treatment (DBT+ALC+cART) exhibited significantly impaired osteocyte quantities. The high intensity of BMP3 immunostaining observed in the present study among the groups with diabetes, (DBT, DBT+ALC, DBT+ALC and DBT+cART+ALC) corroborates the diminished TRAP immunopositivity as BMP3 is antagonistic to osteoblasts. In the present study, both alcohol (ALC) and diabetes (DBT) or a combination of alcohol and diabetes (DBT+ALC) did not change the expression of TGFB1. Evaluating the intracellular expression of TGFB1 in a future study is recommended.

Viewed altogether, these results show that when diabetes was confounded by combination antiretroviral treatment and alcohol consumption (DBT+ALC+cART), osteogenic cells were negatively impacted together with derangement of the hormone profile parathyroid hormone and calcitonin. This is coupled with osteometric changes and bone weakness. Therefore, diabetic patients should be advised to reduce alcohol intake and bone health should be monitored when combination antiretroviral therapy is employed.

TABLE OF CONTENTS

DECLARATION		i
PRESENTATIONS		ii
PUBLICATIONS		ii
DEDICATION		iii
ACKNOWLEDGEMENTS		iv
ABSTRACT		vi
LIST OF FIGURES		xi
LIST OF TABLES		xii
LIST OF ABBREVIATIONS		xiii
CHAPTER 1	Introduction and thesis layout	1
CHAPTER 2	Literature review	10
CHAPTER 3	Diabetic rat model and study design	39
CHAPTER 4	Influence of alcohol and combination antiretroviral treatment on bone regulating hormones in diabetic Sprague Dawley rats	58
CHAPTER 5	Mandibular microstructural alterations from combination antiretroviral therapy and concurrent alcohol intake in the diabetic Sprague Dawley rat	78
CHAPTER 6	Osteometry of the diabetic rat mandible treated with alcohol and combination antiretroviral therapy	100
CHAPTER 7	Influence of alcohol intake and combination antiretroviral treatment on osteocytes and the expression of TGFβ1 and BMP3 in the mandible of diabetic rats	123
CHAPTER 8	General discussion and conclusions	144
REFERENCES		152
APPENDICES		163

LIST OF FIGURES

Figure 2.1: Rat hemimandible landmarks 25
Figure 2.2: Illustration of trabecular and cortical bone. 27
Figure 2.3: Bone remodelling. 29
Figure 2.5: Force-displacement curve. 38
Figure 3.1: Study design. 50
Figure 3.2: Changes in the body mass from weeks 1-12. 51
Figure 3.3: Fasting blood glucose level from 1 to 12 weeks. 52
Figure 3.5: Oral glucose tolerance test 54
Fig. 3.6 Serum insulin concentration at 12 weeks. 55
Figure 4.1: Calcitonin concentration. 64
Figure 4.2: Parathyroid hormone concentration 66
Figure 4.3: Sclerostin concentration 68
Figure 4.4: Osteocalcin concentration.. 70
Figure 4.5:.β-catenin concentration 72
Fig. 5.1: Region of interest. 83
Fig. 5.2 Group membership discrimination 94
Figure 6.1: Morphometric reference points for the linear measurements for mandibular length. 106
Figure 6.2: Morphometric reference points for the linear measurements of rat mandibular height. 107
Figure 7.1 Region of interest. Photomicrographs were taken from the encircled region. 130
Figure 7.3: General histology and relative adipocyte infiltration in the mandible. 133
Figure 7.4: TRAP immunopositive cells quantity in the mandible.. 135
Figure 7.5: TRAP Immunopositive osteocytes in the mandible. 136
Figure 7.6: Mandibular TGFβ1 Immunopositivity graded. 139
Figure 7.7: Mandibular BMP3 Immunopositivity graded. 139

LIST OF TABLES

Table 5.1: Trabecular morphometric parameters 87

Table 5.2. Tensile strength parameters from 3-point bending tests. 92

Table 5.3: Discriminant function analysis of the mandible. 93

Table 5.4: Group membership classification 95

Table 6.1: Measurements for the assessment of the linear mandibular length (mm) 105

Table 6.2: Measurements for the assessment of the linear mandibular height (mm) 106

Table 6.3: Linear mandibular length (mm) 113

Table 6.4: Linear mandibular height 119

Table 7.1: TGFβ1 Immunopositivity 138

Table 7.2: BMP3 Immunopositivity 139

LIST OF ABBREVIATIONS

%:	Percent
°C:	Degree Celsius
β:	Beta
µm:	Micrometer
kg:	Kilogram
mg:	Milligram
AESC:	Animal ethics screening committee
AIDS:	Acquired immunodeficiency disease syndrome
ALC:	Alcohol
BMP-3:	Bone morphogenetic protein (BMP-3)
BV:	Bone volume
BV/TV:	Bone volume to tissue volume ratio
B.W:	Body weight
cART:	Combination antiretroviral therapy
EDTA:	Ethylenedeaminetetraacetic acid
ELISA:	Enzyme–linked immune assay
FBG:	Fasting blood glucose
H & E:	Haemoxylin and eosin
HIV:	Human immunodeficiency virus
IHC:	Immunohistochemistry
Micro-CT	Micro-computed tomography
Necsa:	South African Nuclear Energy Co-operation
NNRTI:	Non-nucleoside reverse transcriptase inhibitor
NRTI:	Nucleoside reverse transcriptase inhibitors
OGTT:	Oral glucose tolerance test
PLWHA:	People living with HIV/AIDS
PI:	Protease inhibitors
PTH:	Parathyroid hormone
ROI:	Region of interest
RANK:	Receptor activator of nuclear factor–Kb
RANKL:	Receptor activator of nuclear factor–Kb ligand
RUNX2:	Runt-related transcription factors
SD:	Sprague Dawley rats
STZ:	Streptozotocin
TbTh:	Trabecular thickness
TbSp:	Trabecular spacing
TbN:	Trabecular number
TGFβ1:	Transforming growth factor beta 1
TGFβRI:	TGF-β type I receptor
TGFβRII:	TGF-β type II receptor

TNF-α:	Tissue necrotic factor- alpha
TRAP:	Tartrate-resistance acid phosphatase
ZDF:	Zucker diabetic fatty rat
ZDSD:	Zucker Diabetic Sprague-Dawley

Chapter 1:

Introduction and thesis layout

1.0 INTRODUCTION

1.1 Background to the study

The prevalence of non-communicable lifestyle and dietary habit diseases such as diabetes mellitus is increasing worldwide (Sun et al., 2022). This adds to socioeconomic hardships associated with the burden of the disease (Guariguata et al., 2014; King and Bowe, 2016). Diabetes mellitus is a chronic condition that depicts a group of metabolic disorders characterised by sustained hyperglycemia (Chao et al., 2018). Diabetes mellitus exists in four main types that can be classified as (i) Type 1 diabetes mellitus, (ii) Type 2 diabetes mellitus, (iii) Gestational diabetes (Zaccardi et al., 2016; Saeedi et al., 2019) (iv) Maturity Onset Diabetes in the Young (MODY), (Nkonge et al., 2020) which describes single-gene disorder causing conditions in younger age groups. Type 2 diabetes mellitus comprises approximately 90- 95% of all cases of diabetes (Wu and Huan, 2007; Fang et al., 2019).

Type 2 diabetes mellitus, excessive alcohol consumption, and infection with the Human Immunodeficiency Virus (HIV) are some of the most common chronic health and socioeconomic problems in South Africa. Individuals infected with HIV are enrolled in combination antiretroviral therapy (cART), adding further difficulty to the country's health system.

Chronic excessive alcohol consumption exacerbates type 2 diabetes mellitus, and it is considered as an independent risk factor for type 2 diabetes mellitus (Kim and Kim, 2012). Since this condition is characterised by hyperglycemia and insulin resistance, chronic alcohol consumption provides excess calories to the body, leading to obesity (Kao et al., 2001). Lack of physical exercise

and excess calories intake leads to obesity and disturbances of carbohydrate and glucose metabolism (Kao et al., 2001; Kim and Kim, 2012). Over a prolonged period, a combination of impaired insulin secretion and reduced insulin sensitivity occurs. This leads to hyperglycemia and subsequently, to type 2 diabetes mellitus (Kao et al., 2001; Kim and Kim, 2012).

Alcohol abuse also impairs the ability to make good behavioural choices, for example, alcohol consumers are more likely to have concurrent multiple sexual partners and have greater chances of engaging in unprotected sex (Carels et al., 2023). This increases the likelihood of HIV infection and subsequent enrolment into a cART regimen.

Combination antiretroviral therapy (cART), particularly Atripla® is a first line treatment drug in HIV patients. The pill consists of two nucleoside reverse transcriptase inhibitors (NRTI) and one non-nucleoside reverse transcriptase inhibitor (NNRTI). Emtricitabine (200mg) and tenofovir disoproxil fumarate (300mg) are the NRTIs, while efavirenz (600mg) forms the NNRTI (Julg and Bogner, 2008). It is cost-effective and readily available (Harris et al., 2012) and early treatment removes both the virus and the infected HIV reservoir cells, thus reducing the high risk of transmitting the infection (Li et al., 2022).

Though, cART is effective in reversing the outcomes of HIV, it is associated with metabolic dysregulation characterised by dyslipidaemia and insulin resistance. These metabolic dysregulations exacerbate type 2 diabetes mellitus, as well as the risk of osteoporosis and increased risk of bone fracture (Molina et al., 2014). The associated high risk of developing

diabetes particularly stems from the NNRTI drug, efavirenz (Rebeiro et al., 2021), also found in cART.

The multimorbidity of type 2 diabetes mellitus, HIV, and chronic excessive alcohol consumption has adverse dental implications that can negatively affect the outcomes of advanced dental procedures such the placement of dental implants (Porter and von Fraunhofer, 2005b). Considering this, type 2 diabetes mellitus patients and excessive alcohol consumers as well as those on cART therapy are treated with special precautions which often include modification of the treatment plans. For example, a diabetic patient should be put on medications to control the blood glucose level prior to the placement of dental implants. Furthermore, type 2 diabetes mellitus among other factors such as poor oral hygiene and patient's age are some of the primary indicators of implant success because they affect dental implants osseointegration and implant stability (Porter and von Fraunhofer, 2005b).

Uncontrolled type 2 diabetes mellitus can lead to the loss of osseointegration between the bone and the surface of the dental implant (Sakka and Coulthard, 2009). The osseointegration and stability depend on the good volume (quantity) of trabecular bone and the strength of the cortical bone (Porter and von Fraunhofer, 2005b). Type 2 diabetes mellitus it is among the causes of osteoporosis (Chiodini et al., 2020) and osteoporosis is considered as the most important metabolic bone disorder seen in patients with type 2 diabetes mellitus (de Araújo et al., 2022).

Studies have linked type 2 diabetes mellitus (Hamann et al., 2011; Sun et al., 2015), excessive alcohol consumption and the use of cART, independently to osteoporosis and increased risk of bone fracture (Maurel et al., 2012; Molina et al., 2014; Castronuovo et al., 2015). These three conditions. each have been shown to reduce bone strength and increase fracture risk by causing a reduction in the number of osteoblasts, osteoclasts and bone matrix synthesis, ultimately leading to poor bone strength and decreased bone mineral density (BMD) (Grigsby et al., 2010; Dave et al., 2015; Sun et al., 2015).

Transforming growth factors (TGF-β1) and bone morphogenetic proteins 3 (BMP-3) are notable cytokines that promote bone remodeling, proliferation, and differentiation of mesenchyme bone forming cells (osteogenesis) (Bismar et al., 1999; Janssens et al., 2005; Tang et al., 2009). Alcohol, type 2 diabetes mellitus, and cART individually or together may have detrimental effects on these cytokines. While the singular effects of alcohol, type 2 diabetes mellitus or cART have been reported, their combined effect is unknown. This is despite the high prevalence of coexistence of diabetes, alcohol abuse and cART among individuals.

This study investigates the combined effect of type 2 diabetes mellitus, excessive alcohol intake, and cART on mandibular bone structure using Sprague-Dawley (SD) rats. The investigation starts by inducing and confirming the induction of type 2 diabetes mellitus in the appropriate rat groups. This was achieved by monitoring fasting blood glucose (FBG) levels, bone mass measurements, evaluation of glucose handling characteristics via oral glucose tolerance tests (OGTT), and serum insulin levels. The study then queries serum levels of hormones that regulate

bone health are shown for all rat groups in the study. Mandibular osteometric measurements were then taken and evaluated. This was followed by an evaluation of cortical bone thickness (CtTh) and trabecular microarchitecture and organisation with respect to their thickness (TbTh), spacing (TbSp) and number (TbN) from three dimensional microfocus X-ray computed tomography (Micro CT). The bones were tested for strength using a computer-controlled universal tensile testing machine. The bones were histologically evaluated for normal morphology and quantification of bone marrow adipocytes. The expression of osteocytes was assessed by immunohistological means. The expression of a cytokine that promote osteogenesis transforming growth factor beta-1 (TGF-β1) and its antagonist, bone morphogenic protein-3 (BMP-3) was assessed from immunolabeled slides.

Rationale for the study

Despite type 2 diabetes mellitus, excessive alcohol consumption, and cART being a common burden in the South African health system, not enough attention is paid to the skeletal health of these comorbidity. Independent studies have shown the detrimental effects of (i) type 2 diabetes mellitus (ii) excessive alcohol use and (iii) cART on mandibular bone health, but the effects of their co-existence on the mandible in a single study is lacking in the literature. This study may provide clinicians with valuable information on the bone structure of patients with this comorbidity when considering implant therapy, internal rigid fixation, or orthopaedic surgery.

1.2 Aim:

To determine the effect of the interaction of alcohol and combination antiretroviral treatment (cART) on the diabetic Sprague Dawley rat mandible.

1.3 Objectives:

1. To induce diabetes mellitus by 20% fructose diet and a single intraperitoneal injection of Streptozotocin 40mg/kg and to confirm the development of diabetes in an experimental animals by measuring the following parameters:
   - i) Weekly body mass using a calibrated scale.
   - ii) Weekly fasting blood glucose levels using a glucometer.
   - iii) Oral glucose tolerance tests (OGTT) using a glucometer.
   - iv) Terminal insulin levels using ELISA

2 To use ELISA to measure the serum levels of insulin, parathyroid hormones, osteocalcin, calcitonin, sclerostin, and catenin. Additionally, to evaluate the effects of alcohol and antiretroviral therapy on these hormones that are involved in bone homeostasis in diabetic rats.

3. To investigate the combined effect of diabetes, chronic alcohol, and combination antiretroviral therapy on mandibular size and shape by taking osteometric measurements using a sliding calliper as follows:
   - i) Mandibular heigh
   - ~~ii)~~ Mandibular length

4. To characterise mandibular bone strength and trabecular morphometric parameters in diabetic rats that consumed alcohol and were treated with combination antiretroviral therapy by analysing the following parameters:
    i) The mandibular tensile strength was analysed using 3-point bending tests using a universal tensile tester.
    ii) The thickness of the trabeculae, spacing, and trabeculae numbers were analysed using Micro-focus X-ray Computed Tomography (MicroCT).

5. Characterisation of bone by histological and immunohistochemical analysis in diabetic rats that consumed alcohol and were treated with combination antiretroviral therapy.
    a) Histological analysis of bone trabecular morphology and adiposity was performed using hematoxylin and eosin (H&E) stain.
    b) Immunohistochemical analysis:
        i) The expression of the osteogenic growth factor (TGF-β1) and the antagonistic growth factor (BMP-3) was evaluated by immunohistochemistry.
        ii) To assess osteolysis, osteocytes were immunolabelled using the anti-TRAP antibody.

1.4 Hypothesis

Null hypothesis: Diabetes negatively affects skeletogenic cytokines, increases bone marrow adiposity, and increases bone fragility in rats that consumed alcohol and received combination antiretroviral therapy.

Alternative hypothesis: Diabetes has no effect on skeletogenic cytokines, increases bone marrow adiposity, and increases bone fragility in rats that consumed alcohol and received combination antiretroviral therapy.

1.5 Layout of the thesis

The thesis consists of eight chapters follows:

Chapter 1

Describes the general introduction, aims, objectives, and rationale for the study.

Chapter 2

This chapter presents a concise literature review that discusses diabetes mellitus, its history, pathophysiology and prevalence, and its associated health burden.

It also discusses the comorbidity of chronic alcohol consumption together with type 2 diabetes mellitus, comorbidity of chronic alcohol consumption and cART. The functional anatomy of rat mandible, bone remodeling, the effect of alcohol and cART on bone remodeling, and its biomechanical properties described. Lastly, it describes three-point biomechanical bending tests.

Chapter 3

This chapter lays out the experimental design. It describes in detail the methodology used to induce diabetes, administration of alcohol and cART.

Chapter 4

This chapter describes the influence of alcohol and combination antiretroviral treatment on bone regulating hormones in diabetic Sprague Dawley rats.

Chapter 5

This chapter describes osteometric measurements in estimation of general mandibular size through use of linear mandibular height, and the linear mandibular length measurement.

Chapter 6

This chapter describes the use of Micro-CT to analyse the 3D trabecular parameters such BV/TV, TbTh, TbSp and TbN. The effects of type 2 diabetes mellitus, alcohol consumption and the cART on the structural and material properties of the Sprague- Dawley rat mandible using three-point bending tests is included in this chapter.

Chapter 7

This chapter describes the regulation of osteoblasts, and osteocytes number by the TGF-β1, BPM-3 and TRAP using immunohistochemistry.

Chapter 8

This chapter gives a summary of the results, the overall discussion and conclusion. It contains limitations and recommendations.

Chapter 2

Literature review

2.0 LITERATURE REVIEW

2.1 The burden of non-communicable lifestyle diseases

The prevalence of non-communicable lifestyle diseases is increasing worldwide, and this adds to socio-economic hardships associated with the burden of the disease. Type 2 diabetes, excessive alcohol consumption and infection with the Human Immunodeficiency Virus (HIV) are some of the most common socio-economic problems in South Africa. Individuals infected with HIV are enrolled on antiretroviral therapy, adding further pressure to the country's health system. Studies link diabetes (Hamman et al., 2011; Sun et al., 2015), excessive alcohol use (Dyer et al., 1998; Maurel et al., 2012; Kusy et al., 1989; Molina et al., 2008) and antiretroviral therapy (ART) (Castronuovo et al., 2015; Bristol-Meyer Squibb and Gilead Sciences, LLC, 2016) to osteoporosis and increased bone fracture risk. Clinically, periodontal disease may occur, adversely affecting implant stability which rely on good bone quality. Though diabetes-HIV co-infection with heavy alcohol drinking abounds in our society, we have not found literature reporting on the multi-morbidity of these three aspects regarding mandibular bone health.

2.2 Pathophysiology of type 2 diabetes mellitus

The pathogenesis of type 2 diabetes mellitus involves insulin resistance and hyperglycemia with some degree of genetic predisposition (Ramlo-Halsted and Edelman, 1999; Polonsky, 2012). Type 2 diabetes mellitus (DM) is a heterogeneous disorder that results from an interaction between genetic predisposition and environmental risk factors such as ageing, obesity, alcohol consumption, lack of physical activity, and excessive refined sugar consumption (Holt, 2004).

Under normal physiological conditions, there is a feedback loop between insulin actions that promote insulin sensitivity in tissues such as liver, muscle, and fatty tissues (Holt, 2004). The secretion of insulin is through tightly controlled and effective regulation of insulin sensitive tissues and insulin secretion (Galicia-Garcia et al., 2020). These interaction mechanisms maintain normal plasma glucose concentration within the normal range despite the wide changes in demand and supply of glucose (Holt, 2004).

In type 2 diabetes mellitus, there is a dysregulation of these mechanisms resulting in insulin resistance (primary defect) and impaired insulin secretion through the failure of dysfunctional pancreatic β-cells to secrete insulin (secondary defect) (Ramlo-Halsted and Edelman, 1999; Holt, 2004; Zheng et al., 2018). Initially, the pancreatic β-cells can compensate by increasing insulin levels leading to hyperinsulinemia; this compensatory hyperinsulinemia can keep plasma glucose concentration normalised for a period (up to several years). However, impaired glucose tolerance in the prediabetic state develops with hyperglycaemia and metabolic syndrome (Ramlo-Halsted and Edelman, 1999). Metabolic syndrome describes a cluster of risk factors that include insulin resistance, hypertension, and dyslipidaemia and increases cardiovascular risks (Polonsky, 2012; Blaslov et al., 2018). This group of risks is identified with glucose intolerance, eventually leading to type 2 diabetes mellitus (Polonsky, 2012).

2.3 A brief history of diabetes

Numerous researchers have reported on how diabetes has evolved in the past 400 years (Polonsky, 2012; Lakhtakia, 2013; Blaslov et al., 2018; Zheng et al., 2018). Scientific literature

reports that diabetes was first recognised by the ancient Egyptians around 1500-1552 B.C. (Polonsky, 2012; Blaslov et al., 2018). The ancient Egyptians considered it a rare condition characterised by excessive urination, weight loss, and death (Polonsky, 2012; Blaslov et al., 2018). Apollonius was the first to use the term 'diabetes' around 230 BC (Zajac et al., 2010; Zaccardi et al., 2016). This term 'diabetes' was derived from the ancient Greek word 'diabainen', which means 'to go through' (dia through, bêtes-to go) to indicate excessive passage of urine through the kidney (Zajac et al., 2010; Zaccardi et al., 2016).

The famous ancient Indian physician Sushruta and the surgeon Charaka in the fifth century (400-500 AD) were able to identify the two types of diabetes, later named Type 1 and Type 2 (Zajac et al., 2010; Lakhtakia, 2013). At this time, they observed that in type 1 diabetes individuals developed the disease at a younger age but did not survive long after diagnosis. On the contrary, type 2 diabetes had a late onset and was observed in older and obese individuals who also lived longer after diagnosis (MacFarlane, 1990; Zajac et al., 2010).

The sweet taste of diabetic urine was recognised at the beginning of the first millennium (Tattersall and Matthews, 2024). The term '*diabetes mellitus'* meaning 'honey' and 'syphon' was first used by the Greek physician Aretaeus of Cappadocia, who practised in Rome and Alexandria in the second century AD, after the detection of a sweet taste among diabetic patients (Polonsky, 2012; Blaslov et al., 2018). In the 17th century (1600s), Thomas Willis of England, an anatomist and physician, coined the term 'mellitus' (sweet) to differentiate this condition from excessive urination of non-sweet urine (diabetes 'insipidus') (Zaccardi et al., 2016). In 1776, the British

physiologist Mathew Dobson of Liverpool measured the concentration of glucose in the urine of people living with diabetes and found that the 'sweet taste' was due to an excess concentration of glucose in the urine and blood (Zajac et al., 2010; Polonsky, 2012; Lakhtakia, 2013; Zaccardi et al., 2016).

Discovery of Insulin

In the 19th century, the French physiologist Claude Bernard discovered the glycogenic action of the liver, which made it easier to study the progression of the disease (Karamanou et al., 2016). In 1889, Joseph von Mering and Oskar Minkowski, for the first time, linked diabetes to a specific organ (pancreas) after discovering that pancreatomised dogs developed symptoms of diabetes (Zaccardi et al., 2016; Tattersall and Matthews, 2024). This became the first evidence that insulin plays a vital role in the regulation of glucose concentration (Polonsky, 2012).

In 1893, Laguesse suggested that the pancreatic 'islets' previously described by Langerhans in 1869 produced an internal chemical secretion that controls glucose metabolism (Tattersall and Matthews, 2024). In 1910, Edward Alber Sharpey-Schaffer indicated that people living with diabetes lacked a single chemical substance produced by pancreatic islets and named it 'insulin' (Zaccardi et al., 2016). Frederick Banting, Charles Best, John Macleod and Bertram Collip; made acid-ethanol extracts from the pancreas to isolate insulin in1921, and it was first used for treatment in 1922 (Karamanou et al., 2016; Tattersall and Matthews, 2024).

2.4 Prevalence of type 2 diabetes mellitus

In 2021, it was estimated that the global prevalence of diabetes in the age 20-79 years was 10.5% (536.6 million people), and it is expected to rise to 12.2% (783.2 million) in 2045, with the prevalence similar in both men and women (Sun et al., 2022). The largest significant increase in the prevalence of DM between the years 2021 and 2045 is expected to occur in the middle-income countries like South Africa (21.1%), compared to high (12.2%) and low-(11.9%) income countries (Sun et al., 2022). The possible explanation for this increase in the prevalence of diabetes in middle-income countries lies in the high urbanization rate. As urbanization increases, lifestyle changes such as sedentary lifestyles and processed foods, consequently, follow (Guariguata et al., 2014; Saeedi et al., 2019). Therefore, the prevalence of diabetes is estimated to be higher in urban areas (12.1%) than in rural areas (8.3%) (Sun et al., 2022).

Type 2 diabetes mellitus is the most common type of diabetes and accounts for approximately 90% of diabetic conditions in Africa, as in other parts of the world (Manyema et al., 2015; Pheiffer et al., 2018; Saeedi et al., 2019). It constitutes an ever-increasing public health and economic burden in South Africa, and its high prevalence is mainly due to the immense increase in the consumption of refined carbohydrate-based diets coupled with sedentary life leading to obesity (Zheng et al., 2018).

2.5 Financial implications associated with type 2 diabetes mellitus.

In 2015 the Global Burden of Disease Study ranked high body mass index (BMI) and hyperglycemia as the second and third contributors to mortality and disability in South Africa,

respectively (Pheiffer et al., 2018). In South Africa, 76% of deaths of individuals under the age of 60 years are due to type 2 diabetes mellitus (Pheiffer et al., 2018). This presents an economic challenge for the country because type 2 diabetes mellitus appears to affect the most economically active sectors of the population.

In addition to diabetes itself, multiple diabetic complications such as macro/microvascular disease, neuropathy, retinopathy, kidney disease, hypertension, and low extremity amputations (LEA) exacerbate the economic burden on the health system, leading to increased morbidity and mortality (Bertram et al., 2013; Mtshali and Mahomed, 2020).

Data obtained from the provincial health information system from 2013-2017, suggested that there was an increase in the rate of LEA due to type 2 diabetes mellitus (Mtshali and Mahomed, 2020). In addition, LEA has a major psychological and economic cost to patients and directly affects the South African health system (Mtshali and Mahomed, 2020). The economic burden is linked to the costs of hospitalization and chronic drugs, disability allowances and absentness from work of diabetic patients and caregivers (Manyema et al., 2015; Pheiffer et al., 2018). Health expenditure on diabetes is projected to increase by 50 per cent between 2010 and 2030, with a capital expenditure of between $1.1 billion and $2.2 billion by 2030 (Manyema et al., 2015).

2.6 Chronic alcohol consumption and type 2 diabetes mellitus

Excessive chronic alcohol consumption exacerbates type 2 diabetes mellitus (Kao et al., 2001). Since this condition is characterised by hyperglycemia and insulin resistance, alcohol abuse

provides excess calories. This leads to obesity and the disturbances in carbohydrate and glucose metabolism. Over a prolonged period, a combination of impaired insulin secretion and a reduction in insulin sensitivity occurs (Kim and Kim, 2012).

Chronic alcohol consumers sometimes forget to take their antidiabetic medications, which fails to adequately monitor their blood glucose level, which worsens their diabetic condition (Hu et al., 2001; Engler et al., 2013). Additionally, poor adherence to diabetic treatment protocols and counselling due to impairments of judgments induced by alcohol intoxications, lack of physical exercises, and poor dietary intake also contribute to the negative effects that alcohol consumption has on diabetic individuals (Hu et al., 2001; Engler et al., 2013).

2.7 Diabetes and combination antiretroviral treatment (cART)

Excess alcohol use also impairs the ability to make good behavioural choices. For example, alcohol abusers are more likely to have multiple concurrent sexual partners and have greater chances of engaging in unprotected sex. This increases the likelihood of HIV infection (Carels et al., 2023) and subsequent enrolment into an antiretroviral therapy programme. Although HIV infection itself has not been associated with an increased risk of type 2 diabetes mellitus, long-term use of cART has been found to increase the risk of diabetes mellitus in HIV-infected individuals (Rebeiro et al., 2021).

With the advent of cART, HIV/AIDS has become a chronic but manageable condition. However, there are metabolic complications such as type 2 diabetes mellitus and dyslipidaemia associated

with cART (Salam et al., 2019). Antiretroviral therapy is associated with metabolic dysregulation characterized by dyslipidaemia and insulin resistance (Molina et al., 2014).

The prevalence of diabetes mellitus among HIV-infected patients is reported to be 2-19%; therefore, diabetes mellitus screening among the HIV-infected patient has become inevitable (Shankalala et al., 2017; Noubissi et al., 2018; Kousignian et al., 2021). Atripla® is an combination antiretroviral drug used as a first line of treatment in HIV patients. The pill consists of two nucleoside reverse transcriptase inhibitors (NRTI) and one non-nucleoside reverse transcriptase inhibitor (NNRTI). Emtricitabine (200mg) and tenofovir disoproxil fumarate (300mg) are NRTI, while efavirenz (600mg) forms the NNRTI component (Julg and Bogner, 2008).

All three components of Atripla® target the reverse transcriptase enzyme. However, the NRTI acts by intracellular conversion of these drugs to their active metabolites, which then competitively inhibit HIV reverse transcriptase activity and viral replication. On the NNRTI's action is through the non-competitive inhibition of HIV reverse transcriptase (Horberg and Klein, 2010).

Tenofovir disoproxil fumarate targets HIV reverse transcriptase and prevents the synthesis of viral DNA. Inhibiting DNA synthesis through the induction of nucleoside pool imbalance, oxidative stress, and DNA damage may be another alternative way in which tenofovir disoproxil fumarate works (Grigsby et al., 2010). NRTI has been implicated in metabolic alterations observed in diabetes mellitus, emtricitabine, and to a lesser extent tenofovir and efavirenz have been found to increase the risk of incident diabetes (Shankalala et al., 2017; Salam et al., 2019).

2.8 Influence of diabetes in compromising bone quality

Type 2 diabetes mellitus reduces bone strength and increases the risk of fractures. This bone weakness is believed to be due to a reduction in the trabecular volume, thickness, and number of trabeculae (Hamann et al., 2011). In chronic cases that remain untreated, reduced insulin secretion can lead to a reduction in osteoblasts number and bone matrix synthesis leading to poor bone strength (Sun et al., 2015). Other researchers suggested that diabetes promotes osteoblast apoptosis by inhibiting new bone formation (He et al., 2004). In the mandible, type 2 diabetes mellitus has been shown to negatively affect bone mineralisation and new bone formation surrounding dental implants (von Wilmowsky et al., 2011). This may lead to poor surgical outcomes.

2.9 Alcohol effects on bone

Alcohol exposure significantly reduces bone turnover as expressed by fewer osteoblasts and osteoclasts on the osteoid surface (Diez et al., 1997; Dyer et al., 1998; Lauing et al., 2008). Alcohol exposure significantly reduces the volume, thickness, and number of trabeculae (Dyer et al., 1998; Maurel et al., 2012). Biomechanical properties such as bone strength, stiffness, toughness, and ductility are significantly decreased in experimental rats exposed to alcohol (Kusy et al., 1989; Lauing et al., 2008). This makes bone more vulnerable to fatigue and fracture due to poor bone quality (Molina et al., 2014).

2.10 Influence of cART on bone

Osteoporosis is a common skeletal bone disease in rural South Africa, and older women with HIV may experience bone loss more than women without HIV (Gregson et al., 2022). Use of cART is associated with a decrease in bone mineral density (BMD) leading to osteoporosis, decreased bone strength, and increased susceptibility to fracture (Natukunda et al., 2023). Efavirenz was associated with a low BMD among HIV-positive individuals (Dave et al., 2015).

2.11 The anatomy of the mandible of the rat

The rat mandible consists of paired bones known as the left and right hemimandibles. These hemimandibles are joined in the midline by a fibrous connective tissue called the mandibular symphysis (Kufley et al., 2017). Each hemimandible has a ramus and the body with its alveolar process which anchors and supports the dentition (Fig. 2.1).

The rat dentition is monophyodont, having a single set of three molar teeth and one large, chisel-shaped incisor teeth that runs beneath the molar teeth and the entire length of the mandible. Rat dentition has no precursors (primary dentition) or successors (permanent dentition) (Crossley, 1995). The dentition consists of 1 Incisor tooth (I), no canine tooth (C), no premolar tooth and 3 molecular teeth (M) in each quadrant of the jaw (I 1-1, C 0-0, P 0-0, M 3-3). Both the mandible and the maxilla have 8 teeth, making a total of 16 teeth in both the maxilla and the mandible.

The mandibular skeletal unit consists of the condylar (Cr), the coronoid (Cd), the angle of the mandible, the mandible body and the alveolar process. The condylar (Cr) and coronoid (Cd) processes are part of the ramus of the mandible, while the alveolar process, the angle (angular process), and the mandibular body form the unit of the body of the mandible (Fig. 2.1). The entire body of the mandible inside the mandibular canal (MC) is the mandibular nerve, together with the mandibular blood vessels. The mental foramen (MF) found in the body of the mandible contains the mental nerves and vessels (Fig. 2.1).

Some important anatomical landmarks on the hemimandible include the Gonion (Go), which is the lowest posteroinferior point on the angle of the mandible, Ante-gonion (Ag) is the highest point of the notch or concavity of the lowest border of the ramus of the mandible where it joins the body of the mandible), and Menton (Me) is the most inferior point of the mandible symphysis (Kufley et al., 2017) (Fig. 2.1)

2.12 Histology of bone

Composition of bone

The bone composition is approximately 70% mineral crystals, 20% organic matrix that includes cells, and 10% water (Rosen, 2009) (Fig. 2.2). The inorganic aspect consists of hydroxyapatite ($Ca_{10}(PO4)_6(0H)_2$ which is a naturally occurring calcium phosphate (Morgan and Gerstenfeld, 2021). The organic component consists predominantly of type 1 collagen, a variety of non-collagenous proteins, and bone remodelling cells (osteoblasts, osteocytes, osteoclasts, bone lining cells), all embedded in a proteoglycan and glycoprotein substance to form bone tissue

(Junqueira and Carneiro, 2003; Morgan and Gerstenfeld, 2021). The human skeleton is made of 20% trabecular bone, and which is enclosed by cortical bone (80%) (Chappard et al., 2008). On the contrary, the rat mandibular bone consists mainly of cortical bone with a small volume of trabecular bone at approximately 11% (Elovic et al., 1995; Jiang et al., 2004; Bagi et al., 2011; Tsai et al., 2011).

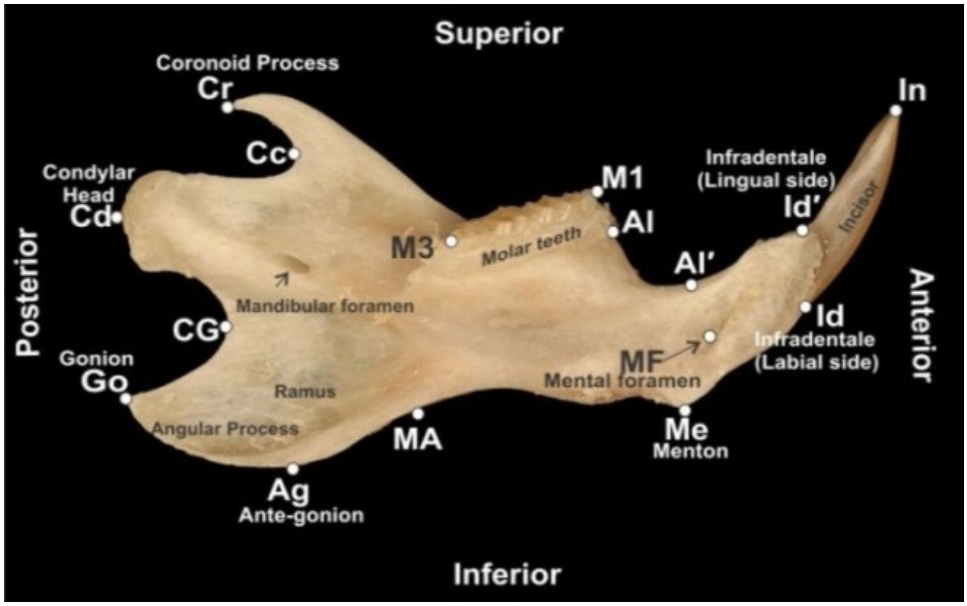

Figure 2.1: Rat hemimandible landmarks Cr, the most posterior point of the coronoid process; CC, the upper mandibular notch, the point of the line Cd-Cr;CG, lower mandibular notch; MA, the deepest point of the outer margin of bone that connects; Me and Ag; Ag, Ante-gonion; Me, Mention; In, the lowest incisor; Id, Infradentale (labial side); Idl, Infradentale (lingual side), Al; the highest point of the mesial alveolar bone at the lower first molar; All; the deepest point of the outer margin of the bone connecting Al and Idl; M1, the highest point of the mesiobuccal cusp of the lower first molar; and M3, the highest point of the central cusps of the lower third molar.

Trabecular bone

Trabecular bone forms the inner layer of bone. It has a highly porous structure consisting of a dense network of lamellar bone rods and plate-shaped trabeculae organised in approximately

perpendicular directions that surround an interconnected pore space that is filled with bone marrow and bone marrow cells, especially in long bones (Hsu et al., 2016; Morgan and Gerstenfeld, 2021) (Fig. 2.2). The bone marrow is found between the trabeculae and supplies nutrients and oxygen to the trabeculae by diffusion since the trabeculae lack blood vessels (McCreadie et al., 2001; Osterhoff et al., 2016; Morgan and Gerstenfeld, 2021). The trabeculae are arranged as an irregular network of its collagen fibres (Morgan and Gerstenfeld, 2021). In small rodents, the thickness of the trabeculae ranges from 20 µm to 60µm (Kinney et al., 1995; Bouxsein et al., 2010), while in humans it ranges from 50µm to 300µm (Morgan and Gerstenfeld, 2021).

Trabecular bone gives strength and structural support to bone despite its lower BMD and performs its metabolic function (Fang et al., 2019) Trabecular bone has a highly porous architecture (40-95%), its porosity is age dependent, and it allows the transmission of stress loads to the much stronger cortical bone (Feng and McDonald, 2011; Lin et al., 2021). It is the site of bone remodelling; it is also the site of many pathological conditions of bone remodelling, of which osteoporosis is a classic example (Feng and McDonald, 2011).

In advanced age-related osteoporosis, bone loss starts with loss of the trabecular bone and later progresses to loss of the cortical bone (Chappard et al., 2008). The loss in trabecular bone mass is due to transformation from dense plate-shaped trabeculae with high connectivity to rod-shaped free-ending trabeculae with less connectivity, which leads to low bone mass and gradual

decline of the bone trabecular and cortical microstructure, which increase bone fragility with a consequent increase fracture risk (Chappard et al., 2008).

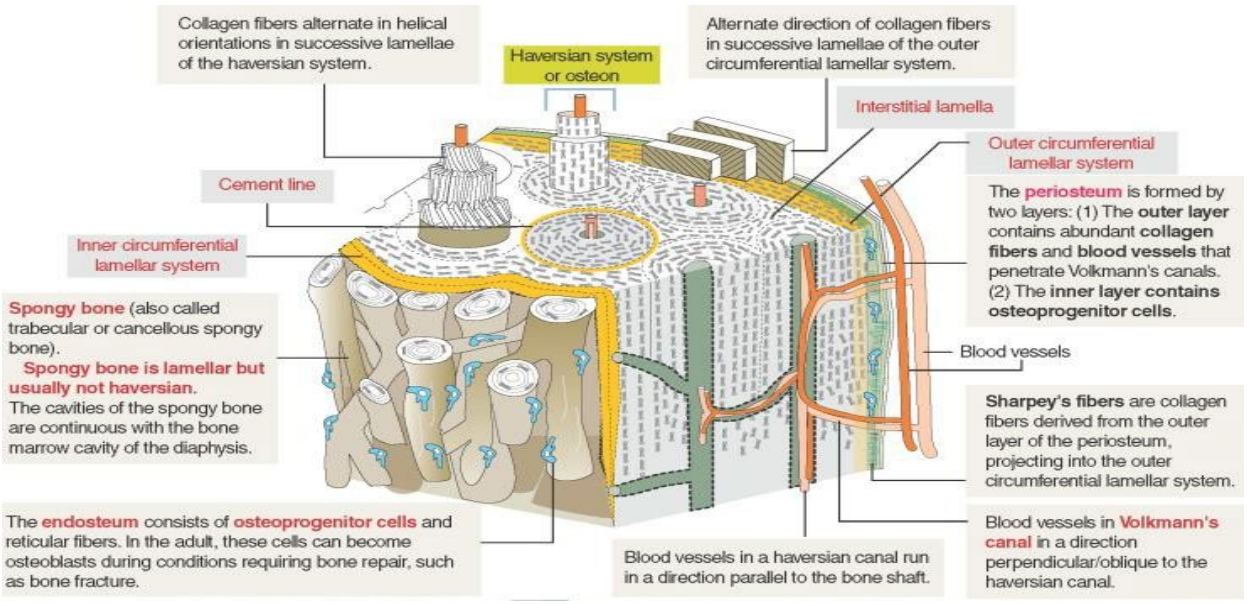

Figure 2.2: Illustration of trabecular and cortical bone (Kierszenbaum and Tres 2015)**.**

Cortical bone

Cortical bone is the outer layer of bone which consists of dense, solid parallel concentric lamellar units (Kierszenbaum and Tres, 2015). These are called osteons and contain a high amount of mineral (hydroxyapatite) and collagen fibres (Klintstrom et al., 2018) (Fig. 2.2). Each osteon is fed and interconnected with each other by the Haversian and Volkmann canals, as well as the canaliculi (Osterhoff et al., 2016). On the outer surface, the cortical bone is covered by the periosteum. The periosteum consists of two types of layers, an outer layer that contains an abundant matrix of connective tissues consisting of bundles of predominantly type 1 collagen fibres (Sharpey's fibres) which connects the periosteum to the endosteum that contains osteoprogenitor cells (Kierszenbaum and Tres, 2015; Osterhoff et al., 2016) (Fig. 2.2) Cortical

bone contains active osteocytes that sense strain and mechanical forces on the bone and send signals for bone resorption or formation (Rosen, 2009).

2.13 Bone remodelling

In dentistry, the mandibular and maxillary bones are crucial organs that give structure, protection, and anchor to teeth. To maintain bone volume and strength, old bone matrices are constantly replaced by newly formed bone in a process known as re-modelling (Chappard et al., 2008). This process is performed by a functional and anatomic structure known as the basic multicellular unit (BMU) and requires coordinated signaling between the six major types of cells: osteoblasts, osteocytes, osteoclasts, bone lining cells, adipocytes, and immune cells (Morgan and Gerstenfeld, 2021). It is also tightly regulated and coordinated by osteoregulatory hormones (Seibel, 2005; Feng and McDonald, 2011; Henneicke et al., 2014), cytokines, and growth factors (Seibel, 2005). An imbalance in bone remodelling results in osteoporosis or osteoporotic bone diseases that are characterised by increased bone fragility (Florencio-Silva et al., 2015). The remodelling cascade (Fig. 2.3) follows four main distinct and interconnected processes, as outlined below:

1. **Activation**: Osteocytes play an important 'mechanosensory' function through their peri-lacunae and peri-canaliculi networks (Qing et al., 2012; Dole et al., 2017). This network enables osteocytes to assess the presence of microdamage and microcracks due to fatigue, bone strain sustained during overloading or due to ageing (Davison et al., 2006; Kaya et al.,

2017). Osteocytes also express the tartrate resistant acid phosphatase (TRAP) catabolic enzyme of bone matrix, a standard intracellular marker for osteoclasts (Kaya et al., 2017)

2. **Resorption**: Osteoclasts are bone resorptive cells (Rosen, 2009). Bone resorption by osteoclasts involves demineralisation of the inorganic matrix and collagen matrix by acidification followed by enzymatic degradation of the organic matrix (Boyle et al., 2003; Janssens et al., 2005). TRAP hydrolyses and solubilises the inorganic component of bone (Charles and Aliprantis, 2014).
3. **Reversal**: This stage reverses the resorption process initiated by osteoclasts by lining the resorption lacunae with osteoid matrix (Parry, 2005; Picke et al., 2019; Pierce et al., 2019). Osteoblasts can be identified by several bone markers such as ALP (Goltzman, 2018; Pierce et al., 2019).
4. **Formation**: At the completion of remodelling, osteoblasts continue to secrete nonmineralised osteoid which becomes mineralized. Osteoblasts are trapped in the mineralised matrix and are now called osteocytes.

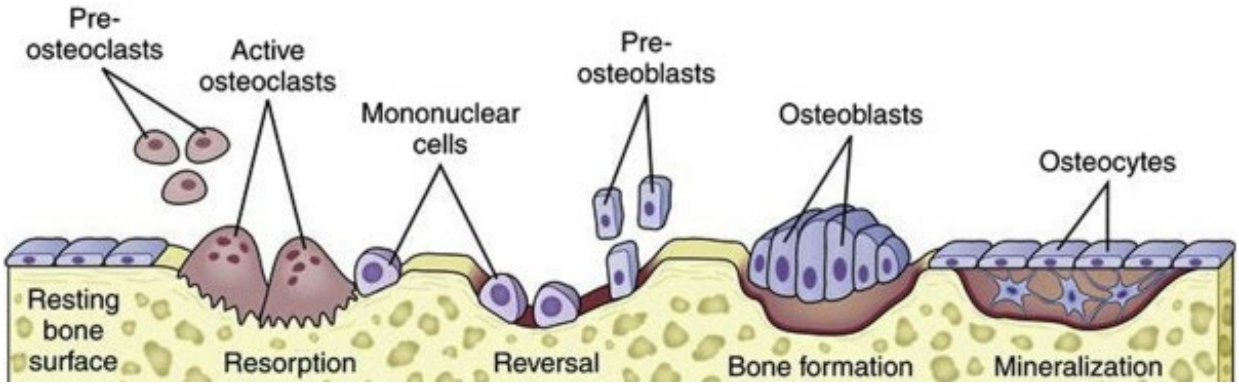

Figure 2.3: Bone remodelling. Schematic representation of the phases of the bone remodelling process. Adapted from Bolamperti et al. (2022).

2.14 Hormonal Influence of bone health

Insulin and osteocalcin

Insulin is a polypeptide hormone secreted by the β-cells in the islets of the pancreas and its main action is to coordinate with glucagon to maintain blood glucose levels (Rahman et al., 2021). It acts in an anabolic pathway to regulate glucose levels and also induces glucose uptake for storage by the liver, skeletal muscles, and adipose tissues (Rahman et al., 2021). Insulin also acts on important organs of the body like the brain, heart, liver, kidneys, and bones, and it promotes bone formation (Rahman et al., 2021).

Insulin has osteo-anabolic effects on bone that cause an increase in osteoblast number while inhibiting osteoclast activity (Hoang et al., 2003; Thrailkill et al., 2005). Osteocalcin is an osteoblast-derived endocrine hormone, synthesized by osteoblastic lineage cells and secreted in the ECM (Li et al., 2016). It plays a vital role in bone formation, resorption, remodelling, and skeletal development (Karsenty, 2017). Osteocalcin increases cortical bone thickness and density, as well as an increase in the amount of mineralised bone matrix (Li et al., 2016). Osteocalcin has been shown to promote the recruitment and attachment of preosteoclasts into the bone matrix via cell signaling and the presence of osteocalcin in the bone matrix is recognized signal for bone resorption and deposition (Ritter et al., 2020).

Insulin acts in synergy with the hormone osteocalcin to regulate glucose metabolism, increase insulin sensitivity in tissues, increase pancreatic beta cell proliferation and increase insulin

secretion (Lee et al., 2007; Booth et al., 2013; Kanazawa, 2015). Both carboxylic and non-carboxylic osteocalcins directly increase the glucose transport of adipocytes and muscle cells.

Parathyroid hormone

Parathyroid hormone (PTH) is produced by the parathyroid gland, and it is important in regulating calcium (Ca^{2+}) and phosphate metabolism. PTH promotes Ca^{2+} reabsorption and inhibits phosphate re-absorption in the renal tubule of the kidney, and it also increases the renal synthesis of 1,25-dihydroxy vitamin D, increasing intestinal absorption of Ca^{2+} (Goltzman, 2018). PTH-induced stimulation of osteoblast differentiation and proliferation and inhibition of apoptosis results in an increase in bone mass and bone formation. PTH regulates osteoblast function by activating PTH receptors type 1 (PTH1R) on the bone marrow osteoblasts lineage cells, including the osteoprogenitors, BLC, pre-osteoblasts, mature osteoblasts, and osteocytes, stimulating increased proliferation of bone marrow mesenchymal stem cells (Goltzman, 2018).

Sclerostin

Sclerostin is a glycoprotein secreted primarily by osteocytes, chondrocytes and osteoclasts (Sharifi et al., 2015; Vasiliadis et al., 2022). Sclerostin is a negative regulator of bone formation and bone remodelling, as it inhibits the canonical wingless-related integration site (Wnt) pathway (Sharifi et al., 2015). It binds to the complex of low-density lipoprotein receptor-related proteins 5 and 6 (LRP5 / 6) and the BMP receptors. Therefore, it is considered a BMP antagonist (Sharifi et al., 2015; Vasiliadis et al., 2022).

Sclerostin prevents mesenchymal stem cell (MSC) differentiation into mature osteoblasts / osteoocytes, and inhibits the differentiation of mature osteoblasts/osteocytes, and inhibition the differentiation of matured osteoblasts into osteocytes, therefore it reduces osteoblastic bone formation (Sharifi et al., 2015). In addition to this, sclerostin is also involved in the regulation of bone marrow adipocyte tissues. Sclerostin also indirectly affects bone resorption by up-regulation of RANKL-expressing osteocytes, and the promotion of osteoclastogenesis and bone resorption by decreasing the expression of osteoprotegerin (Vasiliadis et al., 2022).

Calcitonin

Calcitonin, a 32 amino acid peptide hormone produced primarily by the thyroid, and its receptor (CTR) are well known for their ability to decrease plasma Ca^{2+}concentrationby inhibiting osteoclast-mediated bone resorption and by promoting Ca2 + excretion by the kidney (Pondel, 2000; Masi and Brandi, 2007; Silverman, 2010). Therefore, calitonin plays an important role in skeletal homeostasis, being an important regulator of bone resorption, and therefore its therapeutic use in the treatment of osteoporosis (Masi and Brandi, 2007).

Calcitonin acts directly on calcitonin receptors (CTR) to inhibit bone resorption (Pondel, 2000). Calcitonin has also been proven to interfere with osteoclast differentiation from precursor cells (pre-osteoclasts) to form multinucleated bone-resorbing osteoclasts in the bone marrow (Pondel, 2000; Masi and Brandi, 2007). Calcitonin enhances Ca^{2+} excretion by inhibiting renal tubular reabsorption of Ca^{2+} by the kidney, and therefore Calcitonin can maintain normal plasma calcium concentration in individuals (Pondel, 2000; Silverman, 2010).

2.15 Bone regulation by cytokines

Transforming growth factor beta-1 (TGF- β1)

One of the most abundant multifunctional osteogenic cytokines in the bone matrix is TGF-β1 (Bismar et al., 1999; Janssens et al., 2005; Tang et al., 2009) which plays an important role in bone remodelling by regulating the migration, proliferation, survival, and differentiation of osteoprogenitors cells, as well as production of ECM (Janssens et al., 2005; Tang et al., 2009). TGF-1 bone formation occurs by TGF-β1 is through stimulating osteoblast proliferation by chemotactic attraction of osteoblasts ((Janssens et al., 2005; Tang et al., 2009; Wu et al., 2016).

TGF-β exists as a latent protein stored in the ECM, its activation by proteases depends on osteoclastic bone resorption, activated TGF-β subsequently binds to TGF-β type I receptor (TGFβRI), also known as activin receptor-like kinases (ALK5) and type II (TGFβRII) receptors (TGFRII) to trigger the intracellular signaling cascade (Ehnert et al., 2010; Yang et al., 2014; Wu et al., 2016; Chen et al., 2021) (Fig. 2.4).

TGFβRII induces the phosphorylation of TGFβRI which then phosphorylates receptor-mediated (R-Smad) Smad 2 and 3 specific proteins, and other non-Smad receptors specific proteins within the cytoplasm (Horbelt et al., 2012). On the contrary, inhibitory (I) Smads 6 and 7 compete with R-Smads for receptors and negatively regulate R-Smad signalling by inhibiting the phosphorylation of specific R-Smad proteins as well as the translocation of Smad complexes into the nucleus, therefore inhibiting signal transduction (Yang et al., 2014; Wu et al., 2016; Chen et al., 2021). Phosphorylated R-Smads2 and 3 bind to their common (Co) mediator Smad4, or bind

to other non-Smad receptors, for example, the CREB-binding protein (CBP) or p300, to form Smad complexes that translocate to the nucleus.

In the nucleus, Smad complexes bind to the deoxyribonucleic acid (DNA), where the Smad complexes together with several transcriptional cofactors, coactivators, corepressors to regulate gene transcription and promote osteoprogenitor cell differentiation, proliferation, chemotaxis, and subsequent osteoblast bone deposition (Janssens et al., 2005; Ehnert et al., 2010; Horbelt et al., 2012; Yang et al., 2014; Wu et al., 2023). Smads 6 and 7 regulate the Smad signaling cascade by blocking the translocation of co-Smad complexes into the nucleus (Wu et al., 2016). Smad 6 is an inhibitor of BMP signaling, while Smad7 inhibits both TGF-β1/activin and BMP signaling (Janssens et al., 2005). The mechanisms through which TGF-β1 may influence bone remodelling in type 2 diabetes mellitus with alcohol and cART are unknown, and this study may shed light.

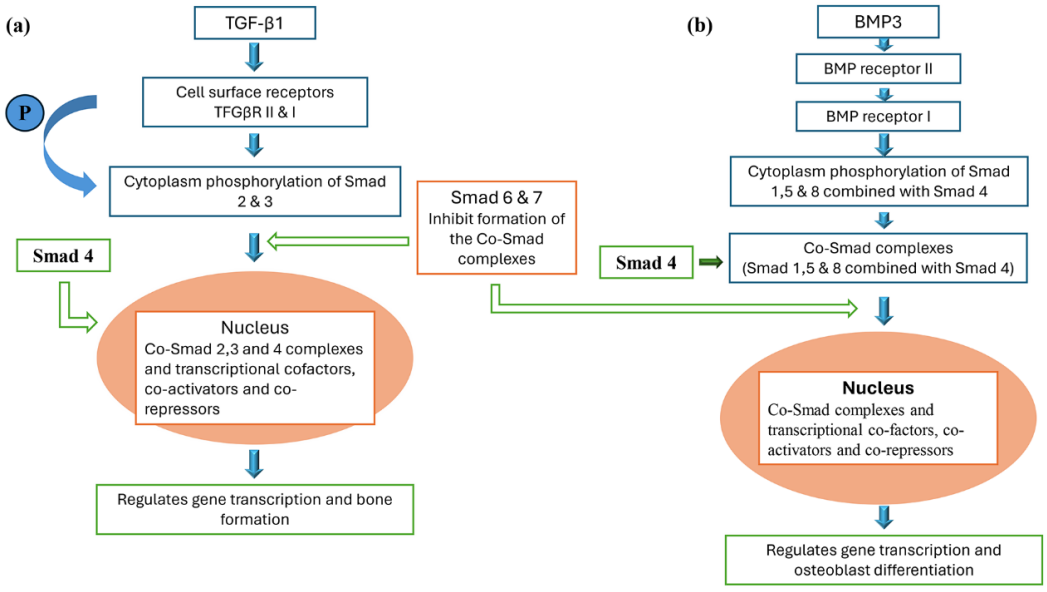

Figure 2.4: Bone regulation by cytokine pathways. (a) **TGF-β** and (b) BMP receptor-Smad signal pathway**. Illustration by Dr. I Eguavoen.**

Anti-osteogenic cytokine BMP-3

BMP-3 also known as osteogenin is an antiosteogenic cytokine produced mainly by osteoblasts and osteocytes (Wu et al., 2016; Kokabu and Rosen, 2018). It is the most abundant BMP within the bone matrix, accounting for approximately 65% of the total BMP content in demineralised adult bone (Daluiski et al., 2001; Kokabu and Rosen, 2018). BMP-3 is a nonsignalling molecule, which competes via the TGFβ-Activin-like pathway, leading to antagonism of BMP-2-induced osteogenic cell commitment; hence, BMP-3 is a negative regulator of osteoblastogenesis and bone mass (Bahamonde and Lyons, 2001; Daluiski et al., 2001; Kokabu and Rosen, 2018). It binds competitively to the activin receptor II2b (ActRIIB) and suppresses BMP-R-Smads 2 and 3 (Wu et al., 2016; Kokabu and Rosen, 2018). It suppresses bone formation by suppressing BMP-Smad signaling (Wu et al., 2016; Kokabu and Rosen, 2018) and therefore it is a negative determinant of BMD (Daluiski et al., 2001). The effects of BMP manifest as reduced volume of BMD, reduced trabecula, and thinner cortical bone, resulting in increased bone fragility (Gamer et al., 2009; Horbelt et al., 2012; Wu et al., 2016; Kokabu and Rosen, 2018).

2.16 Effects of Type 2 diabetes mellitus on bone

Type 2 diabetes mellitus reduces bone strength and increases the risk of fracture. This bone weakness is believed to be due to a reduction in the volume, thickness, and number of trabeculae (Hamann et al., 2011). In chronic cases that remain untreated, reduced insulin secretion can lead to a reduction or inhibition in osteoblastic cell proliferation and collagen production (bone matrix synthesis), leading to diminished mechanical properties and poor bone strength (Sun et al., 2015). Other researchers suggested that type 2 diabetes mellitus promotes osteoblast apoptosis

(He et al., 2004). In the mandible, type 2 diabetes mellitus negatively affects bone mineralisation and new bone formation surrounding dental implants (von Wilmowsky et al., 2011).

Diabetes mellitus that exists singularly or occurring as comorbidity can occur together with osteoporosis being more prevalent in type 1 compared to type 2 diabetes mellitus (Starup-Linde and Vestergaard, 2016). However, fractures are common in both types. Bones are reported to be narrower despite increased cortical bone thickness in type 2 diabetes mellitus (Oei et al., 2013). This indicates a decrease in biomechanical competence. It is suggested that there may be an imbalance in the interactions of bone cells, such as osteoclasts, osteocytes, and osteoblasts, resulting in poor bone integrity (Starup-Linde and Vestergaard, 2016).

2.16 Alcohol effects on bone remodelling and biomechanical properties

Alcohol consumption during adolescence is a risk factor for trabecular bone loss, which could be a significant factor contributing to bone loss, osteoporosis, and susceptibility to fracture (Lauing et al., 2008). Biomechanical properties such as bone strength, stiffness, toughness, and ductility are significantly decreased in experimental rats exposed to alcohol (Kusy et al., 1989; Lauing et al., 2008). This makes bone more vulnerable to fatigue and fracture due to poor bone quality (Molina et al., 2014). Alcohol exposure significantly reduces the volume, thickness, and number of trabeculae (Maurel et al., 2012). All these are thought to be caused by alcohol exposure, which significantly reduces bone turnover, expressed by the low levels of osteoblasts and osteoclasts on the bone surface, affecting the rate of bone formation and resorption. (Leung et al., 1993; Diez et al., 1997).

2.17 Bone mechanical properties

The parameters that reflect the different properties of bone are computed or derived from the load-displacement curve and represent the structural property of bone. These whole bone or structural properties characterise bone tissue in its original intact form (Oksztulska-Kolanek et al., 2016). The three-point bend test (Leppanen et al., 2006) is a widely used method for assessing the biomechanical properties of long bones. This is done by placing a whole bone on a material testing machine that is slowly loaded until it breaks. Several parameters are derived from the force displacement curve (Fig. 2.5), and describes the following:

i) Displacement (Deflection) – the amount of vertical deviation from the horizontal plane required to fracture the bone.

ii) Maximum force - the amount of force required to cause deformation.

iii) Break Force – the amount of force required to fracture the bone.

iv) Time - the duration that the bone withstands the force until a fracture. v) Work to fracture (Energy-to-fracture) is defined as the total area under the curve. It represents the work that must be done to fracture the bone. A tough bone requires more work to fracture (Jepsen et al., 2015).

v) Stiffness (bending stiffness) (N/mm) - The amount of vertical deviation from the horizontal plane required to fracture the bone. This is the extent to which the bone can resist deformation in response to an applied load or force (resistance to deformation)

vi) Yield point indicates the load value at the yield point where the load displacement diagram is deviating from linearity.

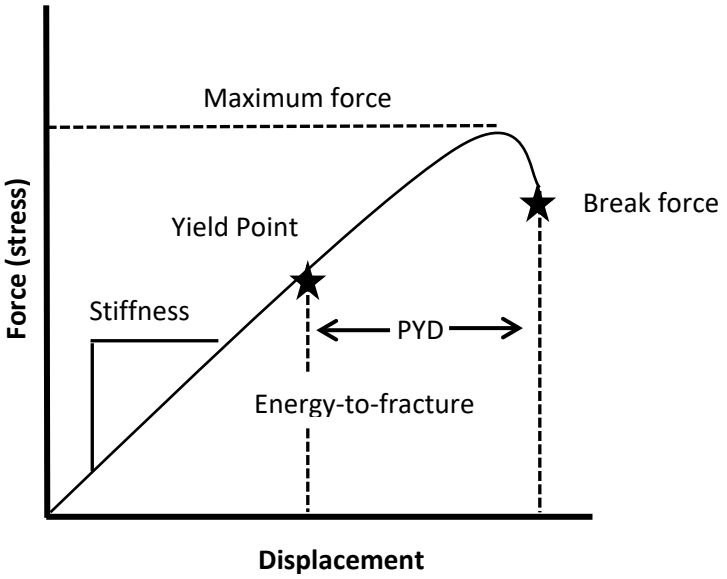

Figure 2.5: Force-displacement curve. A graphical illustration of the properties of compact bone. PYD (post-reward displacement). Illustration by D Pillay.

Chapter 3

Diabetic rat model and study design

3.0 INTRODUCTION 41
3.1 Various disease models of diabetes mellitus 41
3.1.1 Rodent models of diabetes mellitus 41
Chemical (drugs) induction (diabetogenic agents) 42
Dietary and chemical induction 43
Spontaneous, obese, and genetic induction 43
Genetically engineered diabetic rats 45
Surgical induction of diabetes 46
3.2 MATERIALS AND METHODS 47
3.2.1 Ethics 47
3.2.2 Animal husbandry 47
3.2.3 Group allocation 47
3.2.4 Treatment of animals 48
Diabetes induction 48
Alcohol administration 49
Combination antiretroviral therapy (cART) 49
3.2.5 Blood tests 49
Blood glucose tests 49
Oral glucose tolerance tests (OGTTs) 49
3.3 RESULTS 51
3.3.1 Body mass 51
3.3.2 Fasting blood glucose 52
3.3.3 Non-fasting blood glucose 53
3.3.4 Oral glucose tolerance test 53
3.3.5 Serum insulin concentration 55
3.4. DISCUSSION 56
3.4.1 Conclusions 57

3.0 INTRODUCTION

3.1 Various disease models of diabetes mellitus

Diabetes can be studied by cell culture (Russell et al., 1999; Green et al., 2018) or animal models (King, 2012; Kottaisamy et al., 2021). The use of animal diabetes models is more effective in understanding its complexity aetiology and the body multi-system interactions (Kottaisamy et al., 2021). Therefore, various diabetic animal models are currently used to evaluate specific aspects of diabetes. These are rodent diabetes models and non-rodent diabetes models. Non-rodent-diabetic models include the invertebrates (Kottaisamy et al., 2021), the cat (King, 2012), the diabetic pig model and the dog (King, 2012; Kleinert et al., 2018; Zakaria et al., 2021).

3.1.1 Rodent models of diabetes mellitus

In rodent type 2 diabetic model, many of the diabetic rats are obese which reflects the human condition in which obesity has a strong connection with the development of T2DM (Fang et al., 2019). This preclinical rodent type 2 diabetic model has helped researchers to understand how type 2 diabetes can be prevented and their extrapolation to human condition. The rodent diabetic model can be developed by two major mechanisms: genetic manipulation or experimental diabetic disease induction with specific drugs or diets or using both combinations (King, 2012; Green et al., 2018; Kottaisamy et al., 2021).

Diet-induced rodent model of diabetes.

The main diet-induced models of diabetes mellitus in rodents include a high-fat diet, a high-carbohydrate diet, or the combination of high-fat and high-carbohydrate diet (Angelova and

Boyadjiev, 2013), or the combination of high-fat and fructose in drinking water (Mahmoud and Elshazly, 2014).

High fat diets induce obesity and accumulation of fats in the liver (hepatic fat accumulations), which induces hyperinsulinaemia (Alwahsh et al., 2017). Hyperinsulinaemia causes increased insulin production and decrease insulin signalling (insulin resistance) leading to hyperglycaemia (Alwahsh et al., 2017), and also free fatty acid (FFA) accumulated in the insulin-sensitive tissues disrupts insulin action (Morigny et al., 2016). High-fat diets (HFD) are useful for studying human metabolic disorders, such as obesity and type 2 diabetes. The disadvantage the disruption of lipid metabolism and insulin resistance caused by long-term HFD consumption can lead to serious health problems, including hyperlipidemia, cardiovascular diseases, and non-alcoholic fatty liver disease. High fructose diets facilitates the increased production of FFA accumulation in plasma and adipose cells as a result of the conversion of excess fructose to lipid in the liver cells leading to obesity and insulin resistance (Zakaria et al., 2021).

The diet-induced model is assumed to be better than genetic diabetes induction because it is caused by environmental manipulation rather than genetic manipulation (King, 2012). This is because diet-induced diabetes is accompanied by a progressive weight gain in rats associated with insulin resistance and abnormal glucose metabolism as observed in humans (King and Bowe, 2016; Kleinert et al., 2018). However, the diet-induced model requires special diet formulations. In most developing countries, it is difficult to obtain all the necessary food ingredients.

Chemical (drugs) induction (diabetogenic agents)

The chemical induction model appears to be the most popular method of inducing diabetes mellitus (Etuk, 2010; Singh et al., 2024). Glucocorticoids and corticosterone have been used to induce diabetes in animal models (Zakaria et al., 2021). Mice treated with corticosterone in drinking water develop metabolic syndrome, including glucose intolerance, insulin resistance, high plasma cholesterol and triglycerides, hyperinsulinemia, obesity, and type 2 diabetes mellitus (Zakaria et al., 2021). Streptozotocin (STZ) can be used alone or in combination with nicotinamide to induce diabetes mellitus (Masiello et al., 1998; Islam and Wilson, 2012; Ghasemi et al., 2014; Chao et al., 2018). Alloxan is also used to induce diabetes, including type 1 and type 2 diabetes mellitus. Alloxan and STZ are the most used diabetic drugs to induce diabetes (Etuk, 2010; Kottaisamy et al., 2021). STZ is useful because it targets pancreatic β-cells allowing researchers to study diabetes and its complications. The administration can be manipulated to produce models of both type 1 and type 2 diabetes. The disadvantage is that STZ has complications as low doses can cause inflammation.

Dietary and chemical induction

A combination of dietary modifications and STZ can be used to induce diabetes. This includes a high fat diet with a single high dose of STZ (Reed et al., 2000; Islam and Wilson, 2012), a high fat diet with multiple low doses of STZ (Vatandoust et al., 2018; Furman, 2021), a fruit diet with a single low dose of STZ (Kumar and Sandhya, 2018). In addition, a combination of high fat and high fructose with several low doses of STZ (Tchoubou et al., 2023) and low doses of fructose in drinking water with low doses of STZ can be used (Sadeghi et al., 2017).

Spontaneous, obese, and genetic induction

The Zucker Diabetic Fatty (ZDF fa/fa) rat (King, 2012; Green et al., 2018; Zakaria et al., 2021), Zucker Diabetic Sprague-Dawley (ZDSD) rat (Zakaria et al., 2021; Dlamini and Ndou, 2023), diabetic mouse (db/db) rat (King, 2012; Green et al., 2018; Zakaria et al., 2021), Goto-Kakizaki (GK) (Fajardo et al., 2014) are spontaneous obese rats that have been genetically modified to induce type 2 diabetes.

The ZDF rat is most widely used for the study of type 2 diabetes mellitus. It originated from a colony of outbred Zucker rats in Walter Shaw's laboratory in Indianapolis in 1991, and it reflects a typical type 2 diabetes mellitus (Kottaisamy et al., 2021). The disease progresses from prediabetic to diabetic states, and with its characteristics such as insulin resistance and hyperphagia to a leptin receptor gene defect (King, 2012). The leptin receptor gene (fa/fa) defect on chromosome 5 makes the rat diabetic before maturity (Peterson et al., 2015; Kottaisamy et al., 2021). Leptin is a hormone produced by adipocytes to inhibit hunger. Mutations in the gene or its receptor in rats can lead to obesity or hyperglycaemia (Zakaria et al., 2021).

The ZDF rat model is the most used leptin-deficient rat model for obesity and type 2 diabetes mellitus (Peterson et al., 2015). This model of diabetes induction is characterised by an abnormality in insulin release but with lack of complete destruction of β-cells indicating that the diabetes is often not as severe as observed in human type 2 diabetes mellitus (King, 2012). The ZDF may not display all human features of diabetes (King, 2012; Peterson et al., 2015; Zakaria et al., 2021). Additionally, the aetiology of type 2 diabetes mellitus in humans is hardly caused by a monogenetic or single gene-based mutation (King, 2012; Zakaria et al., 2021).

The ZDSD rat was bred to overcome the challenges of the ZDF rat and was created by cross-breeding the ZDF lean homozygous wild-type (+/+) rats which do not carry the leptin receptor mutation (fa) (Reinwald et al., 2009; Peterson et al., 2015). This created a polygenetic model of obesity and diabetes that develops type 2 diabetes mellitus at an older age than the ZDF (Yagihashi, 2023). This is good for bone studies as the ZDSD develops type 2 diabetes mellitus at skeletal maturity, and at older age than the ZDF rats.

The phenotypic and genotypic characteristics of ZDSD rats may be more advantageous adaptation of the preclinical to the clinical compared to the ZDF (Wang et al., 2022). This is because the ZDSD rat does not carry the leptin receptors mutations (fa/fa), therefore the mechanism of type 2 diabetes mellitus in the ZDSD rats may be similar to those in humans since the leptin receptors mutations are rare in humans (Wang et al., 2022). Furthermore, although sex, age and diet contributed to the differences in ZDSD rats, its phenotype and type 2 diabetes mellitus disease progression model the characteristics of humans who develop pre-diabetes and diabetes including co-morbidities (Wang et al., 2022).

Genetically engineered diabetic rats

These are transgenic, knock-out, and tissue-specific knock-out models used to induce type 2 diabetes mellitus (Chandrasekera and Pippin, 2014; Zakaria et al., 2021). Rats can be produced to express proteins that play an important role in glucose metabolism (Etuk, 2010). This model enables researchers to understand insulin resistance and pancreatic cell functions (King and

Bowe, 2016). Transgenic mice have contributed to explaining important genes in insulin signaling, such as insulin receptor substrate 1 (IRS-1), insulin receptor 2 (IRS-2), and glucose transporters (GLUT2, GLUT4) (King and Bowe, 2016). Furthermore, many important genes for normal pancreatic cell function and maintenance of pancreatic cell mass have been discovered in re-expressed mice. KK mice (polygen model) and obese hyperglycaemic rats (Wistar) are examples of genetically modified diabetic rats (Kottaisamy et al., 2021).

Surgical induction of diabetes

This model uses the regenerative capacity of the pancreatic cells or their precursors and involves partial or total elimination of the pancreas (Kottaisamy et al., 2021). In mice, about 60–90% of the pancreas is removed and diabetes occurs within 3 months (King and Bowe, 2016). This is a very invasive model that causes damage to other healthy tissues than the pancreas, so it is considered technically insignificant (Kottaisamy et al., 2021). This model allows researchers to study the effects of the reduction of cell mass and pancreatic regeneration mechanisms.

Sprague-Dawley rat model

The male Sprague-Dawley rats were used in this study because they are more susceptible to STZ induced diabetes mellitus than the females (Deeds et al., 2011). The protective effect of oestradiol (a type of oestrogen) on pancreatic β cell apoptosis may be responsible for this decreased susceptibility; furthermore, oestrogen plays a role in the maintenance of energy and glucose homeostasis (Alemany, 2021).

3.2 MATERIALS AND METHODS

3.2.1 Ethics

Ethics approval for the study has been granted by the University of the Witwatersrand Animal Ethics Committee (2018/011/58/C) (Appendix A).

3.2.2 Animal husbandry

A total of 71 male Sprague-Dawley rats (ten-week-old) weighing approximately 250-300g were used for the study. All animals were bred and kept at the Central Animal Services (CAS) of the University of the Witwatersrand (Wits), Johannesburg, Republic of South Africa under standard experimental conditions as approved by the ethics committee. These animals were housed in individual well-ventilated plastic cages of L43mm long, W220mm wide and H200 height with free movement within the cages. Food and water intake was unlimited. The animal house was kept at a regulated temperature (23± 2ºC), humidity (40-60%), and day a 12h light and 12h dark cycle. The rats were weighed weekly.

3.2.3 Group allocation

The rats were allowed to acclimatize to their environment for 2 weeks before they were randomly distributed into 10 groups consisting of 3 control groups, 3 non-diabetic groups and 4 diabetic groups. The animals were placed in the following groups: (i) Untreated control group which received no treatment (n=8); (ii) Citrate buffer controls (CB), received a once of injection of citrate buffer (n=6); (iii) Gelatine group (GEL), received gelatine (n=8); (iv) Alcohol (ALC), consumed alcohol (n=8); (v) received combination antiretroviral treatment (cART) (n=8); (vi)

ALC+cART, received alcohol and cART (n=7); (vii) DBT, diabetic group (n=7). The study included additional diabetic groups that received alcohol or cART or both as follows; (viii) diabetic animals treated with alcohol (DBT+ALC) (n=6); (ix) diabetic animals treated with cART (DBT+cART) (n=7); and (x) diabetic animals treated with both alcohol and cART (DBT+ALC+cART) (n=6).

3.2.4 Treatment of animals

Diabetes induction

This research adopted a type 2 diabetes mellitus model described by Wilson and Islam (2012), which incorporated a formulated fructose-enriched diet (Appendix B1) and an STZ injection. The enriched-fructose diet is an effective dietary means of inducing obesity, insulin resistance, increased hypertension and hyperglycaemia in laboratory rats and mimics symptoms of type 2 diabetes mellitus in humans(Bell and Polonsky, 2001; Ang and Yu, 2018; Chao et al., 2018). The rats in the diabetic groups (DBT, DBT+ALC, DBT+cART and DBT+ALC+cART) were fed rat chow modified with 20% fructose (Nature's Choice™) Whole Food Specialists, Randvaal, South Africa) for two weeks before receiving a single injection of 40 mg/kg streptozotocin (STZ) (Appendix B2) (Sigma, St. Louis, MO, USA) in freshly prepared citrate buffer at 0.05 M (pH 4.5).

After 72 hours following the STZ administration, the non-fasting blood glucose (NFBG) level were measured and values above >200mg/dL (>11.1mmol/L) were considered diabetic (Deeds et al., 2011). Once the type 2 diabetes mellitus was confirmed, the STZ-induced type 2 diabetes mellitus rats were withdrawn from the 20% fructose diet and placed on the standard rat chow diet.

Alcohol administration

The rats were given 10% v/v alcohol daily in drinking water for 12 weeks.

Combination antiretroviral therapy (cART)

Rats were treated with an extrapolated adult dose of 0.023mg/g body weight of cART (ATRIPLA® Bristol–Myers Squibb and Gilead Sciences Foster City, CA, USA) in gelatine cubes daily (Appendices B3 and B4).

3.2.5 Blood tests

Blood glucose tests

Fasting blood glucose tests were conducted bi-weekly using a hand-held AccuCheck compact glucometer (Roche Diagnostics, South Africa. Blood samples were obtained by pricking the tail vein. Non fasting blood glucose tests were conducted bi-weekly using the same glucometer.

Oral glucose tolerance tests (OGTTs)

Oral glucose tolerance tests were conducted once every four weeks throughout the experimental period. Rats were fasted for 12hours overnight before administering a single dose of 2g/kg body weight of glucose solution 0.5g/ml by oral gavage. Blood glucose (glycaemic response) levels were measured at 4 different times within 2 hours; 0 (prior to glucose load), 15, 30, 60 and 120 min after the glucose load (Abeeleh et al., 2009).

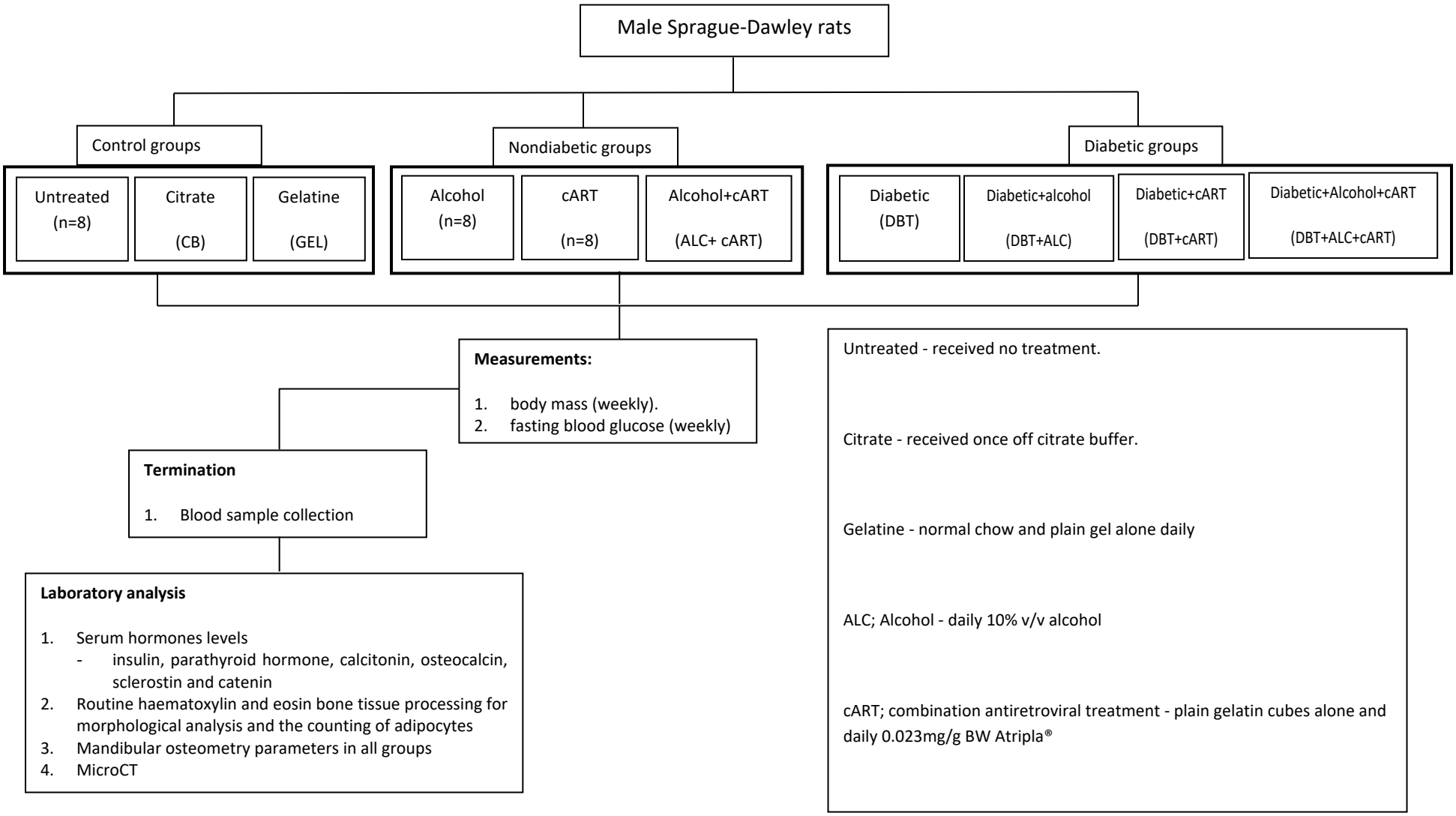

Figure 3.1: Study design. CB, citrate buffter; Gel, Gelatine; ALC, alcohol; cART, combination antiretroviral treatment; ALC+cART, alcohol and cART; DBT, diabetic; DBT+ALC, diabetes and alcohol; DBT+cART, diabetes and cART; DBT+ALC+cART, diabetes, alcohol and cART

3.3 RESULTS

3.3.1 Body mass

The rats in the citrate, gelatine, alcohol, and cART groups exhibited similar mass to the untreated group. From week 5 onwards, all the diabetic groups (DBT, DBT+ALC, DBT+cART and DBT+ALC+cART) had significantly lower mass than the untreated control group ($p<0.001$ for all comparisons).

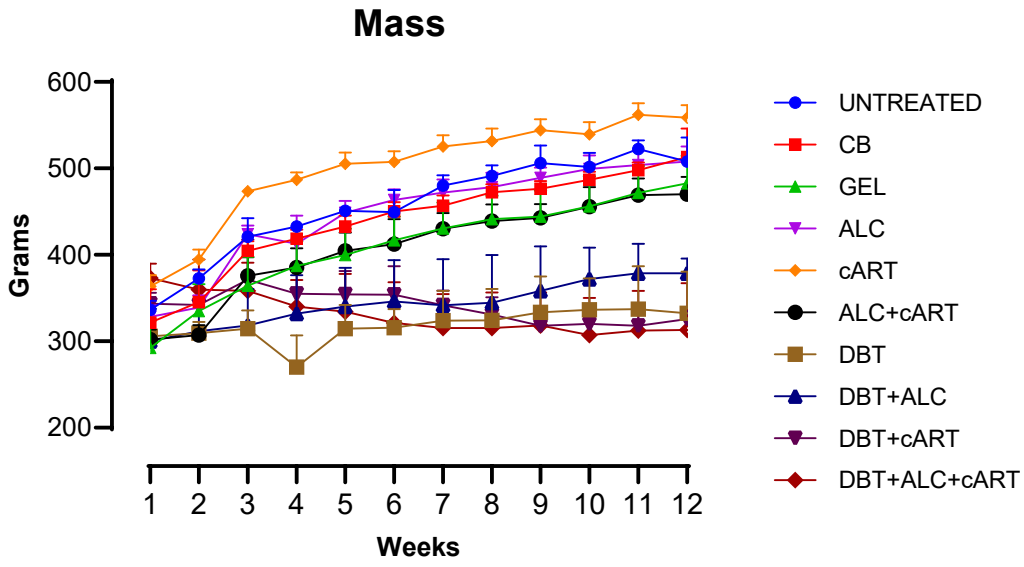

Figure 3.2: Changes in the body mass from weeks 1-12. The diabetic groups had significantly lower mass than non-untreated from week 5 to 12 ($p<0.001$ for all comparisons)

CB, citrate buffter; Gel, Gelatine; ALC, alcohol; cART, combination antiretroviral treatment; ALC+cART, alcohol and cART; DBT, diabetic; DBT+ALC, diabetes and alcohol; DBT+cART, diabetes and cART; DBT+ALC+cART, diabetes, alcohol and cART.

3.3.2 Fasting blood glucose

The FBG level of the diabetic groups was significantly higher compared to the untreated, control and non-diabetic groups from the 2nd to the 12th week ($p<0.001$ for all comparisons with the untreated). The highest FBG level was observed in the DBT+cART group followed by the DBT, DBT+ALC and the DBT+cART+ALC respectively.

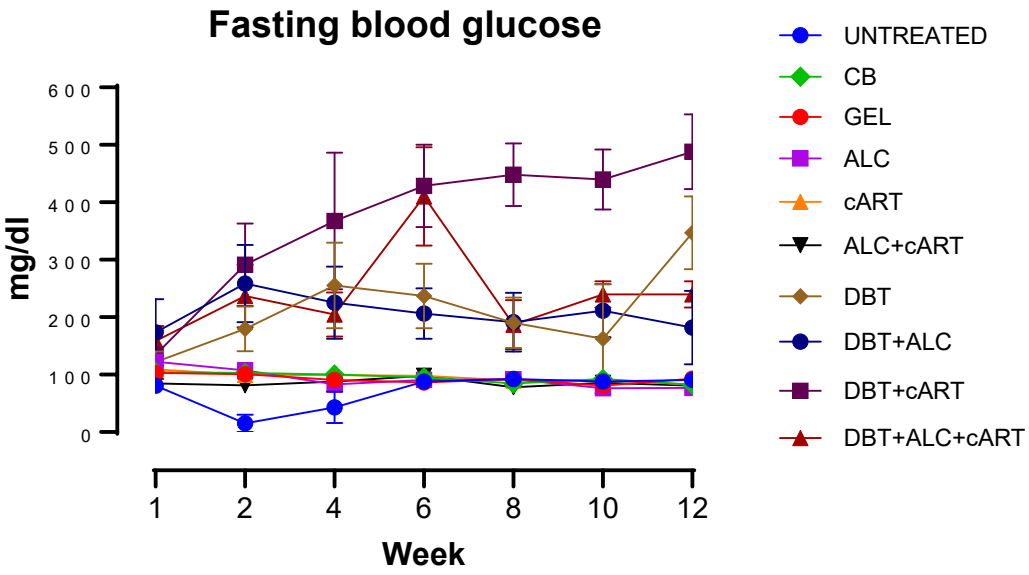

Figure 3.3: Fasting blood glucose level from 1 to 12 weeks.

CB, citrate buffter; Gel, Gelatine; ALC, alcohol; cART, combination antiretroviral treatment; ALC+cART, alcohol and cART; DBT, diabetic; DBT+ALC, diabetes and alcohol; DBT+cART, diabetes and cART; DBT+ALC+cART, diabetes, alcohol and cART.

3.3.3 Non-fasting blood glucose

All the rats in the diabetic groups had non-fasting blood glucose levels above 250mg/dL (13.9mmol/L).The rats in the non-diabetic group had non-fasting blood glucose levels of less than 150mg/dL (8.3mmol/L). The diabetic groups had significantly higher blood glucose than the untreated in all weeks ($p<0.001$ for all comparisons)

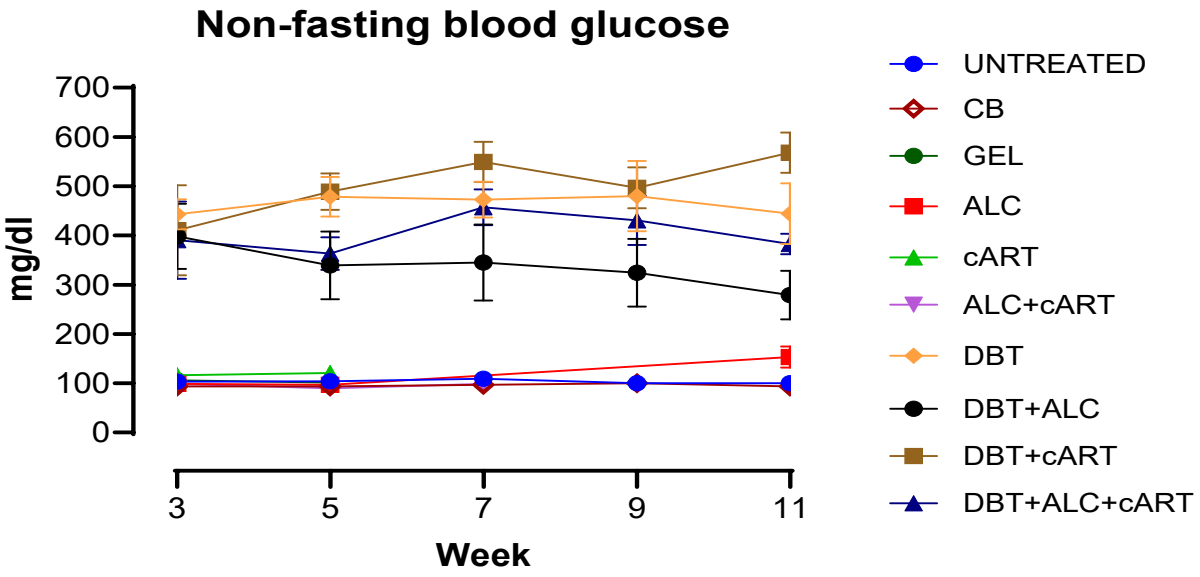

Figure 3.4: Non-fasting blood glucose from 3 to 11 weeks.

CB, citrate buffter; Gel, Gelatine; ALC, alcohol; cART, combination antiretroviral treatment; ALC+cART, alcohol and cART; DBT, diabetic; DBT+ALC, diabetes and alcohol; DBT+cART, diabetes and cART; DBT+ALC+cART, diabetes, alcohol and cART.3.3.4 Oral glucose tolerance test

3.3.4 Oral glucose tolerance test

The diabetic groups had higher blood glucose readings at 0 and at 120 minutes compared to the untreated, control, and non-diabetic groups. The DBT+ALC had the highest blood glucose levels at 15 minutes, while the DBT and DBT+cART had the highest blood glucose levels at both 60 and 120 minutes. There are significant differences in the blood glucose levels between the groups. At the 120th minutes of OGTT, all the diabetic rats blood glucose levels above 250mg/dL (13.9mmol/L)

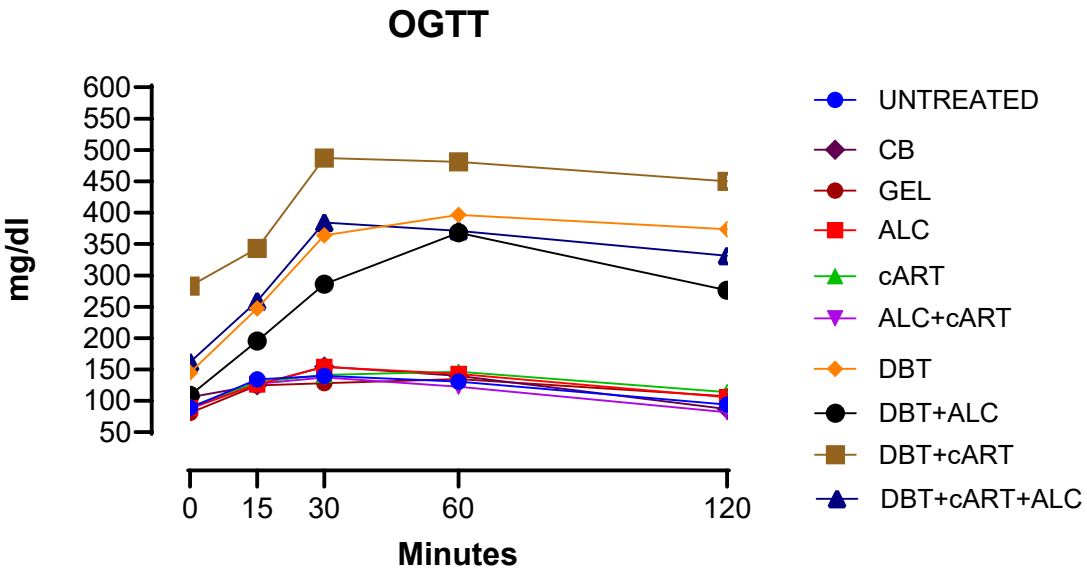

Figure 3.5: Oral glucose tolerance test

CB, citrate buffter; Gel, Gelatine; ALC, alcohol; cART, combination antiretroviral treatment; ALC+cART, alcohol and cART; DBT, diabetic; DBT+ALC, diabetes and alcohol; DBT+cART, diabetes and cART; DBT+ALC+cART, diabetes, alcohol and cART.

3.3.5 Serum insulin concentration

Serum insulin levels detected in the ALC+cART (1290pg/mL±146.6), ALC (1152pg/mL±150.3), and cART (1050pg/mL±18.83), were similar compared to the untreated control group (1251pg/mL±47.2) (p=0.998, p=0.760 and 0.080, respectively) (Fig. 3.6). On the contrary, DBT+cART (813.8pg/mL±92.2), DBT+ALC+cART (801.1pg/mL±85.59), DBT (771.2pg/mL±146.2) and the DBT+ALC (693pg/mL±52.87) groups had significantly lower insulin levels than the untreated control group (p<0.001 for all comparisons) (Fig. 3.6).

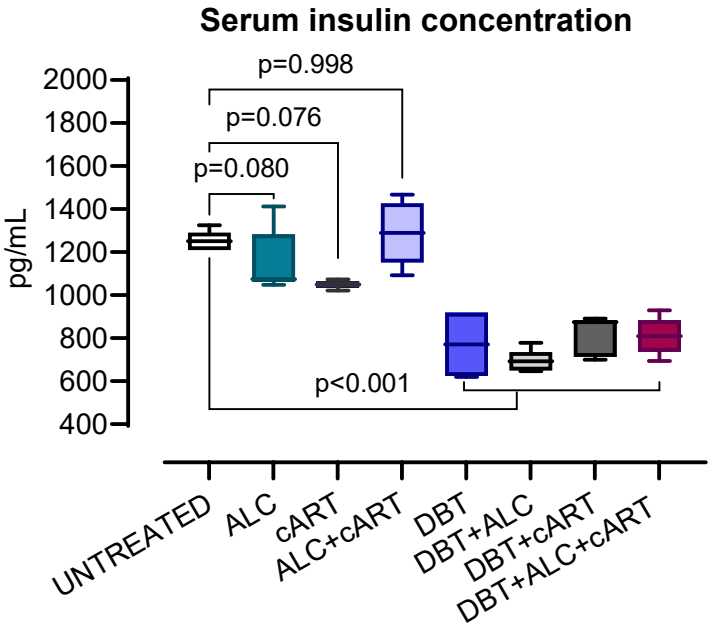

Fig. 3.6 Serum insulin concentration at 12 weeks.

Box-and-whisker plots of adipocyte quantity in various study groups. The line inside the box represents the mean, whereas the bottom and top lines of the box show the 25th and 75th percentiles, respectively. The whiskers below and above the box show the minimum and maximum values, respectively. Untreated control; ALC, alcohol; cART, combination antiretroviral treatment; ALC+cART, alcohol and cART; DBT, diabetic; DBT+ALC, diabetes and alcohol; DBT+cART, diabetes and cART; DBT+ALC+cART, diabetes, alcohol and cART.

3.4. DISCUSSION

The rats assigned to diabetic groups developed signs that are typical of type 2 diabetes such as loss of body mass, low insulin levels, high blood glucose levels and abnormal OGTTs. The citrate buffer and gelatine groups did not have any effect on either the non-diabetic parameters or the diabetic parameters (insulin, blood glucose levels and OGTT) as there was no significant difference found in these parameters compared with the untreated group. This demonstrates that the citrate buffer and gelatine cubes used as the experimental vehicles for administration of STZ and cART respectively did not have any diabetogenic effect on the induction of type 2 diabetes mellitus.

In rodent diabetic studies, rats with a basal blood glucose level ≥200mg/dL (≥11mmol/L) have been considered to be diabetic (Deeds eta al., 2011; Qinna and Badwin, 2015). In this present study, rats in the diabetic groups with the basal glucose level of ≥250mg/dL (≥13.9mmol/L) are considered to be diabetic. All the rats in the diabetic groups had blood glucose levels of ≥250mg/dL (≥13.9mmol/L) in FBG, NFBG and OGTT at 120th minutes and maintained this level of diabetic blood glucose levels throughout the experiments confirming the induction of the type 2 diabetes, and also the diabetic states were maintained.

The diabetic state as confirmed by FBG and NFBG levels, and monitored by OGTTs , low blood insulin levels and the loss of body mass are well-defined characteristic of type 2 diabetes mellitus. Lipolysis and sarcopenia seen in diabetic cases are responsible for the gradual loss of body mass.

The cART is associated with metabolic dyregulations characterised by dyslipidaemia, insulin resistance and obesity (increased gain in body mass), these metabolic dysregulations exacerbate type 2 diabetes mellitus due prolong use of cART. This explains the highest blood glucose levels in the FBG, NFBG and OGTT (at 60th and 120th minutes) in the DBT+cART group. All the above results confirm that type 2 diabetes has been successfully induced in rats that received a modified 20% fructose diet together with a single dose of IP 40mg/kg BW Streptozotocin.

The induction of diabetes led to development of hypoinsulinemia in the diabetic rat groups. Deficiencies in the function and quantity of the beta cell pancreas play an important role in diabetes development and progression. Increased beta cell deficit and apoptosis have been observed in patients with type 2 diabetes. In the early stages, the cells adapt to insulin resistance and insulin secretion increases, but ultimately becomes exhausting, and the pancreatic number of beta cells decreases (Khin et al., 2023). Hypoinsulinemia in the diabetic groups suggests beta cell failure.

3.4.1 Conclusions

This study successfully induced diabetes in Sprague Dawley ratsT2D, as shown by various markers confirming the presence of diabetes. There have been body mass losses, abnormal OGTTs as well as high fasting and random non-fasting blood glucose that are consistent with WHO definitions of type 2 diabetes. There was a reduction in insulin levels in diabetic rats, a feature that is a pancreatic beta cell failure symptom due to long-term hyperglycemia.

Chapter 4

Influence of alcohol and combination antiretroviral treatment on bone regulating hormones in diabetic Sprague Dawley rats

4.0 INTRODUCTION 59
4.1 MATERIALS AND METHODS 61
4.1.1 Study animals. 61
4.1.2 Serum 61
4.2.3 Enzyme-linked immunoassay (ELISA) for the concentration of calcitonin, parathyroid hormone, sclerostin, osteocalcin and catenin 61
4.2.4 Statistical analysis 62
4.2.0 Results 63
4.2.1 Calcitonin concentration 63
4.2.2 Parathyroid hormone 65
4.2.3 Sclerostin concentration 67
4.2.4 Osteocalcin concentration 69
4.2.5 β-catenin concentration 71
4.3 DISCUSSION 73
Calcitonin and parathyroid hormone 73
Sclerostin 75
Osteocalcin 75

4.0 INTRODUCTION

Several hormones are involved in the regulation of bone health and homeostasis such as parathyroid hormone, calcitonin, osteocalcin, sclerostin and β-catenin. These hormones may have anabolic or catabolic actions and may be antagonistic to each other. For example, the anabolic action of parathyroid hormone involves the suppression of sclerostin (Vasiliadis et al., 2022). Sclerostin inhibits the proliferation, function, and differentiation, resulting in a decrease in bone mass (Dreyer et al., 2023). Conversely, osteocytes are the target cells of parathyroid hormone in bone where it inhibits the expression of the sclerostin, thereby increasing bone formation (Vasiliadis et al., 2022).

Calcitonin protects the skeleton from calcium loss by inhibiting osteoclast activity (Keller et al., 2014). In contrast to the action of parathyroid hormone, calcitonin increases the deposition of calcium in bone and lowers the level of calcium in the blood. The major target site for calcitonin is bone, where it inhibits osteoclastic bone resorption (Duan et al., 2018).

Total serum osteocalcin concentrations in humans are either carboxylated or uncarboxylated and are inversely associated with the measures of glucose metabolism (Booth et al., 2013). Though both the carboxylated and the uncarboxylated have been detected in serum; studies have indicated that the endocrine function of osteocalcin is in its uncarboxylated form (Ferron and Lacombe, 2014). The carboxylated form is the most important component of the bone extracellular matrix and the most abundant non-collagenous protein in the bone extracellular matrix (Li et al., 2016; Mizokami et al., 2017).

β-catenin is an important component of the Wnt signaling pathway and plays an important role in the proliferation of osteoblasts (Huang et al., 2022). The Wnt/β-catenin pathway, involves the nuclear translocation of β-catenin and activation of target genes through transcription factors. Switching off the Wnt/β-catenin signalling pathway causes inhibition of the β-catenin in the cytoplasm (Liu et al., 2022).

This chapter sought to evaluate the influence of alcohol and combination antiretroviral treatment on bone regulating hormones in diabetic Sprague Dawley rats through assessing the serum hormone levels by ELISA.

4.1 MATERIALS AND METHODS

4.1.1 Study animals.

Animal husbandry was as described under section 3.2.2 (Animal husbandry) The animal animals were assigned into various groups as described in section 3.2.3 (group allocation). The induction of diabetes, administration of alcohol and cART are all described under section 3.2.4.(treatment of animals).

4.1.2 Serum

Intracardiac blood was aspirated at termination and collected into serum separating tubes, then centrifuged at relative centrifugal force (RFC) of 1409 for 10 minutes. Serum was decanted into aliquots that were stored at minus 80◦C for serum analysis of the concentration of calcitonin, parathyroid hormone, sclerostin, osteocalcin and catenin.

4.2.3 Enzyme-linked immunoassay (ELISA) for the concentration of calcitonin, parathyroid hormone, sclerostin, osteocalcin and catenin

All the ELISA kits were sourced from Elabscience® Houston Texas USA. as follows: Rat CT (Calcitonin) ELISA Kit (E-EL-R0047), Rat I-PTH (Intact Parathormone) ELISA KitE-EL-R0535Rat SOST (Sclerostin) ELISA Kit (E-EL-R3032), Rat OC/BGP(Osteocalcin) ELISA Kit (E-EL-R0243), and Catenin Beta 1 (CTNNb1) E-AB-36471.The Standard working solution was added to the first two columns, the micro-ELISA 96 well plate provided with the kit. Each concentration of the solution was added in duplicate, to one well each, side by side (100 uL in each well). Then the serum samples were added to the other wells (100 uL for each well). The plate was then covered with the sealer provided in the kit before incubating for 90 min at 37℃. Care was taken to ensure the solutions were added to the bottom of the micro-ELISA plate well,

avoiding touching the inside wall. The liquid was then removed from each well and 100 µL of Biotinylated Detection Ab working solution was added to each well. The plate was then covered with the sealer and gently mixed before incubating for 1 hour at 37°C. The solution was then decanted from each well and 350 uL of wash buffer was added to each well. After soaking for 2 minutes, the solution was decanted from each well and dried by gently patting against a clean absorbent paper. This wash step was performed thrice using a microplate washer (ELx50 Microplate Strip Washer, BioTek Instruments, Inc). The HRP Conjugate working solution was then added (100 µL) to each well and covered with the plate sealer before incubating for 30 min at 37°C. The solution was then decanted from each well, and the wash process was repeated five times. The Substrate Reagent (90 µL) was then added to each well and covered with a new plate sealer before incubating for about 15 min at 37°. Care was taken to protect the plate from light. The Stop Solution (50 µL) was then added to each well taking care to the stop solution the same order as the substrate solution. The optical density (OD value) of each well was then determined at with a micro-plate reader (ELx800 Absorbance Microplate Reader, BioTek Instruments, Inc) set to 450 nm.

4.2.4 Statistical analysis

The data were managed in Microsoft Excel Office 365 (Microsoft Corporation) and analysed using GraphPad Prism version 10. ANOVA with Tukey post-hoc was used for multiple group comparisons of means. The data was presented as means and standard deviation. Significance level was set at $p < 0.05$.

4.2.0 RESULTS

4.2.1 Calcitonin concentration

While the cART group (=1473pg/mL±89.6) had the highest serum calcitonin concentration, this did not show a significant difference compared to the untreated group (1438pg/mL±80.33) (p=0.999) (Fig. 4.1). No difference in serum calcitonin concentration levels were detected in the DBT (=1233pg/mL±187.7) and DBT+ALC (1211pg/mL±152.5) (p=0.128, and p=0.062) respectively compared to the untreated group) (Fig. 4.1) The serum calcitonin level was lowest in the DBT+cART group (753.9pg/mL±110.3), followed by the ALC=1107pg/mL±46.82), DBT+ALC+cART (1124pg/mL±34.52), ALC+cART (=1146pg/mL±127.2) groups, respectively. All these groups had significantly lower serum calcitonin levels when compared to the untreated group ($p<0.001$, p=0.001, p=0.003 and $p<0.001$, respectively) (Fig. 4.1).

The ALC group had a serum calcitonin concentration similar to that detected in the ALC+cART, DBT+ALC and DBT+cART+ALC (p=0.999, p=0,8294 and p>0,9999, respectively) (Fig. 4.1). In contrast, the concentration was higher in the cART compared to the ALC group ($p<0.001$). The DBT group serum calcitonin level was similar to the DBT+ALC and DBT+ALC+cART (p=0.999, p=0.799) (Fig. 4.1). However, the concentration in the ALC alone was similar to the DBT group (p=0,657). Additionally, the DBT+cART had significantly lower calcitonin levels than the DBT group ($p<0.001$) (Fig. 4.1). In contrast, the cART alone had higher serum calcitonin concentration than the DBT group (p=0,041) (Fig. 4.1).

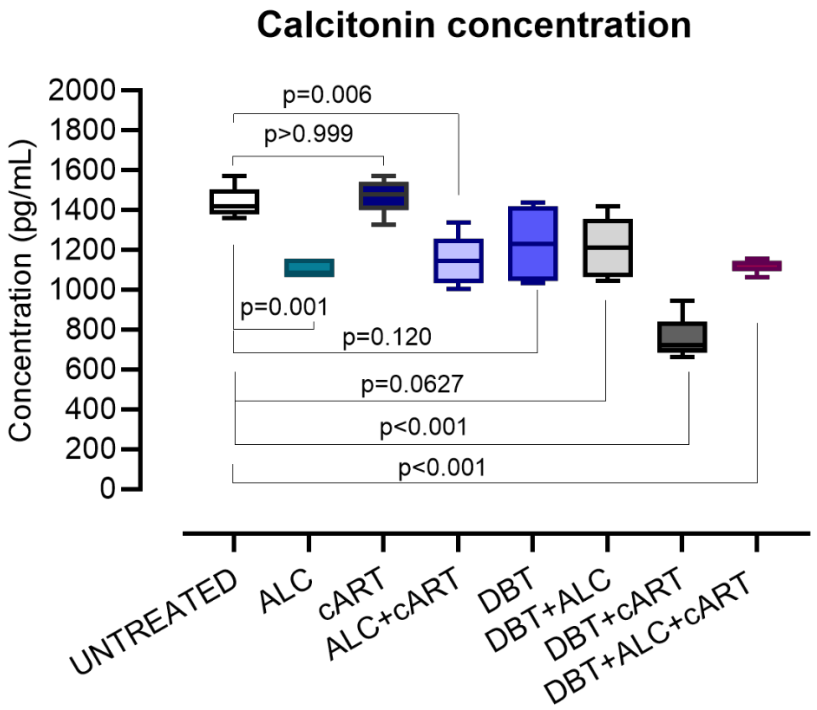

10**Figure 4.1: Calcitonin concentration.** Box-and-whisker plots show calcitonin concentration in various study groups. The line inside the box represents the mean, whereas the bottom and top lines of the box show the 25th and 75th percentiles, respectively. The whiskers below and above the box show the minimum and maximum values, respectively.

ALC vs cART, ALC+cART, DBT+ALC, DBT+cART+ALC (p<0,001, p=,999, p=0,8294 and p>0,9999, respectively); cART vs ALC+cART, DBT+cART, DBT+cART+ALC (p<0.001 for all); DBT vs ALC, cART, DBT+ALC, DBT+cART, DBT+cART+ALC (p=0,657, p=0,041,p>0,999,p<0,001, p=0,799 and p<0.001, respectively); DBT+ALC vs DBT+cART, DBT+cART+ALC (p<0.001, p=0,925, respectively).

ALC, alcohol; cART, combination antiretroviral treatment; ALC+cART, alcohol and cART; DBT, diabetic; DBT+ALC, diabetes and alcohol; DBT+cART, diabetes and cART; DBT+ALC+cART, diabetes, alcohol and cART

4.2.2 Parathyroid hormone

The highest serum parathyroid hormone concentration was detected in the DBT+cART (94425pg/mL±3292) and ALC+cART (=64952pg/mL±630.2) group compared to the untreated group (47575pg/mL±3292) ($p<0.001$ for both comparisons) (Fig. 4.2). The ALC (46279pg/mL±3166) and the cART group (47121pg/mL±3166) had similar serum parathyroid hormone concentration to the untreated group (=0.999) for both comparisons. The DBT (18718pg/mL±1784), DBT+ALC (28130pg/mL±5708) and the DBT+ALC+cART (20667pg/mL±3057) groups had lower serum parathyroid hormone concentration than the untreated group ($p<0.001$ for all comparisons) (Fig. 4.2).

The ALC alone and cART group had similar serum parathyroid hormone concentration ($p=0.999$) (Fig. 4.2). On the contrary, the ALC+cART group had higher in the ALC alone or cART group ($p<0.001$, for both). ALC alone and cART group had significant higher values than the ALC+cART, DBT+ALC and DBT+cART+ALC ($p<0.001$ for all comparisons with the ALC or cART group) (Fig. 4.2).

The DBT group exhibited lower serum parathyroid hormone concentration than the DBT+ALC and the DBT+cART groups ($p=0.025$ and $p<0.001$). In contrast, the DBT and DBT+ALC+cART had similar values ($p=0.995$) (Fig. 4.2).

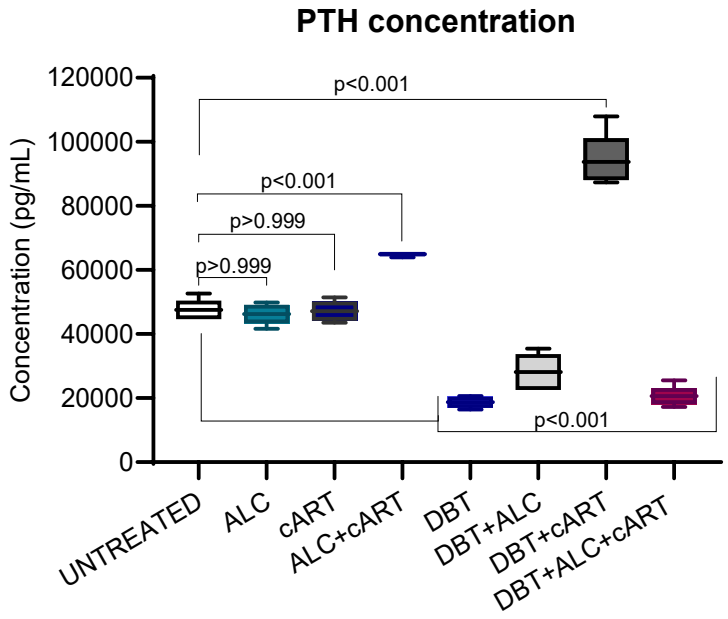

11**Figure 4.2: Parathyroid hormone concentration**

Box-and-whisker plots show parathyroid hormone concentration in various study groups. The line inside the box represents the mean, whereas the bottom and top lines of the box show the 25th and 75th percentiles, respectively. The whiskers below and above the box show the minimum and maximum values, respectively.

ALC vs cART, (p>0,999), ALC vs ALC+cART, DBT+ALC, DBT+cART+ALC (p<0,001, for all); cART vs ALC+cART, DBT+cART, DBT+cART+ALC (p<0,001or all comparisons); DBT vs ALC, cART, DBT+ALC, DBT+cART, DBT+cART+ALC (p<0,001, p<0,001, p<0,001, p=0,025 and p=0,995, respectively); DBT+ALC vs DBT+cART, DBT+cART+ALC (p<0,001, p=0,133, respectively).

ALC, alcohol; cART, combination antiretroviral treatment; ALC+cART, alcohol, and cART; DBT, diabetic; DBT+ALC, diabetes and alcohol; DBT+cART, diabetes, and cART; DBT+ALC+cART, diabetes, alcohol and cART.

4.2.3 Sclerostin concentration

The ALC+cART (11,869pg/mL±1,946) group had the highest concentration of sclerostin than the untreated (3,914pg/mL±481.5) group ($p<0.001$) (Fig. 4.3). The was followed by the DBT+cART (9,568pg/mL±958.4), DBT+ALC (7,309pg/mL±1,827) and cART (6315pg/mL±333.6), groups which also displayed significantly higher concentrations compared to the untreated group ($p<0.001$ for DBT+cART and DBT+ALC and $p=0.033$ for cART, all vs untreated) (Fig. 4.3).

The ALC (4,011pg/mL±806.9), and DBT+ALC+cART (3,971pg/mL±769.8) groups did not display any significant difference in sclerostin concentration compared to the untreated group ($p=0.999$ vs untreated ALC and DBT+ALC+cART, respectively) (Fig. 4.3). While the DBT group (2,139pg/mL±520.8) had the lowest concentration of sclerostin, no statistical significance was detectable against the untreated group ($p= 0.222$) (Fig. 4.3).

The ALC group had a significantly lower serum sclerostin concentration than the cART or ALC+cART group ($p=0,046$, and $p<0.001$, respectively) (Fig. 4.3). The DBT had a lower concentration than the DBT+ALC and DBT+cART groups ($p<0.001$ for both comparisons). However, it was similar to the DBT+ALC+cART group ($p=0,191$) (Fig. 4.3).

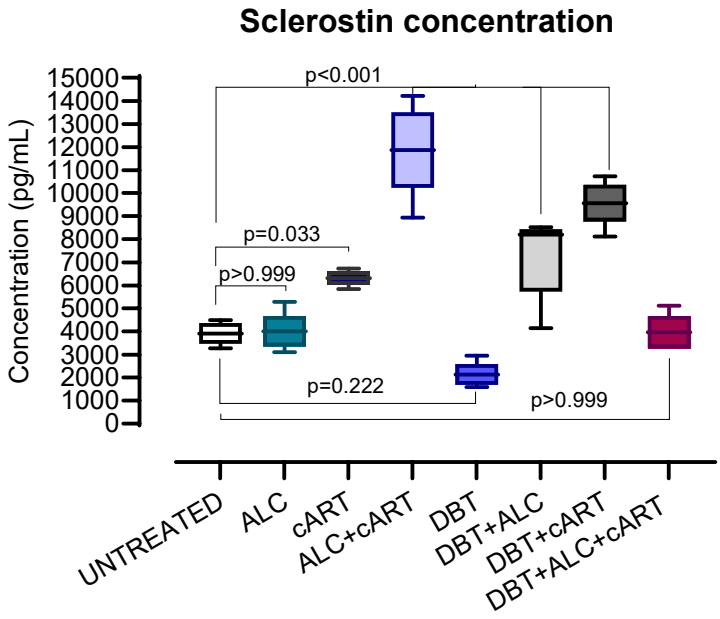

Figure 4.3: Sclerostin concentration

Box-and-whisker plots show sclerostin concentration in various study groups. The line inside the box represents the mean, whereas the bottom and top lines of the box show the 25th and 75th percentiles, respectively. The whiskers below and above the box show the minimum and maximum values, respectively.

ALC vs cART, ALC+cART, DBT+ALC, DBT+cART+ALC (p=0,046, p<0,001, p=0,001 and p>0,999, respectively); cART vs ALC+cART, DBT+cART, DBT+cART+ALC (p<0,001, p=0,001, p=0,040, respectively); DBT vs ALC, cART, DBT+ALC, DBT+cART, DBT+cART+ALC (p=0,171, p<0,001 p<0,001, p<0,001and p=0,191, respectively); DBT+ALC vs DBT+cART, DBT+cART+ALC (p=0.339, p=0.380, respectively).
ALC, alcohol; cART, combination antiretroviral treatment; ALC+cART, alcohol, and cART; DBT, diabetic; DBT+ALC, diabetes and alcohol; DBT+cART, diabetes and cART; DBT+ALC+cART, diabetes, alcohol and cART.

4.2.4 Osteocalcin concentration

Although not statistically significant, the mean osteocalcin concentration was lower in the ALC (13.77pg/mL±0.94), DBT+cART (16.39pg/mL ±2.58), DBT+ALC+cART group (16.71pg/mL±1.59) compared to the untreated (25.92pg/mL±4.27) (Fig. 4.4). On the contrary, the highest concentration was detected in the DBT (78.19pg/mL±15.28) and the DBT+ALC group (72.93pg/mL±14.55) ($p<0.001$ compared to the untreated group). The ALC+cART serum osteocalcin concentration (34.75pg/mL±6.01) was not significantly higher than the untreated group ($p=0.663$) (Fig. 4.4).

There were no significant differences detected between the ALC and the cART group ($p=0.791$) whereas the ALC+cART had significantly larger values than the ALC alone group or the cART group ($p=0.005$ and $p<0.001$, respectively) (Fig. 4.4).

The DBT group serum osteocalcin concentration was similar to the DBT+ALC group ($p=0.964$) (Fig. 4). In contrast, it was lower in the DBT+cART and DBT+cART+ALC ($p<0.001$ for both comparisons). The DBT+ALC group also had lower serum osteocalcin concentration than the DBT+cART and DBT+cART+ALC ($p<0.001$ for both comparisons) (Fig. 4.4).

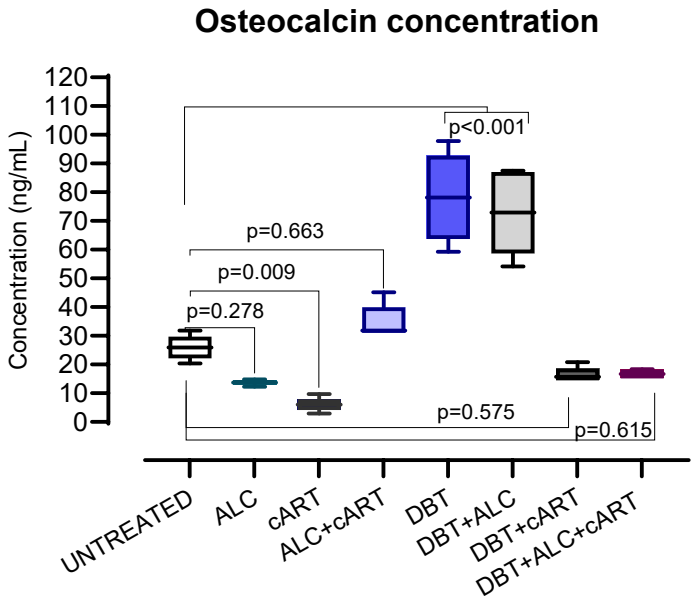

Figure 4.4: Osteocalcin concentration. Box-and-whisker plots show osteocalcin concentration in various study groups. The line inside the box represents the mean, whereas the bottom and top lines of the box show the 25th and 75th percentiles, respectively. The whiskers below and above the box show the minimum and maximum values, respectively.

ALC vs cART, ALC+cART, DBT+ALC, DBT+cART+ALC (p=0,7913, p=0,005, p<0,001 and p=0,998, respectively); cART vs ALC+cART, DBT+cART, DBT+cART+ALC (p<0,0001, p=0,475, p=0,436, respectively); DBT vs ALC, cART, DBT+ALC, DBT+cART, DBT+cART+ALC (p<0,001, <0,001, p=0,9648, p<0,001 and p<0,001, respectively); DBT+ALC vs DBT+cART, DBT+cART+ALC (p<0,001, p<0,001, respectively).

ALC, alcohol; cART, combination antiretroviral treatment; ALC+cART, alcohol and cART; DBT, diabetic; DBT+ALC, diabetes and alcohol; DBT+cART, diabetes and cART; DBT+ALC+cART, diabetes, alcohol and cART.

4.2.5 β-catenin concentration

The DBT+ALC+cART (2.17pg/mL±0.24) and ALC+cART (1.88pg/mL±0.47) group had the highest serum β-catenin concentration although not significantly different from the untreated group (2.06pg/mL±0.18) group (Fig. 4.5).

The ALC (0.51pg/mL±0.00) group, the DBT (0.36pg/mL±0.209), the DBT+ALC (mean=0.86pg/mL±0.05) and the DBT+cART group (0.50pg/mL±0.16) displayed a significantly lower concentration than the untreated group ($p<0.001$) (Fig. 4.5).

While the ALC and cART groups had similar serum β-catenin concentrations, it was higher in the ALC+cART group ($p=0.985$ and $p<0.001$, respectively) (Fig. 4.5). The concentration was similar when comparing the DBT with the DBT+ALC or DBT+cART group ($p=0.498$, $p=0.999$, respectively). However, it was significantly lower when the DBT was compared to the DBT+ALC+cART ($p<0.001$) (Fig. 4.5).

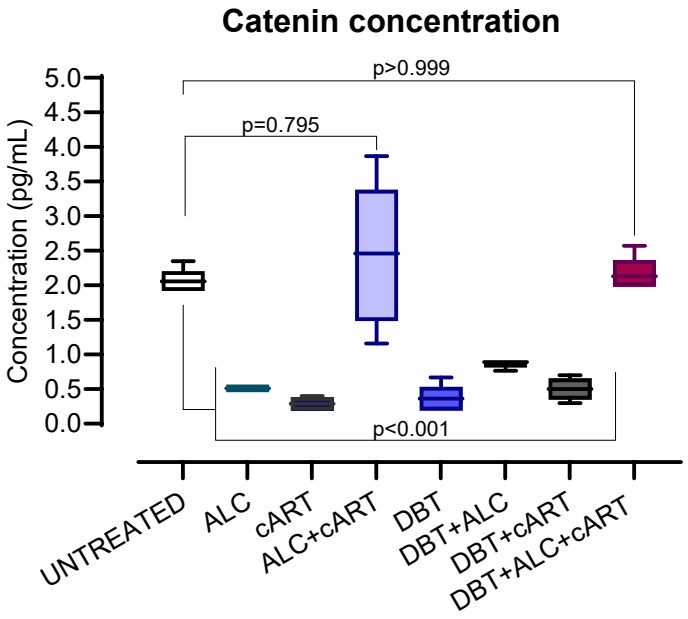

Figure 4.5: β-catenin concentration. Box-and-whisker plots show β-catenin concentration in various study groups. The line inside the box represents the mean, whereas the bottom and top lines of the box show the 25th and 75th percentiles, respectively. The whiskers below and above the box show the minimum and maximum values, respectively.

ALC vs cART, ALC+cART, DBT+ALC, DBT+cART+ALC (p=0,985, p<0,001, p=0,998and p<0,001, respectively);cART vs ALC+cART, DBT+cART, DBT+cART+ALC (p<0,001, p=0,987, p<0,001, respectively); DBT vs ALC, cART, DBT+ALC, DBT+cART, DBT+cART+ALC (p=0,998, p=0,998, p=0,498, p=0,999 and p<0,001, respectively); DBT+ALC vs DBT+cART, DBT+cART+ALC (p=0,835, p<0,001, respectively).

ALC, alcohol; cART, combination antiretroviral treatment; ALC+cART, alcohol and cART; DBT, diabetic; DBT+ALC, diabetes and alcohol; DBT+cART, diabetes and cART; DBT+ALC+cART, diabetes, alcohol and cART.

4.3 DISCUSSION

This chapter evaluates the influence of alcohol and combination antiretroviral treatment on bone regulating hormones in diabetic Sprague Dawley rats.

Calcitonin and parathyroid hormone

Calcitonin protects the skeleton from calcium loss by inhibiting osteoclast activity (Keller et al., 2014). In contrast to the action of parathyroid hormone, calcitonin increases the deposition of calcium in bone and lowers the level of calcium in the blood. Calcitonin levels increase only briefly during acute and short-term alcohol consumption (Sampson, 1998). In the present study, a low dose alcohol (10% v/v), alcohol ALC alone or with antiretroviral treatment (ALC+cART) had low calcitonin concentration. The low calcitonin concentration was due low alcohol which did not have any harmful effect on bone, hence a low calcium deposition in bone and in the serum. The fact that antiretroviral treatment alone (cART) did not influence calcitonin concentration in the present study suggests that the low concentration of calcitonin in the ALC+cART was due to alcohol. Alcohol had interfered with action of cART.

Diabetes (DBT) did not change serum calcitonin concentrations in the current study. This is like the report of (Lunati et al., 2016) who also found no change in calcium among diabetic patients. However, in the present study, calcitonin concentration was low in rats that were diabetic and receiving cART (DBT+cART) or among diabetic rats that received both ALC and cART (DBT+ALC+cART). Since the ALC+cART group in the present study showed low serum calcitonin concentration, these low levels detected in the diabetic rats that received both ALC and cART (DBT+ALC+cART) can be attributed to the effects of combining alcohol and cART.

The liver metabolizes both alcohol and antiretroviral drugs, and when these two compounds combine, liver function is compromised, and the antiretroviral does not work well, and the risk of serious toxicity from antiviral therapy increases (Yu et al., 2021).

Studies investigating the influence of alcohol on parathyroid hormone levels have yielded conflicting results. Some studies have found a decrease in parathyroid hormone levels in alcoholics (Ilich et al., 2002), while most studies have not reported a significant change in parathyroid hormone levels due to alcohol consumption (Andersen et al., 2018). In the present study, parathyroid hormone remained unchanged in the ALC group. This is consistent with the findings of (Andersen et al., 2018) who reported that alcohol did not impair parathyroid hormone secretion. Although alcohol alone (ALC) or cART alone did not alter the serum parathyroid hormone concentration, a combination of the two (ALC+cART) resulted in elevated parathyroid hormone concentration. This group had low calcitonin concentration. Parathyroid hormone increases calcium levels, while calcitonin decreases calcium levels. Parathyroid hormone increases serum calcium levels by activating osteoclastic cells and absorbing calcium into the kidneys. Calcitonin reduces calcium levels by inhibiting osteoclasts (Babić Leko et al., 2021).

In the present study, the diabetic rats (DBT), diabetic rats taking alcohol (DBT+ALC) or taking both alcohol and combination antiretroviral therapy (DBT+ALC+cART) all had lower serum parathyroid hormone concentration than the untreated group. This may be attributed to parathyroid hormone secretion impairment in untreated diabetes mellitus (Paula et al., 2001). While it is not fully comprehended how diabetes affects parathyroid hormone, other researchers rule out the idea that glucose itself directly regulates parathyroid hormone

secretion (Sass et al., 2020). It remains unclear why cART in diabetics (DBT+cART) or when taken with alcohol (ALC+cART) caused an elevation in parathyroid hormone concentration.

Sclerostin

Sclerostin acts as inhibitor of bone formation by inhibiting the Wnt signaling pathway. Mechanical loading in rats and mice reduces sclerostin levels leading to greater bone formation (Shaw and Högler, 2012). Sclerostin remained unchanged in the alcohol (ACL) group. This is contrary to previous research in humans which showed elevated sclerostin concentration among heavy drinkers (Martin-Gonzalez et al., 2023). These authors attribute the high elevated sclerostin concentration among heavy drinkers to liver damage. While no liver tests were performed in the present that, it is likely that the alcohol intake was below the threshold for heavy drinking, hence no increase in sclerostin.

The present study detected a significantly higher levels of serum sclerostin in rats subjected to various combinations of alcohol, CART or diabates (ALC+cART, DBT+cART and DBT+ALC). Antiretroviral therapy (Chwiki et al., 2017) and diabetes (Mohamed et al., 2016; Dangarembizi et al., 2020), individually, adversely affect the liver. Therefore, it is possible that, like the case with alcohol, the elevated serum concentration could be a result of liver damage. However, the diabatic rats that received both alcohol and cART (DBT+ALC+cART) had normal sclerostin levels. This aspect requires further investigation.

Osteocalcin

In the present study, the diabetic only (DBT) and the diabetic rats taking alcohol (DBT+ALC) were the only 2 groups that showed elevated osteocalcin concentration.Circulating undercarboxylated osteocalcin is a predictor of type 2 diabetes (Riquelme-Gallego et al.,

2020). Osteocalcin has shown that it can improve the functioning of pancreatic and fatty tissue and the metabolic, inflammatory, and oxidative parameters that all are affected with diabetes (Desentis-Desentis et al., 2020).

Alcohol decreases the serum levels of osteocalcin (Watt et al., 2019). In contrast, the present study showed no significant lowering of serum osteocalcin concentration in groups receiving alcohol. cART is reported to increase osteocalcin levels (Ofotokun et al., 2016). In this study, cART alone, with alcohol (cART+ALC), in diabetic rats (DBT+cART) and in diabetic rats taking alcohol (DBT+ALC+cART) did not significantly change the serum concentration of osteocalcin.

β-catenin

In the present study the alcohol group had low serum β-catenin concentration. This is consistent with the scientific literature which shows that chronic high-dose ethanol exposures inhibit Wnt/β-catenin signalling pathway (Xu et al., 2015). Low serum β-catenin concentration was also detected in the diabetic group (DBT). This finding is consistent with previous research which report that serum concentrations of catenin in type 2 diabetes patients are lower than those of control patients (Gaudio et al., 2012). A similar finding of low catenin concentration was made when among diabetic rats taking alcohol (DBT+ALC). This shows that alcohol or diabetes inhibit β-catenin among those taking alcohol individually or in diabetics, as well as when diabetic rats consume alcohol. The present study also found low serum catenin concentration catenin in the cART group. This finding is consistent with the previous research reporting that the Wnt/β-catenin signalling pathway is supressed in antiretroviral treatment (Modarresi et al., 2009). In the present study, cART used among diabetics also showed low serum catenin concentration. However, using alcohol with cART (ALC+cART) or the

comorbidity of diabetes, alcohol, and cART use (DBT+ALC+cART) did not change serum catenin concentration, suggesting that this comorbidity may not influence this hormonal level and therefore it function.

4.3.1 conclusions

This study found that serum parathyroid hormone and calcitonin concentrations were low in rats that were diabetic and taking and cART (DBT+cART) or diabetic rats taking both alcohol and cART (DBT+ALC+cART). This shows that the combined effects diabetes with concurrent alcohol intake and while using cART causes derangement of the hormone profile parathyroid hormone and calcitonin. However, sclerostin, osteocalcin and catenin levels were unaffected by diabetes with concurrent alcohol intake and while using cART (DBT+ALC+cART). This is an aspect that requires further investigation. It is possible that other mechanisms could be at play to maintain homeostasis of theses hormones.

Chapter 5

Mandibular microstructural alterations from combination antiretroviral therapy and concurrent alcohol intake in the diabetic Sprague Dawley rat

This chapter was published in the internation journal of morphology as:

"Mandibular trabecular morphometry and tensile strength assessment in the diabetic Sprague Dawley rat mandible consuming alcohol".

The article will be published in Int J Morph, issue 6, volume 42, 2024

5.0 INTRODUCTION 80
5.1 MATERIALS AND METHODS 82
5.1.1 Animal housing 82
5.1.2 Group allocation and treatment of animals 82
5.1.3 Termination procedures 82
5.1.4 Three-Dimensional Microfocus X-ray Computed Tomography (MicroCT) 82
5.1.5 Tensile strength test (3-point bending) 83
5.1.6 Data analysis 84
5.2 RESULTS 85
Bone volume to fraction (BV/TV) 85
Trabecular thickness (TbTh) 86
Trabecular number (TbN) 86
Trabecular spacing (TbSp) 86
5.2.2 Tensile strength 88
Mean maximum force 88
Mean break force 88
Mean displacement 89
Mean time 89
5.2.3 Discriminant function analysis 93
5.3 DISCUSSION 96
5.3.1 CONCLUSIONS 99

5.0 INTRODUCTION

Lifestyle diseases such as diabetes are increasingly becoming common, and in countries such as South Africa, high levels of human immunodeficiency virus (HIV) infection (Gutreuter et al., 2019) and alcohol abuse (Parry, 2005) are common. In sub-Saharan Africa, the incidence of these three conditions (diabetes, antiviral therapy, and alcohol abuse) among individuals is on the rise and constitutes a serious health challenge. Individually, diabetes (Romero-Díaz et al., 2021), cART (Delpino and Quarleri, 2020), and alcohol abuse (Godos et al., 2022) are associated with skeletal pathology. Studies have linked diabetes to osteoporosis and increased bone fracture risk (Lin et al., 2021).

Furthermore, chronic and excessive alcohol consumption has not only contributed to the increase in HIV infections due to poor judgment, multiple sexual exposures and poor lifestyle choices (Shuper et al., 2010), but also exacerbates type 2 diabetes (Kao et al., 2001; Kim and Kim, 2012). Consequently, alcohol abuse is not only indirectly increasing enrollment in antiretroviral therapy regimens, but also producing excess calories that promote hyperglycemia and subsequently lead to obesity and disease of carbohydrate and glucose metabolism (Shah and Hill, 2021). In the longer term, insulin secretion is impaired and insulin sensitivity decreases (Kao et al., 2001; Kim and Kim, 2012). Furthermore, cART therapy is associated with metabolic deregulation and is characterized by dyslipidemia and insulin resistance (Molina et al., 2014; Honnapurmath and Patil, 2017). This exacerbates diabetes and increases the risk of osteoporosis and bone fracture (Lin et al., 2021).

Osteoporosis can lead to periodontal bone loss and eventual loss of teeth, which may require dental implants as a treatment option (Esfahanian et al., 2012). The viability of dental implants is dependent on the amount of cortical and trabecular bone present, and the formation of new bone (Porter and von Fraunhofer, 2005a). The implant tends to fail due to lack of osseointegration in individuals suffering from conditions that enhance bone degeneration, such as osteoporosis (Beikler and Flemmig, 2003; Stevenson et al., 2007; Hasegawa et al., 2008; Yarramsetty et al., 2023).

Alcohol, diabetes, and combination antiretrovirals (cART) have been shown to reduce bone strength. It is not known how the multimorbidity of Type 2 diabetes; excessive alcohol intake and cART therapy affect periodontal bone. Therefore, the current study sought to investigate the combined effect of Type 2 diabetes, excessive alcohol intake, and cART therapy on the mandible using Sprague-Dawley rats as a model. The study used Microfocus X-ray Computed Tomography (MicroCT) to determine possible microstructural alterations and evaluated mandibular trabeculae morphometry such as bone volume fraction (BV/TV), trabecular thickness (TbTh), spacing (TbSP), and number (TbN) were evaluated. Additionally, the tensile strength was tested using a universal tensile tester. Further, the parameters that are most affected by this multimorbidity were identified using discriminant function analysis (DFA).

5.1 MATERIALS AND METHODS

5.1.1 Animal housing

Animal husbandry was as described under section 3.2.2 (Animal husbandry)

5.1.2 Group allocation and treatment of animals

The animal animals were assigned into various groups as described in section 3.2.3 (group allocation). The induction of diabetes, administration of alcohol and cART are all described under section 3.2.4.(treatment of animals).

5.1.3 Termination procedures

At the end of 12 weeks, the animals were deeply anaesthetised with pentobarbitone, and blood samples were collected by cardiac puncture in serum separating tubes (4ml). The mandible was meticulously dissected, bisected into left and right hemimandibles, and fixed in 10% buffered formalin for further analysis.

5.1.4 Three-Dimensional Microfocus X-ray Computed Tomography (MicroCT)

A Nikon XTH 225/320 LC X-ray microtomography was used to scan the mandibles for computed tomography. To keep the samples steady during scanning, the bones were secured in oasis floral foam and positioned on the 360° rotating sample manipulator. The X-ray settings were standardised to a source voltage of 70kV and a source current of 400µA and four-frame average were used to improve the signal to noise ratio. Both hemimandibles from each rat were scanned at a resolution of 18µm. The volume Graphics® 3.2 software was then used for analysis of the following parameters: bone volume fraction (BV/TV), trabecular

thickness (TbTh), spacing (TbSP) and number (TbN). The region of interest (ROI) chosen was based on Lerouxel et al., 2004 report. Region of interest (ROI) was defined as the distance from the start point set on the mesial surface of the first molar (M1) and the end point set at the distal surface of the third molar (M3) (Fig. 5.1).

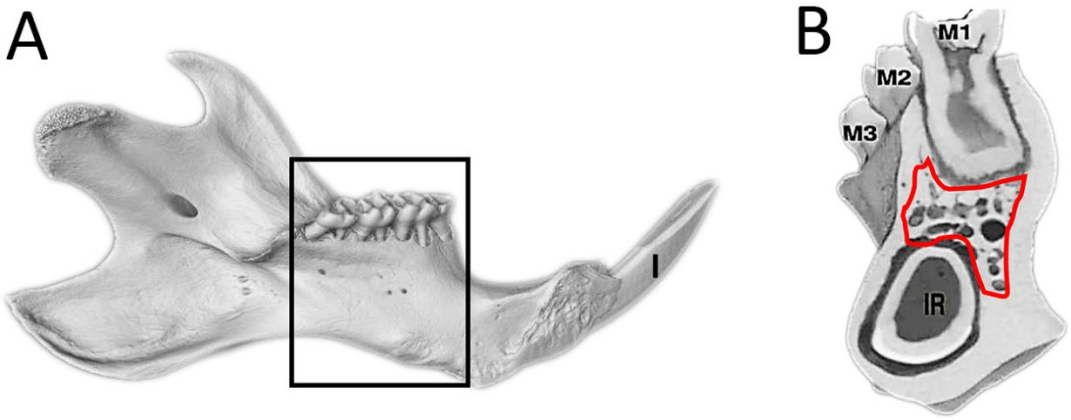

Fig. 5.1: Region of interest (ROI). A three-dimensional rendering of the rat hemimandible. The boxed area shows a mediolateral view of the ROI. B: Cross-sectional anteroposterior view of the mandible showing the ROI (red-bounded area). I, incisor tooth; IR, incisor root; M1 M2 M3, molar teeth.

5.1.5 Tensile strength test (3-point bending)

A Shimadzu universal test machine was used to measure mandibular tensile strength (EZ-X S 200V E SSM346-57320-44, Shimadzu, Honeydew, South Africa). To do this, the left hemi-mandibles with the lingual side facing up, were placed on two rounded bars set at 15mm apart and the load was applied. The load-displacement curves were then recorded at 3mm/min until failure.

5.1.6 Data analysis

Data were managed in Microsoft Excel, Office 365 (Microsoft Corporation®) and analysed using SPSS® version 28 (IBM®). ANOVA with Tuckey post hoc was used for multiple group comparisons of means for the tensile strength and trabecular morphometric parameters. The parameters that are the most disrupted in all groups were identified using discriminant function analysis (DFA). The parameters that are most disrupted were identified using DFA. The results were represented as means and standard deviation. The significance level was established at a confidence interval of $p < 0.05$.

5.2 RESULTS

5.2.1 Trabecular bone morphometric parameters

Bone volume to fraction (BV/TV)

The ALC, DBT+cART+ALC, and DBT+cART groups had the smallest bone to total volume ratio (BV/TV) which were significant compared to the untreated group ($p \leq 0.001$, $p=0.004$ and $p=0.035$, respectively). In contrast, the bone volume fraction (BV/TV) in the cART, ALC+cART, DBT and DBT+ALC had similar values to the untreated group ($p=0.433$, $p=0.621$, $p=0.474$ and $p=0.548$, respectively) (Table 5.1),bone volume fraction (BV/TV), trabecular thickness (TbTh), spacing (TbSP) and number (TbN).

Regarding alcohol effects, the ALC group had the smallest BV/TV, which was significant compared to cART, ALC+cART, DBT, DBT+ALC, DBT+cART ($p \leq 0.001$, for all comparisons, except for DBT and cART ($p=0.017$). However, no significant differences were detected between the ALC and DBT+cART+ALC group ($p=0.147$) (Table 5.1). Although the cART group had a similar BV/TV to that of the DBT and DBT+ALC groups ($p=0.142$ and $p=0.186$, respectively), it was significantly higher than the DBT+cART+ALC group ($p=0.023$). ALC + cART had a higher BV/TV than the DBT+cART+ALC group ($p=0.020$).

There were differences between the treatment groups, with the DBT+cART and DBT+cART+ALC groups having significantly lower BV/TV than the DBT group ($p=0.007$ and $p=0.001$, respectively). On the contrary, DBT+ALC showed similarities with the DBT group ($p=0.934$) (Table 5.1).

Trabecular thickness (TbTh)

None of the study groups showed significant differences in comparison to the untreated ($p>0.05$) (Table 5.1). ALC showed similar TbTh to all groups except the DBT group which had higher values ($p=0.022$). The DBT group had significantly thicker trabeculae than the cART, DBT+cART and DBT+cART + ALC groups ($p=0,023$, $p=0.008$ and $p=0.013$, respectively)

Trabecular number (TbN)

The DBT+cART+ALC and DBT+cART groups exhibited significantly more trabeculae (TbN) than the untreated group ($p<0.001$, for both comparisons). No other groups showed significant differences in comparison to the untreated group ($p>0,05$) (Table 5.1).

There were differences in TbN among the treatment groups, with the ALC group exhibiting significantly less trabeculae than the DBT+cART and DBT+cART+ALC groups ($p<0.001$, for both comparisons). Regarding the treatment with cART, this group showed fewer trabeculae than the DBT+cART group and DBT+cART + ALC ($p<0.001$ and $p=0.001$, respectively). When considering diabetes, the DBT group exhibited significantly fewer trabecula than the DBT+cART and DBT+cART+ALC groups ($p<0.01$, for both comparisons) (Table 5.1). The DBT+ALC group showed fewer trabeculae than the DBT+cART and DBT+cART+ALC groups ($p<0.001$ and $p=0.002$, respectively) (Table 5.1).

Trabecular spacing (TbSp)

None of the study groups showed any significant differences in the trabecular spacing (TbSp) when compared to the untreated group ($p>0.05$) (Table 5.1). Furthermore, all other group comparisons showed similarities except for the smaller trabecular spacing (TbSp) exhibited in the DBT group compared to the DBT+ALC and ALC groups ($p=0.035$, $p=0.053$, respectively).

Table 5.1: Trabecular morphometric parameters.

	Untreated		ALC		cART		ALC+cART		DBT		DBT+ALC		DBT+cART		DBT+cART+ALC	
Parameter	**Mean**	**SD**	**Mean**	**SD**	**Mean**	**SD**	**Mean**	**SD**	**Mean**	**SD**	**Mean**	**SD**	**Mean**	**SD**	**Mean**	**SD**
N	16		16		16		14		14		12		14		12	
[a]BV/TV	58.13	4.96	67.50	4,89	59.69	5,59	59.14	8,08	56.65	4,61	56.83	7,28	62.50	5,47	64.37	1,96
*p value			p≤0.001		0,433		0,621		0,474		0,548		0,035		0,004	
[b]TbTh	0,45	0,09	0,39	0,06	0,39	0,1	0,43	0,29	0,67	0,89	0,47	0,17	0,33	0,03	0,34	0,02
*p value			0.615		0,610		0.634		0.068		0,925		0,352		0,398	
[c]TbN	2,00	0,26	2.00	0.26	2,09	0,09	2,15	0,45	2,02	0,27	2,09	0,49	2,58	0,19	2,47	0,16
*p value			0.503		0,394		0,155		0,691		0,873		p≤0.001		P=0.001	
[d]TbSp	0.06	0.02	0,10	0,02	0,06	0,03	0,06	0,03	0,05	0,02	0,11	0,25	0,06	0,02	0,07	0,01
*p value			0,142		0,969		0,932		0,602		0,091		0,924		0,682	

[a]BV/TV: ALC vs cART, ALC+cART, DBT+ALC (p<0.001 for all), DBT+cART+ALC (p=0.147); cART vs ALC+cART, DBT+cART, DBT+cART+ALC (p=0.791, p=0.174 p=0.031, respectively); DBT vs ALC, cART, DBT+ALC, DBT+cART, DBT+cART+ALC (p<0.001, p=0.142, p=0.934, p=0.012 and p=0.001, respectively); DBT+ALC vs DBT+cART, DBT+cART+ALC (p=0.012, p=0.001, respectively).

[b]TbTh: ALC vs cART, ALC+cART, DBT+ALC, DBT+cART+ALC (p=0.978, p=0.657, p=0.575 and p=0.764, respectively); cART vs ALC+cART, DBT+cART, DBT+cART+ALC (p=0.784, p=0.637, p=0.686, respectively); DBT vs ALC, cART, DBT+ALC, DBT+cART, DBT+cART+ALC (p=0.022, p=0.023, p=0.107, p=0.008 and p=0.013, respectively); DBT+ALC vs DBT+cART, DBT+cART+ALC (p=0.339, p=0.380, respectively).

[c]TbN: ALC vs cART, ALC+cART, DBT+ALC, DBT+cART+ALC (p=0.854, p=0.436, 0.873 and p=0.001, respectively); cART vs ALC+cART, DBT+cART, DBT+cART+ALC (p=0.992, p<0.001, p=0.001, respectively); DBT vs ALC, cART, DBT+ALC, DBT+cART, DBT+cART+ALC (p=0.802, p=0.669, p=0.698, p<0.001 and p<0.001, respectively); DBT+ALC vs DBT+cART, DBT+cART+ALC (p<0.001, p=0.002, respectively).

[d]TbSp: ALC vs cART, ALC+cART, DBT+ALC, DBT+cART+ALC (p=0.159, p=0132, p=0.740 and p=0.338, respectively); cART vs ALC+cART, DBT+cART, DBT+cART+ALC (p=0.903, p=0.956, p=0.715, respectively); DBT vs ALC, cART, DBT+ALC, DBT+cART, DBT+cART+ALC (p=0.053, p=0.581, p=0.035, p=0.0550 and p=0.379, respectively); DBT+ALC vs DBT+cART, DBT+cART+ALC (p=0.120, p=0.228, respectively).

∗ Comparison of respective groups with the untreated group. ALC, alcohol; cART, combination antiretroviral treatment; ALC+cART, alcohol and cART; DBT, diabetic; DBT+ALC, diabetes and alcohol; DBT+cART, diabetes and cART; DBT+ALC+cART, diabetes, alcohol and cART.

5.2.2 Tensile strength

Mean maximum force

The DBT, DBT+cART, DBT+CART+ALC and ALC+cART group showed the lowest values for maximum force which were significant compared to the untreated group ($p<0.001$, p=0,001, p=0,014 and p=0.013, respectively). No other groups exhibited significant differences from the untreated group ($p>0.05$) (Table 5.2).

The ALC group had similar mean value to the cART and ALC+cART treated groups (p=0.702 and p=0.217, respectively) but showed a significantly higher value than the DBT and DBT+cART groups ($p\leq0.001$ and p=0.034, respectively). The cART group had a significantly higher maximum force than the DBT and DBT+cART group ($p<0.001$ and p=0.013, respectively). DBT showed a lower significant value than the ALC+cART, the DBT+ALC and DBT+cART+ALC groups (p=0.011, $p<0.001$ and p=0.017, respectively). The DBT+ALC group exhibited a significantly higher maximum force than the DBT+cART treated group (p=0.039) (Table 5.2).

Mean break force

DBT, DBT+cART and DBT+cART+ALC, ALC+cART treated groups exhibited lower breaking force than the untreated group ($p<0.001$, p=0.001, 0.013, and p=0.010, respectively) (Table 2). On the contrary, the ALC, cART, and DBT+ALC treated groups did not show statistical differences from the untreated group (p=0.119, p=0.346, and p=0.256, respectively) (Table 2).

The ALC group was similar to the cART and ALC+cART groups (p=0.534 and p=0.278, respectively). However, the ALC group had a significantly higher break force than the DBT

(p≤0.001). The cART group had a significantly higher breaking force than the DBT and DBT+cART treated groups (p<0.001 and p=0.011, respectively) (Table 5.2).

The DBT group required significantly less force to fracture than the DBT+ALC or DBT+ALC+ALC treated groups, and but DBT+ALC+ALC groups were similar (p<0.001 and p=0.014, respectively. The DBT+ALC group exhibited a significantly higher break force than DBT+cART (p=0.034) (Table 5.2).

Mean displacement

Lower displacement values were recorded among the DBT+cART+ALC, DBT+ALC and DBT treated groups compared to the untreated group (p≤0.001, p=0.001, p=0.001, p=0.007, respectively) (Table 5.2). No other groups showed significant differences in comparison to the untreated group. The ALC or ALC + cART groups only showed significantly higher displacement compared to the DBT+ cART+ALC group (p=0.001, p=0.003, respectively). Regarding cART, this group had a higher displacement than the DBT+cART+ALC, DBT+ALC, DBT and DBT+cART groups (p<0.001, p=0.001, p=0.006 and p=0.045, respectively) (Table 5.2).

Differences in displacement between treatment groups were noted, with the DBT+cART+ALC group which showed a significantly lower value than DBT+cART and DBT (p=0.006 and p =0,031) (Table 5.2)

Mean time

The DBT+cART+ALC, DBT+ALC and DBT treated groups required the shortest time to fracture the mandible which was significant compared with the untreated group (p<0.001, p=0.003

and p=0.006, respectively). No other groups showed significant differences in comparison to the untreated group (p<0.05) (Table 5.2).

The ALC group showed significantly more time to fracture than the DBT+cART+ALC group (p=0.001). The cART group required more time to fracture than the DBT+CART+ALC, DBT+ALC, DBT, DBT+cART, and ALC+cART groups (p<0.001, p=0.001 and p=0,002, p=0,041 and p=0,050, respectively). The ALC+cART group and the DBT+cART groups had significantly more fracture time than the DBT+cART+ALC group (p=0.003, p=0.006) (Table 5.2).

Mean stiffness

The mean stiffness among the treatment groups showed a varied pattern compared to the untreated group, with the DBT group exhibiting less stiffness than the untreated group (p=0.006). In contrast, the DBT+cART+ALC group showed a greater stiffness value compared to the untreated group (p=0.009). No other groups showed significant differences in the were detected in comparison with the untreated group (p<0.05) (Table 5.2).

Regarding alcohol administration, ALC treatment showed similar stiffness to cART, ALC+cART groups (p=0.464 and p=0.290, respectively). On the contrary, the ALC group had respectively significantly higher and lower stiffness than the DBT and DBT+cART+ALC groups (p= 0.008 and p=0.006). When antiretroviral therapy was included, the ALC+cART group showed a lower value than the DBT+cART + ALC group and the DBT+ALC groups (p<0.001 and 0.013) (Table). Administration of cART alone exhibited a higher stiffness than the DBT and DBT+ALC groups (p=0,049 and p=0,007. In contrast, cART had significantly higher stiffness than the DBT+cART+ALC group (p=0.001) (Table 5.2).

There were differences in stiffness observed between the treatment groups. With respect to diabetes, the DBT group had significantly less stiffness than the DBT+ALC, DBT+cART+ALC and DBT+cART groups ($p<0.001$, $p<0.001$ and 0,049, respectively) (Table 5.2).

Table 5.2. Tensile strength parameters from 3-point bending tests.

	Untreated		ALC		cART		ALC+cART		DBT		DBT+ALC		DBT+cART		DBT+cART+ALC	
Parameter	**Mean**	**SD**	**Mean**	**SD**	**Mean**	**SD**	**Mean**	**SD**	**Mean**	**SD**	**Mean**	**SD**	**Mean**	**SD**	**Mean**	**SD**
N	16		16		16		14		14		12		14		12	
[a]Max Force(N)	117,65	34,24	104,85	31,31	108,58	33,65	92,33	22,08	71,06	25,14	106,30	22,65	83,24	24,39	91,47	25,17
p value			0,191		0,353		0,013		<0,001		0,273		0,001		0,014	
[b]Break Force (N)	117,65	34,24	102,60	29,16	108,58	33,65	91,80	21,11	72,66	27,43	105,83	22,65	82,99	24,61	91,47	25,17
p value			0.119		0.346		0.010		<0,001		0.256		0,001		0,013	
[c]Displacement (mm)	2,08	0,43	1,84	0,22	2,10	0,55	1,81	0,22	1,69	0,29	1,58	0,42	1,79	0,22	1,34	0,61
p value			0,083		0,907		0,068		0,007		0,001		0,057		<0,001	
[d]Time (sec)	40,81	7,43	36,70	4,45	41,97	11,10	36,26	4,31	33,02	6,40	31,52	8,45	35,76	4,47	26,70	12,26
p value			0.143		0.678		0.118		0.006		0.003		0.096		p≤0.001	
[e]Stiffness (N/mm)	59,61	19,08	58,79	21,20	53,79	16,93	51,28	13,36	43,86	15,61	70,36	18,77	49,71	14,03	79,33	33,10
p value			0,905		0,395		0,241		0,006		0,148		0,182		0,009	

[a]Max force: ALC vs cART, ALC+cART , DBT+ALC, DBT+cART+ALC (p=0.702, p=0.217, p=0.890, p=0.206); cART vs ALC+cART, DBT+cART, DBT+cART+ALC (p=0.110, p=0.013 p=0.106, respectively); DBT vs ALC, cART, DBT+ALC, DBT+cART, DBT+cART+ALC (p<0,001, p=0.87, p<0,001, p=0.087 and p=0.017, respectively); DBT+ALC vs DBT+cART, DBT+cART+ALC (p=0.036, p=0.190, respectively).

[b]Break force (N): ALC vs cART, ALC+cART , DBT+ALC, DBT+cART+ALC (p=0.534, p=0.278, p=0.755 p=0.284, respectively); cART vs ALC+cART, DBT+cART, DBT+cART+ALC (p=0.093, p=0.011 p=0.101, respectively); DBT vs ^ALC, ^cART, ^DBT+ALC, DBT+cART, DBT+cART+ALC (^p<0,001, p=0.078 and p=0.014, respectively); DBT+ALC vs DBT+cART, DBT+cART+ALC (p=0.036, p=0.190, respectively).

[c]Displacement: ALC vs cART, ALC+cART , DBT+ALC , DBT+cART+ALC (p=0.064, p=0.880, p=0.092, p=0,001, respectively); cART vs ALC+cART, DBT+cART, DBT+cART+ALC (p=0.053, p=0.045 p<0.001, respectively); DBT vs ALC, cART, DBT+ALC, DBT+cART, DBT+cART+ALC (p=0.286, p=0.005, p<0.515, p=0.482and p=0.031, respectively); DBT+ALC vs DBT+cART, DBT+cART+ALC (p=0.193, p=0.142, respectively).

[d]Time: ALC vs cART, ALC+cART , DBT+ALC, DBT+cART+ALC (p=0.064, p=0.880, p=0.092, p=0.001, respectively); cART vs ALC+cART, DBT+cART, DBT+cART+ALC (p=0.053, p=0.045p<0.001, respectively); DBT vs ALC, cART, DBT+ALC, DBT+cART, DBT+cART+ALC (p=168, p=0.002, p=0.515, p=0482 and p=0.031, respectively); DBT+ALC vs DBT+cART, DBT+cART+ALC (p=0.191, p=137, respectively).

[e]Stiffness: ALC vs cART, ALC+cART , DBT+ALC, DBT+cART+ALC (p=0.464, p=0.290, p=0.119, p=0006, respectively); cART vs ALC+cART, DBT+cART, DBT+cART+ALC (p=0.724, p=0.581p=0.001, respectively); DBT vs ALC, cART, ^DBT+ALC, DBT+cART, ^DBT+cART+ALC (p=0.008, p=0.049, ^p<0,001, p=0.192, respectively); DBT+ALC vs DBT+cART, DBT+cART+ALC (p=0.010, p=0.257, respectively).

∗ Comparison of respective groups with the untreated group; ^ identical value against the comparing group. ALC, alcohol; cART, combination antiretroviral treatment; ALC+cART, alcohol and cART; DBT, diabetic; DBT+ALC, diabetes and alcohol; DBT+cART, diabetes and cART; DBT+ALC+cART, diabetes, alcohol and cART.

5.2.3 Discriminant function analysis

A discriminant function analysis was performed to predict the correct study animal group placement. The structure matrix indicated that displacement, break force, maximum force, time, stiffness, TbN, and TbSp could distinguish the degree of effect of the treatment amongst the study groups (Table 5.3).

Table 5.3: Discriminant function analysis of the mandible. The contributing variables are arranged in descending order based on Function 1, with major contributors (≥ ±0.3) in bold.

Structure Matrix			
Parameter	**Function**		
	1	2	3
	43.9%	28.2%	14.9%
TbN	**0,592**	**-0,151**	**0,6**
Displacement	**-0,504**	**0,472**	**0,417**
Time	**-0,485**	**0,492**	**0,412**
Stiffness	**0,472**	**0,384**	**-0,539**
ThSp	0,071	0,093	-0,415
Breakforce	-0,053	**0,787**	-0,203
Maximum force	-0,058	**0,767**	-0,228
TbTh	-0,185	-0,259	-0,089

The discriminant analysis yielded seven functions, although the Wilk's lambda results exhibited a good fit for functions 1, 2 and 3, Wilk's lambda = 0.218, 0.401 for Functions 1 and 2 ($p<0.001$) and 0.617 for function 3 ($p=0.015$). Functions 1 and 2 accounted for the greatest variability (43.9% and 28.2%, respectively). The cross-validated classification showed that overall, 35.1% of mandibles were correctly classified according to their groups (Table 5.4). The model correctly classified 37% of the mandibles as belonging to the untreated group, ALC (25%), cART (6.3%), ALC+cART (35.7%), DBT (42.9%), DBT+ALC (8.6%), DBT+cART (78.6%) and

DBT+cART+ALC (50%). The centroids of the group for the untreated and cART were in proximity, as well as the ALC and ALC+cART groups (Fig. 5.2).

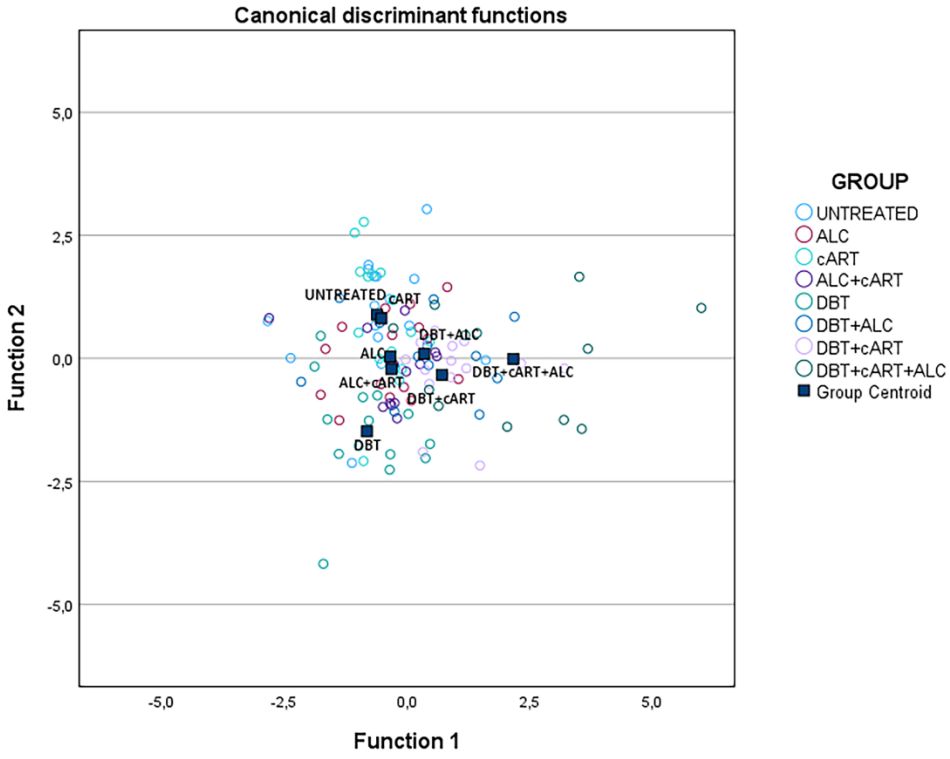

Fig. 5.2 Group membership discrimination

Table 5.4: Group membership classification

Group			Predicted Group Membership							
			UNTREATED	ALC	cART	ALC+cART	DBT	DBT+ALC	DBT+cART	DBT+cART+ALC
Cross-validated	Count	UNTREATED	6	0	5	0	3	1	0	1
		ALC	2	4	1	5	1	3	0	0
		cART	7	0	1	6	1	1	0	0
		ALC+cART	2	1	1	5	2	0	3	0
		DBT	2	1	1	2	6	1	1	0
		DBT+ALC	2	2	0	2	1	1	1	3
		DBT+cART	0	0	0	1	0	0	11	2
		DBT+cART+ALC	0	0	1	0	0	1	4	6
	%	UNTREATED	**37,5**	,0	31,3	,0	18,8	6,3	0	6,3
		ALC	12,5	**25,0**	6,3	31,3	6,3	18,8	0	0
		cART	43,8	,0	**6,3**	37,5	6,3	6,3	0	0
		ALC+cART	14,3	7,1	7,1	**35,7**	14,3	,0	21,4	0
		DBT	14,3	7,1	7,1	14,3	**42,9**	7,1	7,1	0
		DBT+ALC	16,7	16,7	0	16,7	8,3	**8,3**	8,3	25,0
		DBT+cART	,0	0	0	7,1	0	0	**78,6**	14,3
		DBT+cART+ALC	,0	0	8,3	0	0	8,3	33,3	**50,0**

35,1% of cross-validated grouped cases correctly classified.

5.3 DISCUSSION

The main objective of the study was to assess the effect of concurrent alcohol intake and cART treatment on the trabecular morphology and tensile strength of the diabetic rat mandible. The internal bone microarchitecture was assessed from the data obtained using MicroCT. The results found that altered trabecular parameters and tensile strength were negatively impacted using 3-point bending tests and confirmed by discriminant function analysis. This makes a first contribution into how concurrent alcohol intake and cART treatment affect the mandible in diabetic rats.

Aspects of bone trabecular morphometric parameters

In this study, we found that BV/TV and TbN in the DBT+cART and DBT+cART+ALC groups were significantly higher than untreated controls. These groups had poor bone strength parameters, suggesting weaker bones, and consistent with a previous report (Jindal et al., 2018)suggesting that bone quality is a better predictor of bone strength than bone quantity. In the present study, the ACL group had much more BV/TV. This is contrary to another study which have revealed that trabecular morphological parameters have been changed by alcohol (Frazão et al., 2020). It is possible that the amount of alcohol used in this study was lower than the threshold. Low to moderate alcohol consumption leads to increased bone mineral density, and heavy alcohol consumption affects bone mineral density (Godos et al., 2022; LeBoff et al., 2022). Furthermore, this study allowed unlimited access to rodent diets that could have provided adequate nutrition. Alcohol addicts are known for poor diet (Mutuli et al., 2020).

Factors most affected in diabetics with cART treatment and alcohol consumption

The DBT+cART group was correctly classified in more than 78% of the cases using the DFA model. This was followed by the DBT+cART+ALC group, which was correctly classified in half the samples. This means that the parameters considered in the present study differed distinctly for these two groups compared to the rest of the study groups. Therefore, it can be deduced that cART among diabetics as well as concomitant alcohol use had the most severe consequences. These two groups had more TbN than the controls but performed poorly in the tensile test parameters. This suggests that the number of trabeculae may have been high, but with poor bone quality or strength. Therefore, trabeculae number may not be a good determinant of bone quality and/or strength.

The cART group was largely similar to the untreated group, as shown by the group centroids occupying the same spot in the DFA graph. Furthermore, 31% of cART mandibles were misclassified as belonging to the untreated group. This suggests that cART alone may not have so negatively impacted the bone structure as found in a previous report (Delpino and Quarleri, 2020).

Bone tensile strength

Both the maximum and breaking force were lower in the DBT, DBT+cART, ALC+cART, and DBT+cART+ALC group than in the control. These parameters reflect how much load a bone can take before weakening, and the amount of load or force that fractures the mandible once weakened. These values were lowest in the DBT group suggesting the diabetes may have severer

effect on tensile strength than its combination morbidities. This was unexpected, as we hypothesised that ALC and cART could confound the diabetic effects on bone.

The lack of significant differences for the ALC and cART treated groups compared to the untreated controls suggests that alcohol and cART had no adverse effect on maximum and breaking force when used independently. Many studies report that alcohol is detrimental to bone health, as it weakens bone through osteoporosis in a dose dependent manner (Godos et al., 2022; Ke et al., 2023). Therefore, the alcohol dosage in the present study may have been below the threshold for statistical detectable bone deterioration. These results imply that the dose of alcohol did mask the disease drug interactions effects on bone strength indicating that alcohol dosage in the present was invaluable. While no change was seen in the cART group compared to the untreated control, others found a detrimental effect on bone (Delpino and Quarleri, 2020), interestingly, a significant reduction in maximum and breaking force recorded in combined administration of alcohol and antiretroviral therapy (ALC+cART) was observed in the present study. This may imply detrimental effects following the interaction of both drugs concomitantly present in the body. These findings corroborates a recent study in rat testes in which concurrent use of alcohol and antiretroviral therapy were shown to disturb testicular structure and function (Owembabazi et al., 2023).

The stiffness was highest among diabetic animals receiving both alcohol and antiretroviral therapy (DBT+ALC+cART), as well as in the case of diabetic animals treated with ALC (DBT+ALC) which is indicative of better ability to resist deflection under load as corroborated by the less

displacement recorded for these groups. However, these groups showed less time to fracture. This this is characteristic of bones that are both stiff and brittle, a feature observed in osteoporotic bones (Turner, 2006).

5.3.1 Conclusions

While the DBT+cART+ALC group had the highest stiffness, it was characterised by lower values for maximum force and break force, less displacement, and time to fracture, indicating stiff and brittle bones. This finding supports the hypothesis that concomitant cART and alcohol use in diabetes may result in weaker bones. The DFA plot also separated this group from the others, which confirms that these parameters are crucial in diabetes with cART and alcohol use. The high BV/TV and TbN in the DBT, DBT+cART and DBT+cART+ALC did not translate to stronger bones, therefore, the bone was of lower quality. These findings form a foundation for future research on future therapeutics and management of diabetic patients on cART, with regular alcohol intake, and particularly in dental treatments and management.

Chapter 6

Osteometry of the diabetic rat mandible treated with alcohol and combination antiretroviral therapy

6.0 INTRODUCTION 102
6.1 MATERIALS AND METHODS 105
6.1.1 Animals 105
6.1.2 Bone harvesting 105
6.1.3 Mandibular osteometry 105
6.2 RESULTS 108
6.2.1 Length of the mandible 108
Mandibular length (Cd-Id) 108
Mandibular body length (Go-Id) 109
Lingual side of the alveolar bone length (AI-Id) 109
Distance from condyle to base of the lower incisor (Cd-BI) 110
Length of the lower dental arch (M3-Id) 111
6.2.2 Height of the Mandible 115
Mandibular Ramus Height (Cd-Go) 115
Height of condylar process (Cd-Ag) 116
Height of the coronoid process (Cr-Ag) 116
Height of the central portion of the alveolar bone (AI-Me) 117
6.3 DISCUSSION 120
6.3.1 Conclusion 122

6.0 INTRODUCTION

The mandible is an important bone in the facial skeleton. It is formed by both endochrondral and intramembranous bone formation. The hyaline and fibrocartilage arises from the endochrondral bone formation. The hyaline cartilage is associated with the primary growth centre, while the fibrocartilage is associated with the secondary growth centre like the mandibular condyle, both cartilages are associated with bone growth and fracture healing (Chen et al., 2015).

The condylar process develops from the endochrondral bone formation. The endochrondral bone formation begins with the formation of a cartilaginous template within the condylar process region (Chen et al., 2015).

The undifferentiated mesenchyme cells within the cartilaginous process later differentiates to chondrocytes, these chondrocytes undergoes proliferation and hypertrophy and starts to produce type X collagen and mineralized matrix which are continuously being replaced by osteoclasts, also, osteoblasts begins to deposit osteoid along with the invasion of the cartilage by blood vessels and the mineralization of the osteoid promotes the replacement of the cartilage by bone (Chen et al., 2015).

The osseous bone formed from the mineralization of the hyaline or fibrocartilage is the cancellous or trabecular bone, the mandibular condylar bone which made up of cancellous bone undergoes growth and remodelling (from woven or lamellar bone to cancellous bone) postnatally and during early life phase leading to the development, increase in the size of the mandible and the anteroinferior displacement (transposition) of the mandible (Smartt et al., 2005; Mizoguchi et al., 2013; Chen et al., 2015).

The growth remodelling process receives supports from the primary growth centres within the condylar region/cartilage and the response to the local changes in biomechanical/

masticatory forces produced by the surrounding soft tissues including muscles (Smartt et al., 2005). The local factors includes local mediators like bone morphogenic proteins (BMP), Wnts, fibroblast growth factors (FGFs), insulin-like growth factors and systemic factors like growth hormones, thyroid hormones, androgen, vitamin D and glucocorticoids (Chen et al., 2015).

The intramembranous bone formation begins without a cartilaginous template. The mesenchyme cells proliferate and differentiates to pre-osteoblast, which later differentiate to osteoblasts (Chen et al., 2015). The osteoblasts begin to deposits osteoid which later becomes mineralized, some osteoblasts became entrapped in the mineralized osteoid matrix to become osteocytes. The mineralized bone forms the bones the body of the mandible and the cortical bones (Chen et al., 2015) and also the ramus and the alveolar process (Smartt et al., 2005).

Both the endochrondral and intramembranous bone formation including the growth of the mandible during the prenatal, postnatal and into the early life phase, are disturbed by local and systemic factors, the systemic factor include environment factors (mechanical) e.g. gestational alcohol consumption (Chen et al., 2015; Thobane et al., 2024) and biological (genetic factors) (Chen et al., 2015).

Studies have linked some systemic factors like type 2 diabetes mellitus, moderate chronic alcohol use and cART to osteoporosis, the quantitative reduction in bone size and strength, and increased bone fracture risk (Dyer et al., 1998; Maki et al., 2002; Hamann et al., 2011; Sun et al., 2015; Maurel et al., 2012; Kusy et al., 1989; Molina et al., 2008; Castronuovo et al., 2015; Hsu et al., 2016). Mandibular height, length, and general morphology are adversely

affected in osteoporosis (Rehman et al., 2017). Ndou et al., 2024 reported that type 2 diabetes affected both the osteometric and trabecular parameters of the Sprague Dawley rat femur.

In this study, measurements of the, linear length of the mandibular, and linear mandibular height were made in other to detect any changes in the dimensions of the mandibles exposed to conditions linked to osteoporosis.

6.1 MATERIALS AND METHODS

6.1.1 Animals

The animal husbandry was as described under section 3.2.2 (Animal husbandry), group allocation and the induction of diabetes, administration of alcohol and cART are all described under section 3.2.3 (group allocation) and section 3.2.4(treatment of animals), respectively.

6.1.2 Bone harvesting

The mandibles were harvested and handled as described in section 5.1.3

6.1.3 Mandibular osteometry

The measurements of linear mandibular length and linear mandibular height were taken using a digital vernier calliper (to the nearest 0.05mm), according to the method of (Maki et al., 2002). Each measurement was taken 3 times, and the average (mean) was determined to represent the value of each osteometric parameter (Tables 6.1 and 6.2) (Figs. 6.1 and 6.2).

Table 6.1: Measurements for the assessment of the linear mandibular length (mm)

3D Morphometric reference points	Description of the morphometric reference points
Cd-Id	The length of the base of the mandible which is the distance between the condyle to infradentale (labial side). This indicates the mandibular length
Go-Id	Mandibular body length is the distance between the gonion (Go) and the infradentale (Id) on the labial side. This indicates mandibular body length
Al-Id^{l}	Length of lingual side of the alveolar bone. This is the distance between the highest point of the mesial alveolar bone at the lower first molar and the infradentale (Id^{l}) on the lingual side. This indicates the alveolar bone length on the lingual side
M3-Id	Length of the lower dental arch on the labial side. This is the distance between the highest point of the central cusps of the lower third molar (M3) and the infradentale (Id) on the labial side
Cd-B1	Distance from condylar head (Cd) to the alveolar base of the lower incisor (B1). B1 indicates the alveolar base of the lower incisor

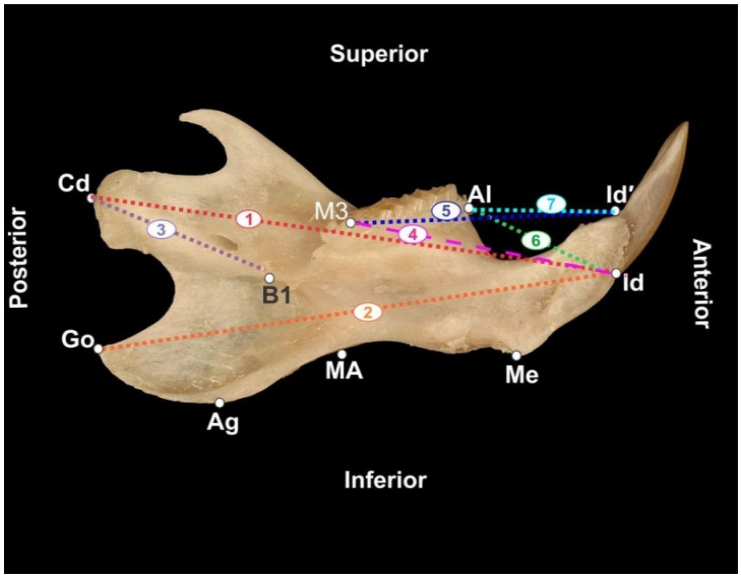

17**Figure 6.1: Morphometric reference points for the linear measurements for mandibular length.** Showing the ten morphological points from which five 3D measurements of the linear mandibular length parameters were analysed. B1 indicates the alveolar base of the lower incisor; ①Cd-Id, mandibular length; ②Go-Id, mandibular body length;③Cd-B1, distance from condyle head to the alveolar base of the lower incisor; ④M3-Id, length of the lower dental arch;⑤M3-Id', length of the lower dental arch;⑥Al-Id; length of lingual side of alveolar bone; and ⑦Al-Id′; length of lingual side of the alveolar bone, this is the distance between the highest point of the mesial alveolar bone at the lower first molar and the infradentale on the lingual side. This indicates the alveolar bone length on the labial side *(Maki, 2002)*. Cd= condyle, Id= infradentale, Go= gonoin , Al=deepest point of the outer margin of the bone, Id'= infradentale, M3= the highest point of the central cusp, Bl= base of the lower incisor. The definitions of the acronyms are given in the table (Image courtesy of Dr. I Eguavoen).

Table 6.2: Measurements for the assessment of the linear mandibular height (mm)

3D Morphometric reference	Description of the reference points
Cd-Go	Indicates mandibular ramus height which is the distance between the condyle (Cd) and the Gonion (Go). This indicates the mandibular height
Cd-Ag	Height of condylar head which is the distance between the Condylar head (Cd) and the Ante-gonion (Ag). This indicates the height of the condylar process
Cr- Ag	Height of coronoid which is the distance between the Coronoid (Cr) and Ante-gonion (Ag). This indicates the height of the coronoid process
Al^{i}-Me	Height of the central portion of alveolar bone which is the distance between the deepest point of the outer margin of bone (Al^{i}) that connects Menton (Me) and the Ante-gonion (Ag) to the Menton (Me). This indicates the height of the central portion of the alveolar

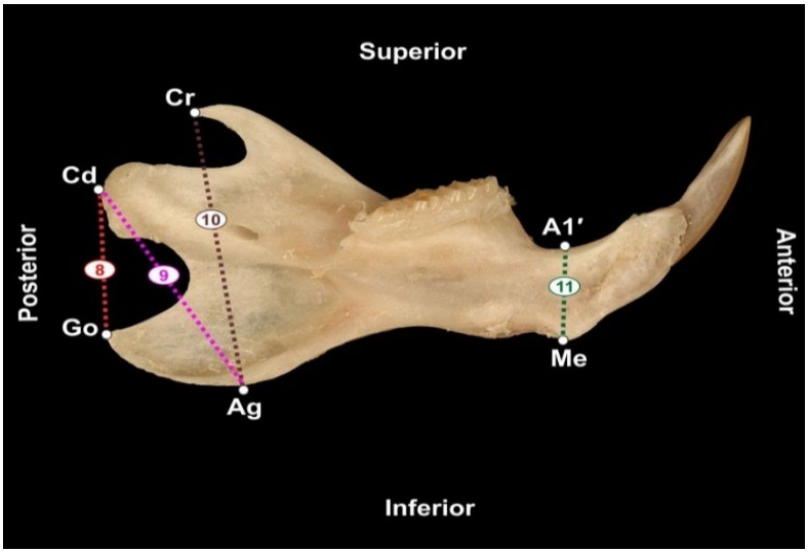

Figure 6.2: Morphometric reference points for the linear measurements of rat mandibular height. Showing the six landmarks from which four 3D measurements of the linear mandibular height parameters were analysed, ⑧Cd-Go indicates mandibular ramus height; ⑨Cd-Ag, the height of condylar head; ⑩Cr-Ag, height of coronoid; and ⑪AI'-Me, height of the central portion of alveolar bone (*Maki, 2002)* (Image courtesy of Dr. I Eguavoen). Cd- Condyle, Go- Gonion, Cd- Condyle, Ag- Ante-gonion, Cr- Coronoid process, Ag- Ante-gonion,Me- Menton, Al'- Deepest point of the outer margin of the bone.

6.2 RESULTS

6.2.1 Length of the mandible

Mandibular length (Cd-Id)

The DBT, DBT+cART and DBT+cART+ALC groups exhibited a significantly smaller distance between the posterior point of the condylar head and infradentale on the labial side (Cd-Id) compared to the untreated control (p≤0,001, p=0,003 and p=0,013, respectively) (Table 6.3). In contrast, the mandibular length in the ALC, cART, ALC+cART and DBT+ALC, had similar values to the untreated control group (p=0,363 p=0,067, p=0,541 p=0,067, respectively).

Regarding alcohol effects, the ALC group had a significantly lower mandibular length in comparison to the cART group (p=0,007), however, exhibited significantly higher mandibular length than the DBT and DBT+cART group (p= 0.004 and p=0,037, respectively). Conversely, a similar mandibular length was observed between the ALC group than the ALC+cART, DBT+ALC and DBT+cART+ALC (p>0,05, for all comparisons) (Table 6.3).

The cART group exhibited significantly higher mandibular length than the ALC+cART, DBT+ALC, DBT, DBT+cART and DBT+cART+ALC groups (p≤0.001, for all comparisons, except p=0,018, for ALC+cART and p=0,001, for DBT+ALC) (Table 6.3). When considering the DBT group exhibited similar mandibular length than the DBT+ALC, DBT+cART and DBT+cART+ALC (p>0,05, for all comparisons). Conversely, a significantly lower mandibular length was observed in the ALC+cART group (p=0,002) (Table 6.3).

Mandibular body length (Go-Id)

The DBT, DBT+ALC, DBT+cART and DBT+cART+ALC groups exhibited a significantly lower distance between the the gonion to the infradentale (labial side) (Cd-Id) compared to the untreated control (p≤0,001, p=0,011 and p=0,003, p=0,005 respectively) (Table 6.3). In contrast, the mandibular body length in the ALC, cART, and ALC+cART had similar values to the untreated control group (p=0,950, p=0,210, and p=0,053, respectively).

Considering, the alcohol effects, ALC group exhibited significantly higher mandibular body length than the DBT, DBT+ALC, DBT+cART and DBT+cART+ALC groups (p≤0,001, p= 0.011, p=0,003 and p=0,005, respectively). Conversely, a similar mandibular body length was observed between the ALC group than the cART and ALC+cART (p=0,188 and p=0,060, respectively. Regarding cART effects, the cART group showed a higher mandibular body length in the ALC+cART, DBT, DBT+ALC, DBT+cART and DBT+cART+ALC groups (p≤0,001, for all comparisons, except, p=0,002, for ALC+cART) (Table 6.3). When considering the diabetes group similar mandibular body lengths were observed among treatment groups (p>0,05) (Table 6.3).

Lingual side of the alveolar bone length (AI-Id)

The DBT+cART group exhibited the lowest alveolar bone length in the lingual side than the untreated control control group, significance was detected (p≤0,001. Again, significantly lower values were also observed between the DBT and DBT+ALC groups than the untreated control controls (p≤0,001 and p=0,003, respectively). Similarities was observed between the ALC,

cART, ALC+cART and DBT+cART+ALC groups when compared to the untreated control (p=0,887, p=0,677, p=0,512 and p=0,311, respectively) (Table 6.3).

With respect the the alcohol effects, the ALC group exhibited significantly higher alveolar bone length (lingual side) than the DBT, DBT+ALC, DBT+cART (p≤0,001, for both DBT and DBT+cART, p=0,005, for DBT+ALC). Similarities of the AI-Id was observed between the ALC in comparison to cART, ALC+cART, DBT+cART+ALC (p=0,783, p=0,604 and p=0,377, respectively). Regarding cART effects, the cART group showed a higher alveolar bone length in the DBT, DBT+ALC, DBT+cART and DBT+cART+ALC groups (p≤0,001, for both DBT and DBT+cART and, p=0,011, for DBT+ALC). Similarities of AI-ID was found between cART and the other treatment groups (p>0,05) (Table 6.3).

Considering diabetes, the DBT, DBT+cART and DBT+ALC, had significantly lower alveolar length than ALC+ cART. However, similarities were observed between ALC+cART and DBT+cART+ALC group (Table 6.3).

Distance from condyle to base of the lower incisor (Cd-BI)

Only the DBT group exhibited significantly lower length of the lower incisor than the untreated control control (p=0,017). Similarities were observed between all other treatment groups compared with the untreated control control (p>0,05) (Table 6.3).

Considering alcohol effects, the length of the lower incisor was significantly lower in the DBT group than the ALC group (p=0,029). Similarities were observed between all other treatment groups compared with the ALC group (p>0,05). The cART group exhibited significantly higher length of the lower incisor than the DBT, DBT+ALC, DBT+cART and DBT+cART+ALC groups (p=0,001, p=0,007, p=0,034 and p=0,031, respectively). Similarities were observed between all other treatment groups compared with the cART group (p>0,05) (Table 6.3).

Considering diabetes, the DBT group exhibited lower length of the lower incisor than the ALC+cART group (p=0,008) (Table 6.3).

Length of the lower dental arch (M3-Id)

The DBT+cART and DBT+cART+ALC groups when compared to the untreated control control exhibited a significantly lesser length of the lower dental arch (p=0,003 and p=0,050, respectively). Similarities were observed between all other treatment groups compared with the untreated control control (p>0,05) (Table 6.3).

Regarding the alcohol effects, DBT+ALC, DBT+cART and DBT+cART+ALC groups exhibited a lower M3-Id than the ALC group (p=0,040, p≤0,001, p=0,014, respectively). Similarities were observed between all other treatment groups compared with the ALC group (p>0,05). With regards to cART, a similar pattern seen in the ALC group continued, where DBT+ALC, DBT+cART and DBT+cART+ALC groups exhibited a lower M3-Id than the cART group (p=0,003, p≤0,001, p=0,001, respectively). Similarities were observed between all other treatment groups

compared with the cART group (p>0,05) (Table 6.3). When considering diabetes, only the DBT+cART group exhibited a shorter length of the lower dental arch (p=0.012) (Table 6.3).

Table 6.3: Linear mandibular length (mm)

	UNTREATED		ALC		cART		ALC+cART		DBT		DBT+ALC		DBT+cART		DBT+cART+ALC	
N	16		16		16		14		14		12		14		12	
Parameters	Mean	SD	Mean	SD	Mean	SD	Mean	SD	Mean	SD	Mean	SD	Mean	SD	Mean	SD
[a]Cd-Id (mm)	27,19	0,92	26,82	1,71	27,96	0,54	26,93	0,54	25,54	1,43	26,37	0,8	25,91	1,41	26,06	1,37
*p value			0.363		0.067		0.541		0.000		0.067		0.003		0.013	
[b]Go-Id(mm)	26,57	0,6	26,54	0,9	27,06	0,68	25,78	1,75	25,04	1,26	25,46	0,85	25,31	0,95	25,35	1,45
*p value			0.950		0.210		0.053		0.000		0.010		0.002		0.005	
[c]AI-Id' (mm)	8,7	0,37	8,68	0,21	8,64	0,2	8,61	0,4	7,8	0,4	8,26	0,26	7,95	0,66	8,55	0,41
*p value			0.887		0.677		0.512		0.000		0.003		0.000		0.311	
[d]Cd-B1 (mm)	11,71	0,89	11,64	1,62	12,11	0,36	11,84	0,5	10,89	1,04	11,12	1	11,37	0,35	11,32	0,95
*p value			0.833		0.240		0.718		0.017		0.100		0.316		0.276	
[e]M3-Id (mm)	14,02	0,33	14,14	0,42	14,35	0,48	13,94	0,42	14,06	0,42	13,69	0,18	13,4	1,07	13,6	0,7
*p value			0.563		0.102		0.680		0.841		0.126		0.003		0.051	

[a]Cd-Id: ALC vs cART, ALC+cART, DBT+ALC, DBT+cART+ALC (p=0.007,p=0.787, p=0.318, p=0.094 respectively); cART vs ALC+cART, DBT+cART, DBT+cART+ALC (p=0.018, p<0.001, p<0.001 respectively); DBT vs ALC, cART, DBT+ALC, DBT+cART, DBT+cART+ALC (p=0.004, p<0.001, p=0.076, p=0.405, and p=0.262 respectively); DBT+ALC vs DBT+cART, DBT+cART+ALC (p=0.325,p= 0.523 respectively).

[b]Go-Id: ALC vs cART, ALC+cART , DBT+ALC, DBT+cART+ALC (p=0.188, p=0.060, p=0.011, p=0.005, respectively); cART vs ALC+cART, DBT+cART, DBT+cART+ALC (p=0.002, p<0.001, p<0.001, respectively); DBT vs ALC, cART, DBT+ALC, DBT+cART, DBT+cART+ALC (p<0,001, p<0.001, p=0.333, p=0.524 and p=0.474, respectively); DBT+ALC vs DBT+cART, DBT+cART+ALC (p=0.721, p=0.808, respectively).

[c]AI-Id': ALC vs cART, ALC+cART , DBT+ALC , DBT+cART+ALC (p=0.783, p=0.604, p=0.005, p=0.377, respectively); cART vs ALC+cART, DBT+cART, DBT+cART+ALC (p=0.800, p<0.011, p=0.529, respectively); DBT vs ALC, cART, DBT+ALC, DBT+cART, DBT+cART+ALC (p<0.001, p<0.001, p=0.003, p=0.304 and p<0.001, respectively); DBT+ALC vs DBT+cART, DBT+cART+ALC (p=0.042, p=0.068 respectively).

[d]Cd-B1: ALC vs cART, ALC+cART , DBT+ALC, DBT+cART+ALC (p=0.167, p=0.572, p=0.147, p=0.371, respectively); cART vs ALC+cART, DBT+cART, DBT+cART+ALC (p=0.437, p=0.034, p=0.031, respectively); DBT vs ALC, cART, DBT+ALC, DBT+cART, DBT+cART+ALC (p=0.029, p=0.001, p=0.526, p=0.176 and p=0.239 respectively); DBT+ALC vs DBT+cART, DBT+cART+ALC (p=0.503, p=0.599, respectively).

[e]M3-Id**:** ALC vs cART, ALC+cART, DBT+ALC, DBT+cART+ALC (p=0.288, p=0.332, p=0.040, p=0.014, respectively); cART vs ALC+cART, DBT+cART, DBT+cART+ALC (p=0.047, p<0.001, p=0.001, respectively); DBT vs ALC, cART, DBT+ALC, DBT+cART, DBT+cART+ALC (p=0.721, p=0.167, p=0.095, p=0.002 and p=0.038, respectively); DBT+ALC vs DBT+cART, DBT+cART+ALC (p=0.182, p=0.691, respectively).

*Comparison of respective groups with the untreated group. ALC, alcohol; cART, combination antiretroviral treatment; ALC+cART, alcohol and cART; DBT; diabetes; DBT+ALC, diabetes and alcohol; DBT+cART, diabetes and cART; DBT+cART+ALC, diabetes, cART+alcohol.

6.2.2 Height of the Mandible

Mandibular Ramus Height (Cd-Go)

All the treatment groups exhibited a smaller mandibular ramus height (Cd-Go) compared to the untreated control, however, significance was only detected for DBT+cART+ALC versus the untreated control (p >0,05 and p=0,001, respectively) (Table).

Regarding alcohol effects, the ALC group had a significantly higher mandibular ramus height than the DBT+cART+ALC group (p=0,002). Conversely, a similar mandibular ramus height was observed between all other treatment groups (p>0,05, for all comparisons). The cART group exhibited significantly higher mandibular ramus height than the DBT+cART+ALC (p=0.014). Similarities were observed between all other treatment groups compared with the cART group (p>0,05).

When considering diabetes, the DBT group exhibited similar mandibular ramus height than the DBT+ALC, DBT+cART, however, a significantly higher mandibular ramus height was observed between the DBT+cART+ALC (p>0,05, for DBT+ALC, DBT+cART and p=0.004). Also, a significantly higher mandibular ramus height was exhibited between the ALC+cART and DBT+cART groups than the DBT+cART+ALC group (p=0,018 and p=0.001).

Height of condylar process (Cd-Ag)

The DBT+cART+ALC group exhibited a significantly lower height of the condylar process than the untreated control (p=0,003) (Table). In contrast, the height of the condylar process was similar amongst all other treatment groups to the untreated control group (p>0,05).

Considering, the alcohol effects, the ALC group had a significantly higher height of the condylar process than the DBT+cART+ALC group (p=0,004). Conversely, a similar height of the conylar process was observed between all other treatment groups (p>0,05, for all comparisons). Regarding cART effects, the cART group showed a higher height of the condylar process than the DBT+cART+ALC group (p=0.046). Similarities were observed between all other treatment groups compared with the cART group (p>0,05). However, when considering ALC+cART group with the DBT+cART+ALC group a significantly higher height of the condylar process was observed (p=0,009)

Regarding the diabetes group similar height of the condylar process were observed among all treatment groups (p>0,05) except between the DBT and DBT+cART+ALC group (p=0,020) (Table).

Height of the coronoid process (Cr-Ag)

All treatment groups exhibited significantly lower height of the coronoid process than the untreated control group (p≤0,001 for DBT, DBT+cART and DBT+cART+ALC, p=0,001 for

DBT+ALC, p=0,005 for ALC+cART, p=0,003 for ALC). Conversely, similarities were observed between the cART group than the untreated control (p=0,741) (Table).

With respect the alcohol effects, the ALC group exhibited significantly lower height of the coronoid process than the cART group(p=0,008). Similarities of the Cr-Ag was observed between the ALC in comparison to all other treatment groups (p>0,05). Regarding cART effects, the cART group showed a higher height of the coronoid process in the ALC+cART, DBT, DBT+ALC, DBT+cART and DBT+cART+ALC groups (p≤0,001, for DBT, DBT+cART and DBT+cART+ALC, p=0,003, for DBT+ALC, p=0,013, for ALC+cART) (Table).

Considering diabetes, the DBT+cART had a significantly lower height of the coronoid process than ALC+cART (p=0,020). However, similarities were observed between ALC+cART and all other diabetic groups (p>0,05) (Table).

Height of the central portion of the alveolar bone (AI-Me)

Most of the treatment groups exhibited significantly lower height of the central portion of the alveolar bone than the untreated control group (p≤0,001 for DBT, DBT+cART and DBT+ALC, p=0,001 for DBT+cART+ALC, p=0,005 for ALC+cART, p=0,003 for ALC). Conversely, similarities were observed between the ALC and cART groups in comparison to the untreated control (p=0,084 and p=0,346, respectively) (Table).

Considering alcohol effects, the height of the central portion of the alveolar bone was significantly lower in the DBT, DBT+ALC and DBT+cART groups than the ALC group (p≤0,001, for both DBT and DBT+cART, p=0,015 for DBT+ALC). Similarities were observed between all other treatment groups compared with the ALC group (p>0,05). The cART group exhibited significantly lower height of the central portion of the alveolar bone in the ALC+cART, DBT, DBT+ALC, DBT+cART and DBT+cART+ALC groups (p=0.034 for ALC+cART, p≤0,001 for both DBT and DBT+cART, p=0,002 for ALC, and p=0,018, DBT+cART+ALC). Similarities were observed between ALC than cART group (p=0,424) (Table).

Considering diabetes, the DBT and DBT+cART groups exhibited significantly lower height of the central portion of the alveolar bone than the ALC+cART group (p=0,005 and p≤0.001, respectively). The DBT+cART exhibited significantly lower height of the central portion of the alveolar bone than the DBT+ALC and DBT+cART+ALC group (p=0.009 and p=0.001, respectively). The DBT group showed a significantly higher height of the central portion of the alveolar bone than the DBT+cART+ALC group (p=0.017) (Table).

Table 6.4: Linear mandibular height

Groups	UNTREATED		ALC		cART		ALC+cART		DBT		DBT+ALC		DBT+cART		DBT+cART+ALC	
N	16		16		16		14		14		12		14		12	
Parameters	Mean	SD	Mean	SD	Mean	SD	Mean	SD	Mean	SD	Mean	SD	Mean	SD	Mean	SD
[a]Cd-Go (mm)	9,66	0,73	9,6	1,15	9,39	0,61	9,39	0,91	9,57	1,17	9,03	0,5	9,06	0,46	8,56	1,1
*p value			0.838		0.390		0.401		0.777		0.061		0.064		0.001	
[b]Cd-Ag (mm)	12,51	1,21	12,46	1,84	12,04	0,7	12,36	1	12,23	1,07	11,7	1,06	11,91	0,71	11,13	1,34
*p value			0.906		0.262		0.740		0.516		0.075		0.170		0.003	
[c]Cr-Ag(mm)	15,93	0,35	15,26	0,82	15,86	0,27	15,29	0,61	14,87	0,65	15,14	0,47	14,74	0,8	14,97	0,76
*p value			0.003		0.741		0.005		<0.001		0.001		<0.001		<0.001	
[d]Al'-Me(mm)	5,49	0,17	5,37	0,23	5,43	0,17	5,28	0,11	5,07	0,19	5,19	0,14	4,99	0,28	5,25	0,19
*p value			0.084		0.348		0.003		<0.001		<0.001		<0.001		0.001	

[a]Cd-Go: ALC vs cART, ALC+cART, DBT+ALC, DBT+cART+ALC (p=0.511,p=0.520, p=0.091, p=0.002 respectively); cART vs ALC+cART, DBT+cART, DBT+cART+ALC (p=0.993, p=0.302, p=0.014 respectively); DBT vs ALC, cART, DBT+ALC, DBT+cART, DBT+cART+ALC (p=0.932, p=0.583, p=0.118, p=0.127, and p=0.004 respectively); DBT+ALC vs DBT+cART, DBT+cART+ALC (p=0.992,p=0.195 respectively).

[b]Cd-Ag: ALC vs cART, ALC+cART, DBT+ALC, DBT+cART+ALC (p=0.315, p=0.827, p=0.094, p=0.004, respectively); cART vs ALC+cART, DBT+cART, DBT+cART+ALC, p=0.451,p=0.771, p=0.046, respectively); DBT vs ALC, cART, DBT+ALC, DBT+cART, DBT+cART+ALC (p=0.592, p=0.663, p=0.258, p=0.482, and p=0.020, respectively); DBT+ALC vs DBT+cART, DBT+cART+ALC (p=0.646, p=0.240, respectively).

[c]Cr-Ag: ALC vs cART, ALC+cART , DBT+ALC , DBT+cART+ALC (p=0.008, p=0.920, p=0.609, p=0.211, respectively); cART vs ALC+cART, DBT+cART, DBT+cART+ALC (p=0.013, p<0.001, p<0.001, respectively); DBT vs ALC, cART, DBT+ALC, DBT+cART, DBT+cART+ALC (p=0.085, p<0.001, p=0.265, p=0.565 and p=0.692, respectively); DBT+ALC vs DBT+cART, DBT+cART+ALC (p=0.097, p=0.488 respectively).

[d]Al'-Me : ALC vs cART, ALC+cART, DBT+ALC,DBT+cART+ALC (p=0.424, p=0.172, p=0.015, p=0.098, respectively); cART vs ALC+cART, DBT+cART, DBT+cART+ALC (p=0.034, p<0.001, p=0.018, respectively); DBT vs ALC, cART, DBT+ALC, DBT+cART, DBT+cART+ALC (p<0.001, p<0.001, p=0.104, p=0.289 and p=0.017 respectively); DBT+ALC vs DBT+cART, DBT+cART+ALC (p=0.009, p=0.451, respectively).

*Comparison of respective groups with the untreated group. ALC, alcohol; cART, combination antiretroviral treatment; ALC+cART, alcohol and cART; DBT; diabetes; DBT+ALC, diabetes and alcohol; DBT+cART, diabetes and cART; DBT+cART+ALC, diabetes, cART+alcohol

6.3 DISCUSSION

The intention of this chapter was to assess the proposition that diabetic rats that take both alcohol and cART have a worse outcome for the mandibular external dimensions. This study is the first to test this proposition. The findings showed that diabetes alone (DBT) as well as when diabetic rats had alcohol (DBT+ALC) or cART (DBT+cART) or both (DBT+cART+ALC) resulted in smaller mandibular dimensions. In contrast, among the rats given alcohol or cART or alcohol combined with cART (ALC+cART), the mandibular dimensions did not change significantly compared to the untreated controls rats.

The DBT group had smaller mandibular length measurements (Cd-Id), mandibular body length (Go-Id) and length of the lower incisor (Cd-BI). When diabetic rats took cART (DBT+cART), the mandibular length (Cd-Id), mandibular body length (Go-Id), lingual side of the alveolar bone length (AI-Id) and length of the lower dental arch (M3-Id) were all smaller than control rats. Only one measurement of length, the mandibular body length (Go-Id) was affected among diabetic rats that took alcohol (DBT+ALC). Among diabetic rats that were given both alcohol and cART (DBT+cART+ALC), mandibular length (Cd-Id), mandibular body length (Go-Id) and length of the lower dental arch (M3-Id) were smaller than the untreated control rats. These results show that diabetes has the most role on mandibular measurement that are a proxy for the mandibular length. This seems to be exacerbated by alcohol and cART. Studies have shown that diabetes alone affects the bones including the mandible (Dyer et al., 1998; Maurel et al., 2012). This is the first study to show that the negative effects of diabetes on the mandible may be exacerbated by concurrent alcohol use and treatment with cART.

The DBT group or when diabetic rats received cART treatment (DBT+cART) had smaller Height of the coronoid process (Cr-Ag) and height of the central portion of the alveolar bone (AI-Me) than the untreated controls. In addition to these measurements, the mandibular ramus height (Cd-Go) and height of the ccondylar process (Cd-Ag) were smaller among diabetic rats given both alcohol and cART (DBT+cART+ALC). This means that all measurements that served as a proxy for mandibular height parameters where smaller than untreated controls when diabetic rats were given both alcohol and cART (DBT+cART+ALC). Again, this further supports the proposition that diabetes is worse for the bone in cases of concurrent alcohol and cART use. This study is the first to test this proposition and report on this finding of a poor mandibular outcome in diabetics taking alcohol with cART use (DBT+cART+ALC).

In the present study, no significant differences were detected in all the linear mandibular length and height parameters among the rats given alcohol or cART or alcohol combined with cART (ALC+cART) compared to the untreated rats. These findings contrast with our expectations as literature reports that alcohol or cART adversely affects bone (Natukunda et al., 2023). This finding in the present study may mean that, the external dimensions of the mandible remain unaffected whereas the internal structure of the mandible is adversely affected. Tensile strength tests show lower break force and maximum force (See 5.2.2) in the ALC+cART. This supports the idea that external dimensions may remain the same while the bone is weaker. This is further supported by the observation that BV/TV was lower than untreated controls in the ALC group although the external mandibular dimensions were unaffected.

6.3.1 Conclusion

Diabetes adversely affected mandibular dimensions and was worsened by concurrent alcohol and cART. The findings support existing literature on the detrimental effects of diabetes on bone but add new knowledge on the combined effects of alcohol and cART among diabetics. It is important to consider external bone dimensions together with internal structurer and bone strength as alcohol or cART or alcohol combined with cART (ALC+cART) did not show osteometric changes although the bones were weaker.

Chapter 7

Influence of alcohol intake and combination antiretroviral treatment on osteocytes and the expression of TGFβ1 and BMP3 in the mandible of diabetic rats

7.0 INTRODUCTION 125
7.1 MATERIAL AND METHODS 127
7.1.1 Animals 127
7.1.2 Bone harvesting 127
7.1.3 Tissue processing for immunohistochemical techniques 127
7.1.4 Haematoxylin and Eosin (H&E) stain 128
7.1.5 Immunohistochemistry for TRAP, TGFβ1 and BMP3 in the mandible. 128
Photography, quantification, and staining intensity of ROI (region of interest) 129
7.2 Results 131
7.2.1 General histological appearance 131
7.2.2 Cells expressing TRAP (Osteocytes) 134
7.2.3 TGFβ1 137
7.2.4 BMP-3 137
7.3 Discussion 140
Anti-osteoblastogenic effects of adipocytes 140
Osteolysis 141
TGFβ1 and its antagonist BMP3 141
7.3.1 Conclusion 142

7.0 INTRODUCTION

Transforming growth factor beta 1 (TGFβ1) is an extracellular complex that is translocated into the intracellular domain to regulate bone cell differentiation and maintains skeletal integrity (Ehnert et al., 2010; Yang et al., 2014; Wu et al., 2016). Conversely, bone morphogenic protein 3 (BMP-3) is an anti-osteogenic cytokine that is secreted by osteoblasts and osteocytes, and it negatively regulates osteoblastogenesis by inhibiting osteoblast differentiation (Rosen, 2009; Wu et al., 2016; Kokabu and Rosen, 2018). The anti-osteogenic effects of BMP-3 manifest as reduced bone mineralization, smaller and thinner trabeculae volume, and thinner cortical bone(Gamer et al., 2009; Horbelt et al., 2012), therefore, increased bone fragility. Increase BMP-3 expression as reported in the diabetic bone may affect osteoblast numbers and function, leading to increased fracture risk associated with T2D (Wang et al., 2022).

In the process of endochrondral and intramembranous bone formation and remodeling, many osteoblasts become entrapped into the mineralized bone matrix which they secrete and differentiate into osteocytes (Picke et al., 2019).

Tartrate resistant acid phosphate (TRAP) is typically used as a reliable immunohistochemical marker for osteocytes andosteoctyes-precursors (Nakano et al., 2004).

The TRAP-positive osteocytes in the cytoplasmic granular structure on the resorption surface of bone is a valuable functional proof of the involvement of osteocytes in the analysis of cellular interaction taking place during bone resorption and bone remodeling (Nakano et al., 2004).

The ability to express TRAP enables osteocytes to participate in bone remodeling through a network of canaliculi and gap junctions of their cytoplasmic process. The osteocytes (former osteoblasts embedded in matrix bone) form functional units with osteoblasts to carry out the work of bone remodeling (Nakano et al., 2004). This network is reduced in T2DM due to an increased rate of apoptosis of osteocytes leading to reduced bone turnover, osteoblast number, osteoclast function, and increased susceptibility to fracture (Kaya et al., 2017; Picke et al., 2019).

The aim of the study was to evaluate whether alcohol intake and combination antiretroviral treatment use would adversely affect the number of osteocytes and the expression of TGFβ1 and BMP3 in the mandible of diabetic rats.

7.1 MATERIAL AND METHODS

7.1.1 Animals

The animal husbandry was as described under section 3.2.2 (Animal husbandry), group allocation and the induction of diabetes, administration of alcohol and cART are all described under section 3.2.3 (group allocation) and section 3.2.4 (treatment of animals), respectively.

7.1.2 Bone harvesting

The mandibles were harvested and handled as described in section 5.1.3

7.1.3 Tissue processing for immunohistochemical techniques

Bone samples were fixed in 10% buffered formalin for a minimum of 14 days, then decalcified in 20% w/v ethylenediaminetetraacetic acid (EDTA, pH 7.4) for 10 days in an incubator with regular gentle shaking at 45˚C. The bones were then rinsed, immersed in 10% buffered formalin for 24 hours before processing for histology. An automatic processor (Citadel 2000, Thermo Fischer Scientific) was used to take the samples through ascending grades of ethanol prior to embedding in paraffin wax. During embedding, bone samples were orientated to enable section in the anteroposterior direction. Bone sections were cut at 5µm thickness using a microtome (Leica RM2125 RTS, Leica Biosystems, USA) and mounted on silane-coated glass slides. Section sequences were mounted in order for specific stains, namely, Hematoxylin and Eosin to assess morphology, and to quantify adipocyte number as well as immunolocalization of TRAP, TGFβ1 and BMP3 for the same regions.

7.1.4 Haematoxylin and Eosin (H&E) stain

This method is also used to determine normal tissue structure (Totty, 2002). Sections were dewaxed in xylene for 10 minutes and hydrated by passing through 3 changes (1 minute each) of absolute alcohol followed by 90% and 70% alcohol (1 minute each) and eventually into running tap water for 1 minute. The sections were then stained for 10 min in haematoxylin, differentiated in periodic acid for 10 seconds, rinsed in tap water for a minute, blued in Scott's tap water for 2 minutes, and rinsed again in tap water. The cytoplasm was stained with eosin by immersing the sections in 70% alcohol followed by eosin for 2 minutes. The sections were then dehydrated in increasing concentrations of alcohol before they were mounted in entellen.

7.1.5 Immunohistochemistry for TRAP, TGFβ1 and BMP3 in the mandible.

Immunohistochemistry was performed using anti-TRAP antibody (ab185716) for osteocyte detection, anti-BMP3 antibody (ab134724), and anti-TGFB 1 antibody (ab92486). All antibodies came from Abcam. The sections were placed for 30 minutes in a 40°C incubator, then deparaffinized, and rehydrated in a series of graded alcohols. Subsequently, they were immersed in citrate buffers (pH=6) and placed in a 60°C water bath for 24 hours to facilitate the extraction of antigens. After 24 hours, the sections were cooled at room temperature for 20 minutes and rinsed in PBS 3x5 minutes (pH=7.4).

Endogenous peroxidase was blocked by 1% hydrogen peroxide (H_2O_2), which was followed by a wash in PBS (3x5 minutes). The sections were, incubated with primary antibodies at appropriate dilution (TRAP, 1: 100, TGFB1, 1:400, BMP3, 1: 75) and placed overnight at 4°C. After 24 hours,

the slides were left on the bench for 20 minutes to reach room temperature, then washed with PBS (3x5 minutes). The slides were incubated for 10 minutes with a secondary biotinylated antibody (Biotinylated Goat Anti-Rabbit IgG (H+L) (ab64256)) and washed again PBS (3x5 minutes).

The sections were then incubated for 10 minutes in streptavidin HRP (ab64269) to detect and improve the antibody binding. After washing inPBS (pH=7.4) PBS (3x5 minutes), the slides were then incubated for 5 minutes in a 3-3' di-aminobenzidine (DAB) working solution. Once the best color was achieved, the sections are washed in running tap water for 5 minutes, then dehydrated by grade alcohol, cleared with xylene and finally installed with entellen

Photography, quantification, and staining intensity of ROI (region of interest)

A light microscope (Zeiss Axioscope 2 plus) fitted with an axiocam HRC digital camera (Zeiss, Germany) connected to a PC (Hewlett-Packard, South Africa) was used to take photomicrographs of the stained slides. Photomicrographs were taken from the region of encircled region of interest (Fig 7.1). Anatomical landmarks were determined using the H&E stained slides, to create consistency in quantification and staining analysis. Nonadjacent fields were selected in the encircled area. Photomicrographs were imported into Fiji Image-J software (National Institute of Health USA) for further analysis. TRAP positive osteocytes (Nakano et al., 2004; Dole et al., 2017), and adipocytes were identified as specified in previous literature (Ferland-McCollough et al., 2018). Cells were counted manually by the investigator at different times in the same region to

check for consistency. Immunolocalization anti-BMP3 antibody, and anti-TGFβ1 antibody was performed. These were graded as no stain, mild, moderate and intense staining.

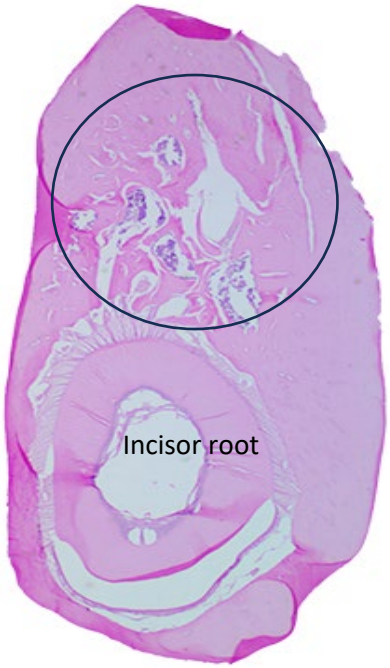

Figure 7.1 Region of interest. Photomicrographs were taken from the encircled region.

7.2 RESULTS

7.2.1 General histological appearance

The trabecular network was more extensive in the untreated controls (Fig. 7.2). The highest number of adipocytes was observed in the ALC+cART (38.33±4.80), cART (31.67±4.80), ALC (28.5±6.06), (11.67±1.86), DBT+ALC (26.17±5.88), DBT (25.67±2.58), and DBT+cART (23.83±4.17) DBT+ALC+cART (21.67±4.63) groups which was significantly more than the untreated controls (11.67 ± 1,86) ($p<0.001$ for all the comparisons except $p=0.034$ for DBT+ALC+cART) (Figs. 7.2 and 7.3).

The ALC group had similar values to the cART group ($p=0.960$) (Figs. 7.2 and 7.3). However, the ALC+cART group had significantly more adipocytes that the ACL but not the cART group ($p=0.038$ and $p=0.350$). The ALC+cART group also had significantly more adipocytes than the DBT, DBT+ALC, DBT+cART and DBT+ALC+cART ($P=0,002$, $P= 0,004$, $P= 0,001$ and $p<0,001$). The cART group showed more adipocytes only when compared to the DBT+ALC+cART ($p=0.033$) (Figs. 7.2 and 7.3).

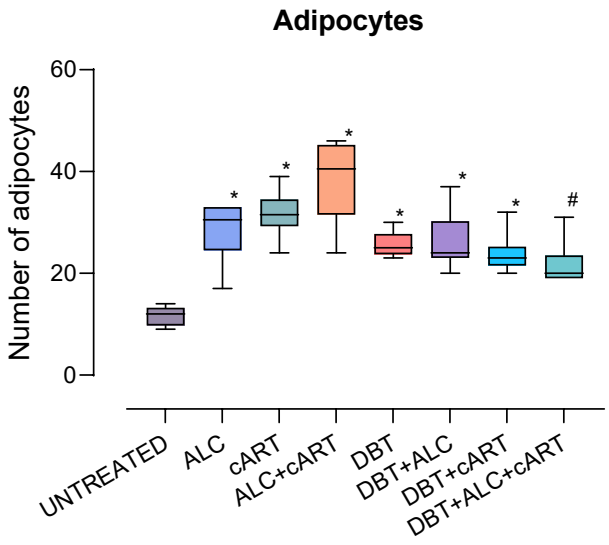

Figure 7.2: Number of adipocytes in the mandible. Box-and-whisker plots of adipocyte quantity in various study groups. The line inside the box represents the mean, whereas the bottom and top lines of the box show the 25th and 75th percentiles, respectively. The whiskers below and above the box show the minimum and maximum values, respectively.

Untreated control; ALC, alcohol; cART, combination antiretroviral treatment; ALC+cART, alcohol and cART; DBT, diabetic; DBT+ALC, diabetes and alcohol; DBT+cART, diabetes and cART; DBT+ALC+cART, diabetes, alcohol and cART

ALC vs cART, ALC+cART, DBT+ALC, DBT+cART+ALC ($p=0.960$, $p>0.038$, $p=0.993$, $p=0.322$); cART vs ALC+cART, DBT+cART, DBT+cART+ALC ($p=0.352$, $p=0.175$, $p=0.033$, respectively); DBT vs ALC, cART, DBT+ALC, DBT+cART, DBT+cART+ALC ($p<0.978$, $p=0.486$, $p>0.999$, $p=0.998$ and $p>0.999$, respectively); DBT+ALC vs DBT+cART, DBT+cART+ALC ($p=0.993$, $p>0.797$, respectively). *****$p<0.001$ vs untreated; #$p=0.033$ vs untreated

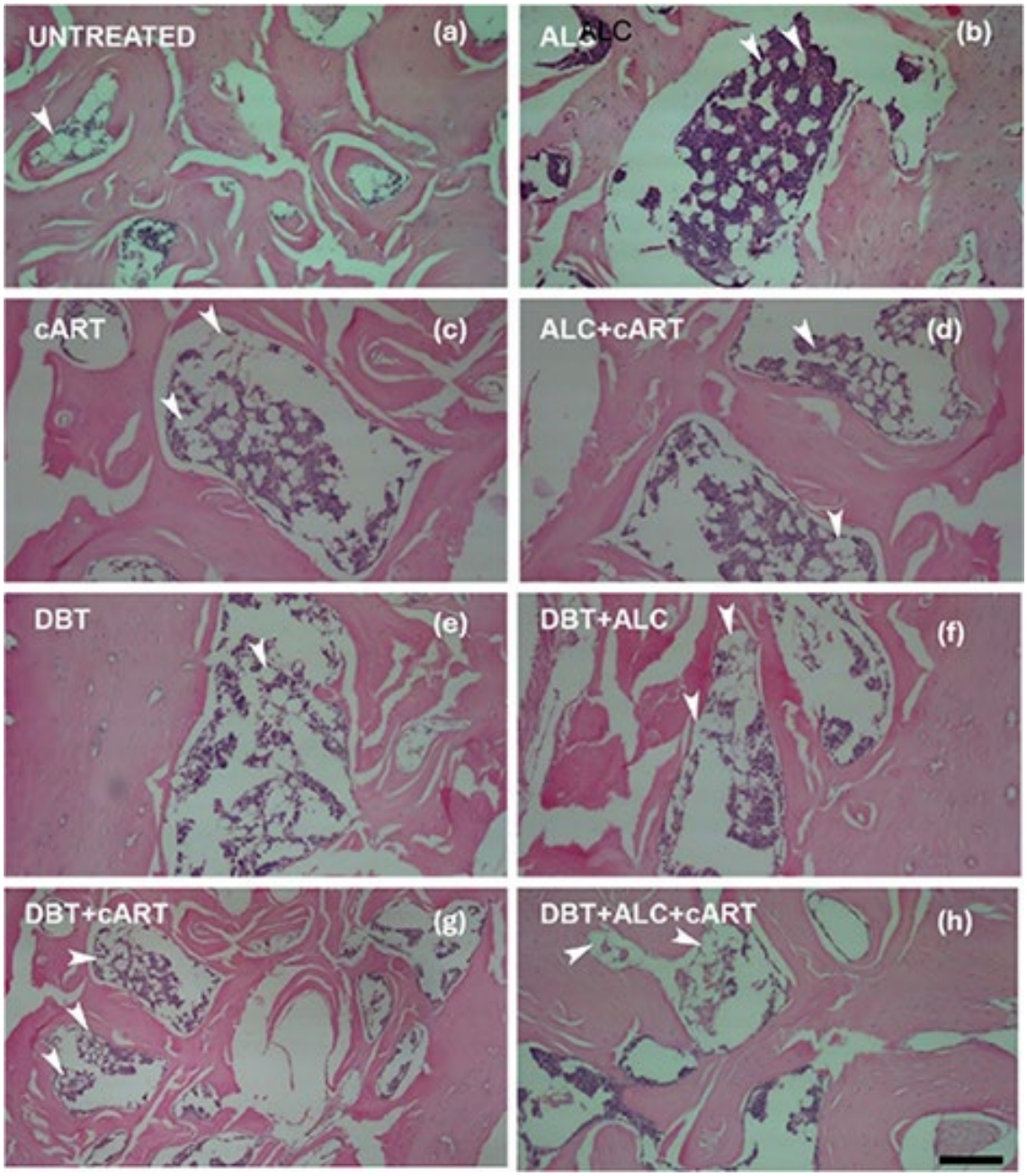

20**Figure 7.3: General histology and relative adipocyte infiltration in the mandible.** Adipocytes are the large round cells with a clear cytoplasm Scale bar represents 40µm and applies all photomicrographs

Untreated control; ALC, alcohol; cART, combination antiretroviral treatment; ALC+cART, alcohol and cART; DBT, diabetic; DBT+ALC, diabetes and alcohol; DBT+cART, diabetes and cART; DBT+ALC+cART, diabetes, alcohol and cART

7.2.2 Cells expressing TRAP (Osteocytes)

The DBT+ALC+cART (16.67±2.07), DBT+ALC (17.33±4.45), DBT (18.17±2.64) and ALC (17.67±2.25) had the least number of TRAP immunopositive cells compared to the untreated controls (25.67±3.67 ($p=0.012$, $p=0.026$, $p=0.022$, $p=0.037$) (Figs. 7.4 and 7.5). These other groups: DBT+cART (18.83±1.84), ALC+cART (23.00±7.34), cART (30.33±6.02) groups were similar to the untreated group ($p=0.114$, $p=0.952$, $p=0.538$) (Figs. 7.4 and 7.5).

The cART group had significantly more TRAP immunopositive cells than the ALC, DBT, DBT+ALC and DBT+cART, DBT+ALC+cART groups ($p<0.001$) (Figs. 7.4 and 7.5). There was no significant difference between the cART and the ALC+cART group ($p=0.073$). The DBT was similar to all other groups (Figs. 7.4 and 7.5).

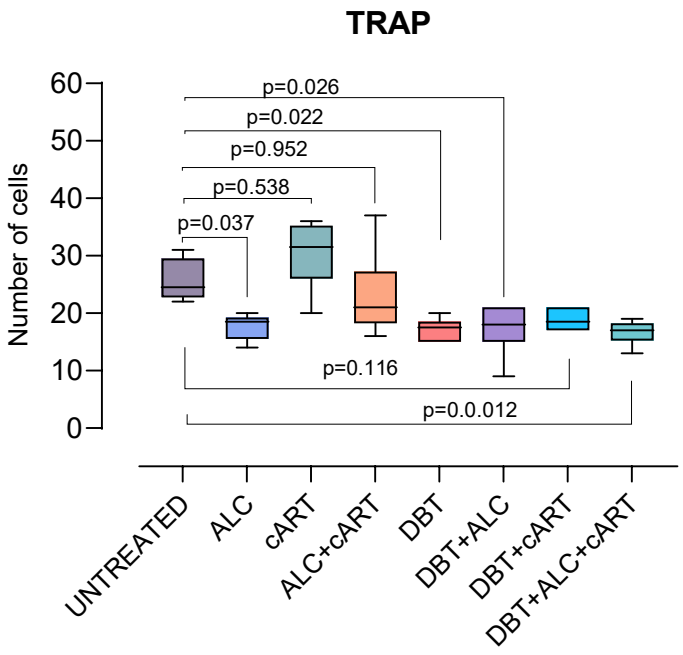

Figure 7.4: TRAP immunopositive cells quantity in the mandible. Box-and-whisker plots of TRAP immunopositive cells in various study groups. The line inside the box represents the mean, whereas the bottom and top lines of the box show the 25th and 75th percentiles, respectively. The whiskers below and above the box show the minimum and maximum values, respectively.

ALC vs cART, ALC+cART, DBT+ALC, DBT+cART+ALC ($p<0.001$, $p=0.369$, $p>0.999$, $p>0.999$); cART vs ALC+cART, DBT+cART, DBT+cART+ALC ($p=0.073$, $p<0.001$, $p<0.001$, respectively); DBT vs ALC, cART, DBT+ALC, DBT+cART, DBT+cART+ALC ($p>0.999$, $p<0.001$, $p>0.999$, $p>0.999$ and $p=0.984$, respectively); DBT+ALC vs DBT+cART, DBT+cART+ALC ($p=0.998$, for both comparisons).

Untreated control; ALC, alcohol; cART, combination antiretroviral treatment; ALC+cART, alcohol and cART; DBT, diabetic; DBT+ALC, diabetes and alcohol; DBT+cART, diabetes and cART; DBT+ALC+cART, diabetes, alcohol and cART

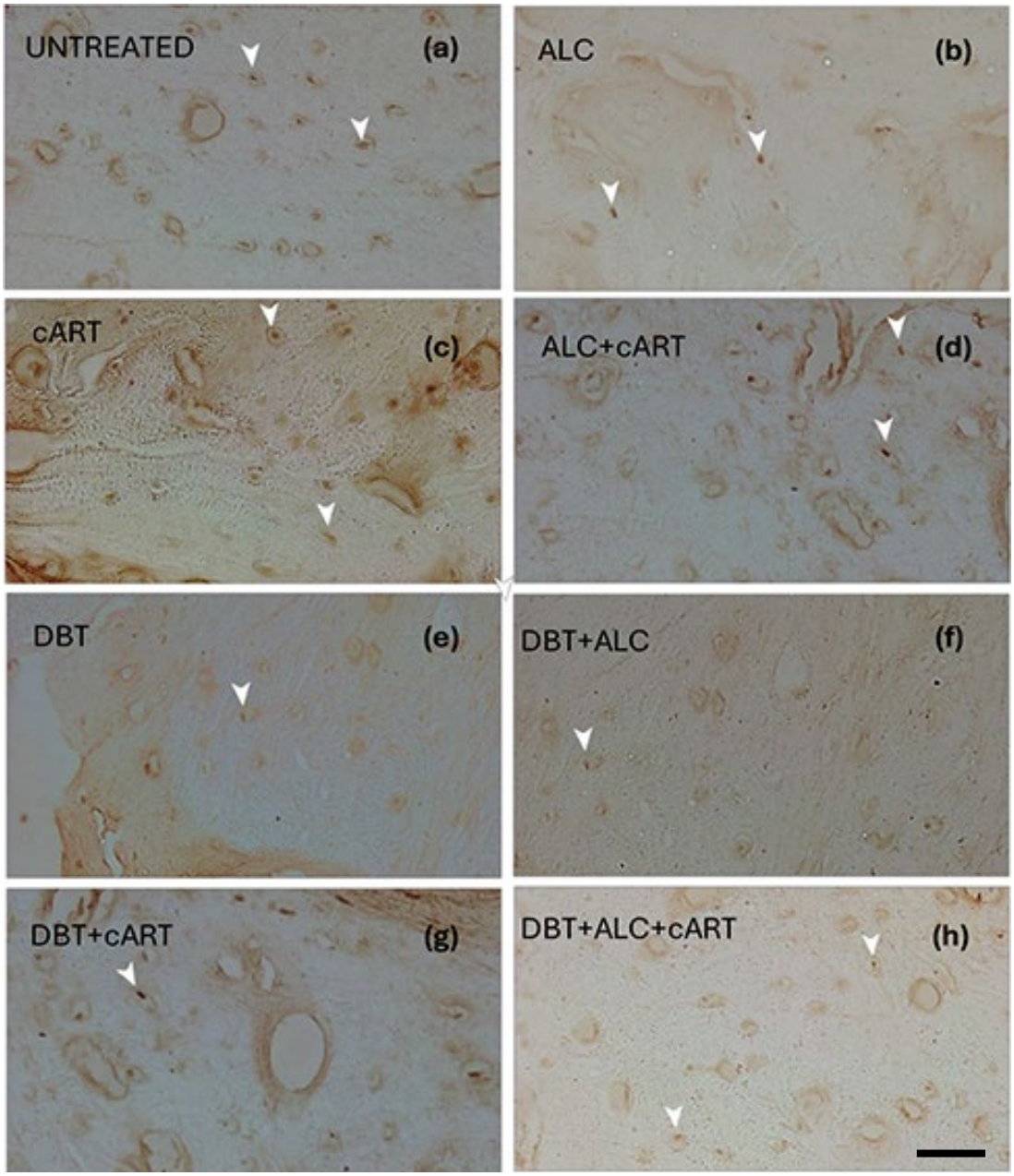

Figure 7.5: TRAP Immunopositive osteocytes in the mandible. Osteocytes are embedded in the bone matrix as depicted by the arrows and are found throughout a-h. Scale bar represents 40µm and applies all photomicrographs

Untreated control; ALC, alcohol; cART, combination antiretroviral treatment; ALC+cART, alcohol and cART; DBT, diabetic; DBT+ALC, diabetes and alcohol; DBT+cART, diabetes and cART; DBT+ALC+cART, diabetes, alcohol and cART

7.2.3 TGFβ1

None of the study group exhibited no staining for TGFβ1 (Table 7.1 and Fig 7.6). Half of the samples in the untreated control group showed mild staining while the other half moderately stained for TGFβ1 (Table 7.1 and Fig 7.6). The ALC group showed that half the samples stained moderately for TGFβ1, and one third showed intense staining but was not significantly deferent from the untreated control group (p=0.052). In contrast, the cART group, significant differences compared to the untreated group were detected as half the samples had intense staining while one third showed moderate staining for TGFβ1 (p=0.017) (Table 7.1 and Fig 7.6). Although two-thirds of the samples in the ALC+cART groups showed moderate staining for TGFβ1, this was not significantly different from the untreated control group (0.052). Majority of the samples in the DBT, DBT+ALC, DBT+cART and DBT+cART+ALC groups showed mild staining, but no significant differences were detected compared to the untreated control group (p=0.620 for all except 0.323 for DBT+cART+ALC) (Table 7.1 and Fig 7.6).

7.2.4 BMP-3

None of the study group exhibited no staining for BMP3 (Table 7.2 and Fig 7.7). The untreated group had half the samples showing mild staining whereas the other half had moderate staining for BMP3. Two thirds of the samples in the ALC and ALC+cART groups had moderate staining whereas only 1 sample in the cART group had moderate staining, with the other being mild. However, all these groups (ALC, cART, ALC+cART did not significantly differ from the untreated group (p=0.657, p=0.376 and p=0.657, respectively) (Table 7.2 and Fig 7.7).

One-third of the samples in the DBT group exhibited intense BMP3 immunostaining which was high compares to the intreated controls (p=0.011). Half of the samples in the DBT+ALC, DBT+cART and DBT+cART+ALC had intense BMP3 immunostaining (Table 7.2 and Fig 7.7). A third of the samples in the DBT+ALC, DBT+cART showed moderate staining and half of the DBT+cART+ALC samples had moderate staining (p=0.031, p=0.031 and p=0.011, respectively compared to the untreated control) (Table 7.2 and Fig 7.7).

The ALC group was significantly different from the DBT or DBT+cART+ALC which had more samples in the intense staining category (p=0.031 for both comparisons) (Table 7.2 and Fig 7.7).

Table 7.1: TGFβ1 Immunopositivity

Groups	N	No stain		Mild		Moderate		Intense		P value
		Count	%	Count	%	Count	%	Count	%	
Untreated	6	0	0	3	50.00	3	50.00	0	0	
ALC	6	0	0	1	16.70	3	50.00	2	33.30	0.052
cART	6	0	0	1	16.70	2	33.30	3	50.00	0.017
ALC+cART	6	0	0	0	0	4	66.70	2	33.30	0.052
DBT	6	0	0	4	66.70	2	33.30	0	0	0.620
DBT+ALC	6	0	0	4	66.70	2	33.30	0	0	0.620
DBT+cART	6	0	0	4	66.70	2	33.30	0	0	0.620
DBT+cART+ALC	6	0	0	5	83.30	1	16.70	0	0	0.323

ALC vs cART, ALC+cART, DBT+ALC, DBT+cART+ALC (p=0.620, p>0.999, p0.017, p=0.005);
cART vs ALC+cART, DBT+cART, DBT+cART+ALC (p=0.620, p=0.005, p=0.005, respectively);
DBT vs ALC, cART, DBT+ALC, DBT+cART, DBT+cART+ALC (p<0.017, p=0.005, p>0.999, p>0.999 and p>0.999, respectively); DBT+ALC vs DBT+cART, DBT+cART+ALC (p=0.017, p>0.999, respectively).

Untreated control; ALC, alcohol; cART, combination antiretroviral treatment; ALC+cART, alcohol and cART; DBT, diabetic; DBT+ALC, diabetes and alcohol; DBT+cART, diabetes and cART; DBT+ALC+cART, diabetes, alcohol and cART

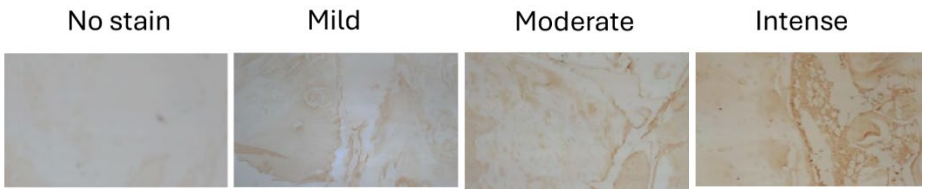

Figure 7.6: Mandibular TGFβ1 Immunopositivity graded. The grading was based on staining intensity

Table 7.2: BMP3 Immunopositivity

Groups	(N)	No stain		Mild		Moderate		Intense		P value
		Count	%	Count	%	Count	%	Count	%	
Untreated	6	0	0	3	50.00	3	50.00	0	0	
ALC	6	0	0	2	33.30	4	66.70	0	0	0.657
cART	6	0	0	5	83.30	1	16.70	0	0	0.376
ALC+cART	6	0	0	2	33.30	4	66.70	0	0	0.657
DBT	6	0	0	1	16.70	1	16.70	4	66.70	0.011
DBT+ALC	6	0	0	1	16.70	2	33.30	3	50.00	0.031
DBT+ALC	6	0	0	1	16.70	2	33.30	3	50.00	0.031
DBT+cART+ALC	6	0	0	0	0	3	50.00	3	50.00	0.011

ALC vs cART, ALC+cART, DBT+ALC, DBT+cART+ALC (p=0.187, p>0.999, p0.081, p=0.0031);
cART vs ALC+cART, DBT+cART, DBT+cART+ALC (p=0.187, p=0.003, p=0.001, respectively);
DBT vs ALC, cART, DBT+ALC, DBT+cART, DBT+cART+ALC (p<0.031, p=0.001, p=0.657, p=0.657 and p>0.999, respectively); DBT+ALC vs DBT+cART, DBT+cART+ALC (p=0.031, p=657, respectively).

Untreated control; ALC, alcohol; cART, combination antiretroviral treatment; ALC+cART, alcohol and cART; DBT, diabetic; DBT+ALC, diabetes and alcohol; DBT+cART, diabetes and cART; DBT+ALC+cART, diabetes, alcohol and cART

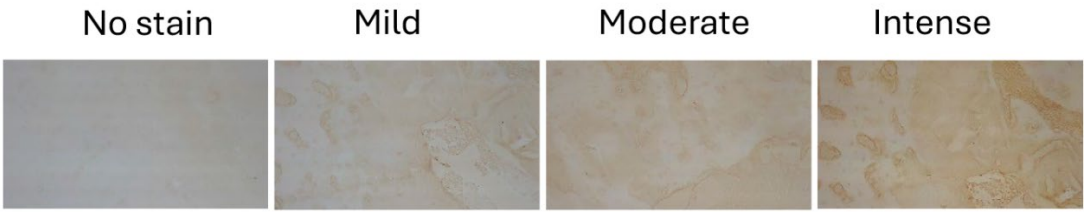

Figure 7.7: Mandibular BMP3 Immunopositivity graded. The grading was based on staining intensity

7.3 DISCUSSION

The purpose of the study was to assess the influence of alcohol intake and combination antiretroviral treatment use on osteocytes and the expression of TGFβ1 and BMP3 in the mandible of diabetic rats. The results showed that when diabetes was confounded by combination antiretroviral treatment and alcohol consumption (DBT+ALC+cART), osteogenic cells were negatively affected.

Anti-osteoblastogenic effects of adipocytes

Bone marrow adiposity contributes to skeletopathy through the development of adipogenic cell lines and suppression of osteogenic cell lineages (Gillet et al., 2017; Ferland-McCollough et al., 2018). In the present study all the treatments, either individually or in combinations exhibited significantly increased adiposity than the untreated controls. This is consistent with previous research which reports that alcohol consumption (Johnson et al., 2022), diabetes (Dlamini and Ndou, 2023) and antiretroviral therapy (Couturier et al., 2018) increase bone marrow adiposity. Adipocytes impair antiretroviral therapy through sequestration of the antiretroviral drugs (Couturier et al., 2018).

These marrow adipocytes secrete the hormone adiponectin that is anti-osteoblastogenic, pro-osteoclastogenic and promotes osteoblast apoptosis (Rharass and Lucas, 2018; Singh et al., 2018). This could partially explain the susceptibility of bones to fracture in diabetes (Gillet et al., 2017; Ferland-McCollough et al., 2018). This could possibly accentuate the increased risk to fracture of the proximal humerus.

Osteolysis

Diabetic rats (DBT), rats receiving alcohol only (ALC), diabetic rats given alcohol (DBT+ALC) and diabetic rats given alcohol and antiretroviral treatment (DBT+ALC+cART) had significantly fewer TRAP immunopositive cells than the untreated controls. TRAP immunolabeling in bone can be used to estimate the number of osteocytes in bone. Osteocytes are cells located within the bone and are "entrapped" osteoblasts. They are post-proliferative and represent the most mature differentiation state of the osteoblast lineage (Mohamed, 2008). The rate of osteogenic differentiation reduced, with defects in proliferation, differentiation and survival of osteoblasts among diabetic patients (Phimphilai et al., 2023) and long-term alcohol users (Sampson 1998). Therefore, it is plausible to attribute the low number of osteocytes in this study to the purported osteoblast disturbances as osteoblasts mature into osteocytes. Additionally, the observation that diabetic rats given alcohol and antiretroviral treatment (DBT+ALC+cART) had the least TRAP immunopositive cells suggest that the low osteocyte quantity was worsened when diabetes was confounded by combination antiretroviral treatment and alcohol consumption.

TGFβ1 and its antagonist BMP3

All the groups with diabetes, (DBT, DBT+ALC, DBT+ALC and DBT+cART+ALC) had significantly more BMP3 showing intense staining. BMP-3 is an anti-osteoblastgenesis cytokine as it inhibits the differentiation of osteoblasts (Wu et al., 2016; Kokabu and Rosen, 2018). The high intensity of BMP3 immunostaining observed in the present study corroborates the diminished TRAP immunopositivity as BMP3 is antagonistic to osteoblasts. The anti-osteogenic effects of BMP-3 are evident in increased bone fragility (Gamer et al., 2009; Horbelt et al., 2012). Increased

expression of BMP-3, as reported in diabetic bone, can affect the number and function of osteoblasts, leading to an increased risk of fracture associated with T2D (Wang et al., 2022).

Only the cART group had significantly more samples exhibiting intense staining for TGFB1 while all other groups did not show significant differences compared to the untreated control group. Alcohol has been reported to increase plasma TGFβ1 levels in alcoholic patients (Kim et al., 2009). Diabetes is known to reduce the expresionTGFB1 in bone (Kum et al., 2022). In the present study, both alcohol (ALC) and diabetes (DBT) or a combination of alcohol and diabetes did not change (DBT+ALC) the expression of TGFB1. This lack of change in TGFB1 expression compared to the untreated controls could be attributed to the method used to detect TGFB1 expression in the present study. TGFβ1 is an extracellular complex that is translocated into the intracellular domain to regulate bone cell differentiation (Ehnert et al., 2010; Yang et al., 2014). If follows, therefore that, for this cytokine to function, it must be translocated into the cytoplasm. The present study assessed extracellular TGFβ1. It is possible that a different finding could have been made had the study evaluated the intracellular TGFβ1 expression.

7.3.1 Conclusion

All groups had more adiposity than the untreated control as seen in previous diabetic studies. Diabetes (DBT), alcohol (ALC), diabetes with alcohol (DBT+ALC) or diabetics consuming alcohol and antiretroviral treatment (DBT+ALC+cART) significantly impaired osteocyte quantities. In addition, this low osteocyte quantity was worsened when diabetes was confounded by

combination antiretroviral treatment and alcohol consumption (DBT+ALC+cART) as this group had the least TRAP immunopositive cells. The high intensity of BMP3 immunostaining observed in the present study among the groups with diabetes, (DBT, DBT+ALC, DBT+ALC and DBT+cART+ALC) corroborates the diminished TRAP immunopositivity as BMP3 is antagonistic to osteoblasts. In the present study, both alcohol (ALC) and diabetes (DBT) or a combination of alcohol and diabetes (DBT+ALC) did not change the expression of TGFB1, possibly because extracellular expression of the cytokine was assessed. Evaluating the intracellular expression of TGFB1 in a future study is recommended. Viewed altogether, these results show that when diabetes was confounded by combination antiretroviral treatment and alcohol consumption (DBT+ALC+cART), osteogenic cells were negatively impacted. Therefore, diabetic patients should be advised to reduce alcohol intake and bone health should be monitored when combination antiretroviral therapy is employed.

Chapter 8

General Discussion and Conclusion

8.0 GENERAL DISCUSSION AND CONCLUSIONS

The deleterious effects of alcohol, combination antiretroviral therapy (cART) or diabetes are well-known. However, this knowledge is based on studies investigating each of these variables (alcohol, combination antiretroviral therapy (cART) or diabetes) separately. The combined effect of alcohol and cART on the mandible of diabetic rats has not been investigated previously. Therefore, the aim of the present study was to determine the impact of the interaction of alcohol and combination antiretroviral treatment (cART) on the diabetic Sprague Dawley rat mandible.

Diabetes was induced in the appropriate rat groups (DBT, DBT+ALC, DBT+cART and DBT+ALC+cART). Confirmation of diabetes was achieved by monitoring the fasting blood glucose levels, bone mass measurements, oral glucose tolerance tests (OGTT) and terminal serum insulin levels. This was followed by the assessment of serum levels of hormones that regulate bone health were. Afterwards, mandibular osteometry measurements were made. The trabecular microstructure parameters were assessed from microfocus X-ray computed tomography (Micro CT) to measure thickness (TbTh), spacing (TbSp), and number (TbN). The bones were tested for strength with a universal tensile tester and histologically evaluated for normal morphology. The expression of osteocytes, transforming growth factor beta-1 (TGF-1), and bone morphogenic protein-3 (BMP-3) was evaluated by immunohistochemistry.

We reported that over the duration of the study, there was hyporinsulinemia, hyperglycemia, weight loss and poor glucose handling as shown by OGTT findings among the diabetic groups (DBT, DBT+ALC, DBT+cART and DBT+ALC+cART) as a manifestation of diabetes.

Serum parathyroid hormone and calcitonin concentrations were low in rats that were diabetic and taking and cART (DBT+cART) or diabetic rats taking both alcohol and cART (DBT+ALC+cART). This may be attributed to parathyroid hormone secretion impairment in untreated diabetes mellitus (Paula et al., 2001). Since the liver metabolises both alcohol and antiretroviral drugs, liver function may be compromised (Yu et al., 2021). The poor regulation of parathyroid hormone and calcitonin concentrations is corroborated by weaker bones in the present study based on the bone strength tests. It remains unclear why in the present study, the diabatic rats that received both alcohol and cART (DBT+ALC+cART) had normal sclerostin and catenin levels. This finding suggests that this comorbidity of diabetes with alcohol intake and cART may not influence the function and concentrations sclerostin and catenin.

Insulin has osteo-anabolic effects on bone that cause an increase in osteoblast number while inhibiting osteoclast activity (Thrailkill et al., 2005; Huang et al., 2022). Therefore, in type 2 diabetes mellitus the bone exhibits a significant increase in trabecular and cortical bone mass and decreased bone strength (Huang et al., 2022). Insulin works in synergy with oestrogen and osteocalcin to regulate glucose metabolism, increase insulin sensitivity to tissues, increase

pancreatic beta cell proliferation, and increase insulin secretion (Lee et al., 2007; Booth et al., 2013; Kanazawa, 2015).

Carboxylated and non-carboxylated osteocalcin directly increase glucose transport in adipocytes and muscle cells (Hill et al., 2014). In the present study, serum osteocalcin concentration in diabetes alone (DBT), cART alone, and when diabetic rats received alcohol (DBT+ALC), these groups also recorded high bone marrow adiposity. It is possible that the high osteocalcin concentration in these groups (DBT, cART and DBT+ALC) could contribute to glucose transport in the abundant adipocytes.

Regarding mandibular external dimensions, the present study found that diabetes adversely affected mandibular osteometric dimensions and was worsened by concurrent alcohol and cART use (DBT+cART+ALC). When linking this to bone strength, the study found that the DBT+cART+ALC group was characterised by lower values for maximum force and break force, less displacement, and time to fracture, indicating stiff and brittle bones. This finding supports the proposition that concurrent use of alcohol and cART among diabetics produces a poor outcome for the bone, particularly the mandible.

Diabetes (DBT), alcohol (ALC), diabetes with alcohol (DBT+ALC) or diabetics consuming alcohol and antiretroviral treatment (DBT+ALC+cART) significantly impaired osteocyte quantities (TRAP immunopositive cells). This finding of diminished TRAP immunopositivity largely corroborates the high intensity of BMP3 immunostaining among the groups with diabetes, (DBT, DBT+ALC,

DBT+ALC and DBT+cART+ALC) as BMP3 has an inhibitory effect on osteoblasts. Since osteocytes originate from osteoblasts (Kierszenbaum and Tres, 2015) and BMP3 inhibits on osteoblastogenesis (Kokabu and Rosen, 2018), it is plausible to deduce that the low osteocyte quantities in the present study was due to the inhibitory effect BMP3.

While alcohol (ALC), diabetes (DBT) or a combination of alcohol and diabetes (DBT+ALC) did not change the expression of TGFB1, we found that when diabetes was confounded by combination antiretroviral treatment and alcohol consumption (DBT+ALC+cART), osteogenic cells were negatively impacted. This is shown by the low quantity TRAP immunopositive cells. This finding of low fewer TRAP immunopositive cells (without a change in the expression of TGFB1) suggests that the inhibitory effect BMP3 may be adequate in lowering osteocyte numbers (TRAP immunopositive cells) without impacting on the expression of TGFB1, which promotes osteoblastogenesis.

The low osteocyte quantities coupled with high intensity of BMP3 immunostaining in diabetic rats consuming alcohol and antiretroviral treatment (DBT+ALC+cART) are corroborated by the bone strength test results. The bones in this group (DBT+ALC+cART) were also weaker as 3 point bending tests showed the highest stiffness, with lower values for maximum force and break force, less displacement, and time to fracture. This indicates stiff and brittle bones and also supports our hypothesis that concomitant cART and alcohol use in diabetes may result in weaker bones.

Furthermore, while there was high BV/TV and TbN recorded in the DBT, DBT+cART and DBT+ALC+cART groups, this did not translate to stronger bones, therefore, these bones were of lower quality. These findings form a foundation for future research on future therapeutics and management of diabetic patients on cART, with regular alcohol intake, and particularly in dental treatments and management.

The results of this study but be interpreted with cognizance of the use of cART without HIV infection. It is recommended that dental practitioners consider the deleterious impact of alcohol and cART among diabetics.

Translationability of the study findings

For diabetic patients receiving combination antiretroviral therapy (cART) who require dental implant surgery, it's crucial to carefully manage their blood sugar levels (glycemic control) before the procedure. This is because well-controlled blood sugar significantly improves the chances of successful osseointegration, which is the process of the implant fusing with the surrounding bone. Essentially, high blood sugar can impair bone healing, making implant failure more likely. Therefore, optimizing blood sugar levels beforehand is a critical step. However, the lack of adequate training on this area of diabetic skeletopathy remains a barrier translate these findings into clinical interventions.

8.1 Limitations

1. Only male rats were used, therefore the findings may not apply to females
2. This is a rat study; therefore, the results must be applied with caution to humans
3. The RAT-OC/BGP (osteocalcin) ELISA kit (E-EL-RO243) did not indicate whether it is in the carboxylated or undercarboxylated form
4. A lager sample size may yield different results
5. The present study uses cART without HIV infection.

8.2 Conclusions

1. Diabetes induction and maintenance was successful in the present study as supported by various markers of type 2 diabetes (loss of body mass, abnormal OGTTs and fasting blood glucose, reduced insulin levels).
2. Rats taking both alcohol and cART (DBT+ALC+cART) had low serum parathyroid hormone and calcitonin concentrations.
3. Osteocalcin, sclerostin and catenin levels remained unaffected by concurrent use of alcohol and cART among diabetic rats.
4. Concurrent use of alcohol and cART among diabetics produces a poor outcome for the bone for the mandibular osteometric dimensions as shown by the smaller dimensions of the DBT+ALC+cART group.

5. Alcohol intake (ALC) or cART or a combination (ALC) or cART) or diabetes alone (DBT) or concurrent use of alcohol and cART among diabetics (DBT+ALC+cART) increased bone marrow adiposity.
6. The inhibitory effect of BMP3 was coupled with a reduction in osteocyte quantities (TRAP immunopositive cells) without a significant change in the expression of TGFB1.
7. Dental practitioners must be acquainted with the deleterious impact of alcohol and cART among diabetics when planning and managing patients

REFERENCES

Abeeleh, M.A., Z.B. Ismail, K.R. Alzaben, S.A. Abu-Halaweh, M.K. Al-Essa, J. Abuabeeleh, and M.M. Alsmady. 2009. Induction of diabetes mellitus in rats using intraperitoneal streptozotocin: a comparison between 2 strains of rats. *Eur J Sci Res*. 32:398-402.

Andersen, S., P. Noahsen, K.F. Rex, I. Fleischer, N. Albertsen, M.E. Jorgensen, L.K. Schaebel, and M.B. Laursen. 2018. Serum 25-hydroxyvitamin D, calcium and parathyroid hormone levels in Native and European populations in Greenland. *Br J Nutr*. 119:391-397.

Ang, B.R.G., and G. Yu. 2018. The role of fructose in type 2 diabetes and other metabolic diseases. *J Nutr Food Sci*. 8:659.

Angelova, P., and N. Boyadjiev. 2013. A review on the models of obesity and metabolic syndrome in rats. *Trakia J Sci*. 11:5-12.

Babić Leko, M., N. Pleić, I. Gunjača, and T. Zemunik. 2021. Environmental Factors That Affect Parathyroid Hormone and Calcitonin Levels. *Int J Mol Sci*. 23.

Bagi, C.M., E. Berryman, and M.R. Moalli. 2011. Comparative bone anatomy of commonly used laboratory animals: implications for drug discovery. *Comp Med*. 61:76-85.

Bahamonde, M.E., and K.M. Lyons. 2001. BMP3: to be or not to be a BMP. *JBJS*. 83:S56-S62.

Beikler, T., and T.F. Flemmig. 2003. Implants in the medically compromised patient. *Crit Rev Oral Biol Med*. 14:305-316.

Bell, G.I., and K.S. Polonsky. 2001. Diabetes mellitus and genetically programmed defects in beta-cell function. *Nature*. 414:788-791.

Bertram, M.Y., A.V. Jaswal, V.P. Van Wyk, N.S. Levitt, and K.J. Hofman. 2013. The non-fatal disease burden caused by type 2 diabetes in South Africa, 2009. *Glob Health Action*. 6:19244.

Bismar, H., T. Kloppinger, E.M. Schuster, S. Balbach, I. Diel, R. Ziegler, and J. Pfeilschifter. 1999. Transforming growth factor beta (TGF-beta) levels in the conditioned media of human bone cells: relationship to donor age, bone volume, and concentration of TGF-beta in human bone matrix in vivo. *Bone*. 24:565-569.

Blaslov, K., F.S. Naranda, I. Kruljac, and I.P. Renar. 2018. Treatment approach to type 2 diabetes: Past, present and future. *World J Diabetes*. 9:209-219.

Bolamperti, S., I. Villa, and A. Rubinacci. 2022. Bone remodeling: an operational process ensuring survival and bone mechanical competence. *Bone Res*. 10:48.

Booth, S.L., A. Centi, S.R. Smith, and C. Gundberg. 2013. The role of osteocalcin in human glucose metabolism: marker or mediator? *Nat Rev Endocrinol*. 9:43-55.

Bouxsein, M.L., S.K. Boyd, B.A. Christiansen, R.E. Guldberg, K.J. Jepsen, and R. Muller. 2010. Guidelines for assessment of bone microstructure in rodents using micro-computed tomography. *J Bone Miner Res*. 25:1468-1486.

Boyle, W.J., W.S. Simonet, and D.L. Lacey. 2003. Osteoclast differentiation and activation. *Nature*. 423:337-342.

Carels, C., M. Florence, S. Adams, and S. Savahl. 2023. Alcohol use as a predictor of risky sexual behaviour among young adults in the Western Cape province of South Africa. *Int J Environ Res Public Health*. 20:7053.

Castronuovo, D., M. Pinzone, S. Moreno, B. Cacopardo, and G. Nunnari. 2015. HIV infection and bone disease: a review of the literature. *Infect Dis Trop Med*. 1:e116.

Chandrasekera, P.C., and J.J. Pippin. 2014. Of rodents and men: species-specific glucose regulation and type 2 diabetes research. *ALTEX*. 31:157-176.

Chao, P.C., Y. Li, C.H. Chang, J.P. Shieh, J.T. Cheng, and K.C. Cheng. 2018. Investigation of insulin resistance in the popularly used four rat models of type-2 diabetes. *Biomed Pharmacother*. 101:155-161.

Chappard, D., M.F. Basle, E. Legrand, and M. Audran. 2008. Trabecular bone microarchitecture: a review. *Morphologie*. 92:162-170.

Charles, J.F., and A.O. Aliprantis. 2014. Osteoclasts: more than 'bone eaters'. *Trends Mol Med*. 20:449-459.

Chen, J., C. Ning, J. Mu, D. Li, Y. Ma, and X. Meng. 2021. Role of Wnt signaling pathways in type 2 diabetes mellitus. *Mol Cell Biochem*. 476:2219-2232.

Chiodini, I., A. Catalano, L. Gennari, and A. Gaudio. 2020. Osteoporosis and fragility fractures in type 2 diabetes. *J Diabetes Res*. 2020:9342696.

Chwiki, S., M.M. Campos, M.E. McLaughlin, D.E. Kleiner, J.A. Kovacs, C.G. Morse, and M.S. Abu-Asab. 2017. Adverse effects of antiretroviral therapy on liver hepatocytes and endothelium in HIV patients: An ultrastructural perspective. *Ultrastruct Pathol*. 41:186-195.

Couturier, J., L.C. Winchester, J.W. Suliburk, G.K. Wilkerson, A.T. Podany, N. Agarwal, C.Y. Xuan Chua, P.N. Nehete, B.P. Nehete, A. Grattoni, K.J. Sastry, C.V. Fletcher, J.E. Lake, A. Balasubramanyam, and D.E. Lewis. 2018. Adipocytes impair efficacy of antiretroviral therapy. *Antiviral Research*. 154:140-148.

Crossley, D.A. 1995. Clinical aspects of rodent dental anatomy. *J Vet Dent*. 12:131-135.

Daluiski, A., T. Engstrand, M.E. Bahamonde, L.W. Gamer, E. Agius, S.L. Stevenson, K. Cox, V. Rosen, and K.M. Lyons. 2001. Bone morphogenetic protein-3 is a negative regulator of bone density. *Nature Genetics*. 27:84-88.

Dangarembizi, R., P. Nkomozepi, and R. Ndou. 2020. Type 2 diabetes mellitus-related non-alcoholic steatohepatitis in the Zucker Diabetic Sprague Dawley rat. *JMLSTSA*. 2:36.

Dave, J.A., K. Cohen, L.K. Micklesfield, G. Maartens, and N.S. Levitt. 2015. Antiretroviral therapy, especially efavirenz, is associated with low bone mineral density in HIV-infected South Africans. *PLoS One*. 10:e0144286.

Davison, K.S., K. Siminoski, J. Adachi, D.A. Hanley, D. Goltzman, A.B. Hodsman, R. Josse, S. Kaiser, W.P. Olszynski, and A. Papaioannou. 2006. Bone strength: the whole is greater than the sum of its parts. *In* Seminars in arthritis and rheumatism. Vol. 36. Elsevier. 22-31.

de Araújo, I.M., M.L.M. Moreira, and F.J.A. de Paula. 2022. Diabetes and bone. *Arch Endocrinol Metab*. 66:633-641.

Delpino, M.V., and J. Quarleri. 2020. Influence of HIV Infection and Antiretroviral Therapy on Bone Homeostasis. *Front Endocrinol (Lausanne)*. 11:502.

Desentis-Desentis, M.F., J.D. Rivas-Carrillo, and S. Sanchez-Enriquez. 2020. Protective role of osteocalcin in diabetes pathogenesis. *J Bone Miner Metab*. 38:765-771.

Diez, A., S. Serrano, J. Cucurull, L. Marinoso, J. Bosch, J. Puig, X. Nogues, and J. Aubia. 1997. Acute effects of ethanol on mineral metabolism and trabecular bone in Sprague-Dawley rats. *Calcif Tissue Int*. 61:168-171.

Dlamini, G.F., and R. Ndou. 2023. Osteoblastogenesis and osteolysis in the Zucker Diabetic Sprague Dawley rat humerus head. *Anat Cell Biol*. 56:552-561.

Dole, N.S., C.M. Mazur, C. Acevedo, J.P. Lopez, D.A. Monteiro, T.W. Fowler, B. Gludovatz, F. Walsh, J.N. Regan, and S. Messina. 2017. Osteocyte-intrinsic TGF-β signaling regulates bone quality through perilacunar/canalicular remodeling. *Cell Reports*. 21:2585-2596.

Dreyer, T.J., J.A. Keen, L.M. Wells, and S.J. Roberts. 2023. Novel insights on the effect of sclerostin on bone and other organs. *J Endocrinol*. 257:e220209.

Duan, L., Q. Yang, J. Yang, Q. Hu, B. Wang, P. Li, and W. Chen. 2018. Identification of serum beta-catenin as a biomarker in patients with HBV-related liver diseases. *J Transl Med*. 16:265.

Dyer, S.A., P. Buckendahl, and H.W. Sampson. 1998. Alcohol consumption inhibits osteoblastic cell proliferation and activity in vivo. *Alcohol*. 16:337-341.

Ehnert, S., J. Baur, A. Schmitt, M. Neumaier, M. Lucke, S. Dooley, H. Vester, B. Wildemann, U. Stöckle, and A.K. Nussler. 2010. TGF-β1 as possible link between loss of bone mineral density and chronic inflammation. *PloS one*. 5:e14073.

Elovic, R.P., J.A. Hipp, and W.C. Hayes. 1995. Ovariectomy decreases the bone area fraction of the rat mandible. *Calcif Tissue Int*. 56:305-310.

Engler, P.A., S.E. Ramsey, and R.J. Smith. 2013. Alcohol use of diabetes patients: the need for assessment and intervention. *Acta Diabetol*. 50:93-99.

Esfahanian, V., M.S. Shamami, and M.S. Shamami. 2012. Relationship between osteoporosis and periodontal disease: review of the literature. *J Dent (Tehran)*. 9:256-264.

Etuk, E. 2010. Animals models for studying diabetes mellitus. *Agric Biol JN Am*. 1:130-134.

Fajardo, R.J., L. Karim, V.I. Calley, and M.L. Bouxsein. 2014. A review of rodent models of type 2 diabetic skeletal fragility. *J Bone Miner Res*. 29:1025-1040.

Fang, J.-Y., C.-H. Lin, T.-H. Huang, and S.-Y. Chuang. 2019. In vivo rodent models of type 2 diabetes and their usefulness for evaluating flavonoid bioactivity. *Nutrients*. 11:530.

Feng, X., and J.M. McDonald. 2011. Disorders of bone remodeling. *Annu Rev Pathol*. 6:121-145.

Ferland-McCollough, D., D. Maselli, G. Spinetti, M. Sambataro, N. Sullivan, A. Blom, and P. Madeddu. 2018. MCP-1 feedback loop between adipocytes and mesenchymal stromal cells causes fat accumulation and contributes to hematopoietic stem cell rarefaction in the bone marrow of patients with diabetes. *Diabetes*. 67:1380-1394.

Ferron, M., and J. Lacombe. 2014. Regulation of energy metabolism by the skeleton: osteocalcin and beyond. *Arch Biochem Biophys*. 561:137-146.

Florencio-Silva, R., G.R.d.S. Sasso, E. Sasso-Cerri, M.J. Simões, and P.S. Cerri. 2015. Biology of bone tissue: structure, function, and factors that influence bone cells. *Biomed Res Int*. 2015.

Frazão, D.R., C. Maia, V.D.S. Chemelo, D. Monteiro, R.O. Ferreira, L.O. Bittencourt, G.S. Balbinot, F.M. Collares, C.K. Rösing, M.D. Martins, and R.R. Lima. 2020. Ethanol binge drinking exposure affects alveolar bone quality and aggravates bone loss in experimentally-induced periodontitis. *PLoS One*. 15:e0236161.

Furman, B.L. 2021. Streptozotocin-induced diabetic models in mice and rats. *Curr Protoc*. 1:e78.

Galicia-Garcia, U., A. Benito-Vicente, S. Jebari, A. Larrea-Sebal, H. Siddiqi, K.B. Uribe, H. Ostolaza, and C. Martín. 2020. Pathophysiology of type 2 diabetes mellitus. *Int J Mol Sci*. 21.

Gamer, L.W., K. Cox, J.M. Carlo, and V. Rosen. 2009. Overexpression of BMP3 in the developing skeleton alters endochondral bone formation resulting in spontaneous rib fractures. *Dev Dyn*. 238:2374-2381.

Gaudio, A., F. Privitera, K. Battaglia, V. Torrisi, M.H. Sidoti, I. Pulvirenti, E. Canzonieri, G. Tringali, and C.E. Fiore. 2012. Sclerostin levels associated with inhibition of the Wnt/beta-catenin signaling and reduced bone turnover in type 2 diabetes mellitus. *J Clin Endocrinol Metab*. 97:3744-3750.

Ghasemi, A., S. Khalifi, and S. Jedi. 2014. Streptozotocin-nicotinamide-induced rat model of type 2 diabetes (review). *Acta Physiol Hung*. 101:408-420.

Gillet, C., A. Dalla Valle, N. Gaspard, D. Spruyt, P. Vertongen, J. Lechanteur, S. Rigutto, E.R. Dragan, A. Heuschling, V. Gangji, and J. Rasschaert. 2017. Osteonecrosis of the femoral head: Lipotoxicity exacerbation in MSC and modifications of the bone marrow fluid. *Endocrinology*. 158:490-502.

Godos, J., F. Giampieri, E. Chisari, A. Micek, N. Paladino, T.Y. Forbes-Hernández, J.L. Quiles, M. Battino, S. La Vignera, G. Musumeci, and G. Grosso. 2022. Alcohol Consumption, Bone Mineral Density, and Risk of Osteoporotic Fractures: A Dose-Response Meta-Analysis. *Int J Environ Res Public Health*. 19.

Goltzman, D. 2018. Physiology of parathyroid hormone. *Clin Endocrinol Metab*. 47:743-758.

Green, A.D., S. Vasu, and P.R. Flatt. 2018. Cellular models for beta-cell function and diabetes gene therapy. *Acta Physiol (Oxf)*. 222:e13012.

Gregson, C.L., T. Madanhire, A. Rehman, R.A. Ferrand, A.R. Cappola, S. Tollman, T. Mokoena, L.K. Micklesfield, A.N. Wade, and J. Fabian. 2022. Osteoporosis, rather rhan sarcopenia, Is the predominant musculoskeletal disease in a rural South African community where Human Immunodeficiency Virus rrevalence Is high: a cross-sectional study. *J Bone Miner Res*. 37:244-255.

Grigsby, I.F., L. Pham, L.M. Mansky, R. Gopalakrishnan, and K.C. Mansky. 2010. Tenofovir-associated bone density loss. *Ther Clin Risk Manag*. 6:41-47.

Guariguata, L., D.R. Whiting, I. Hambleton, J. Beagley, U. Linnenkamp, and J.E. Shaw. 2014. Global estimates of diabetes prevalence for 2013 and projections for 2035. *Diabetes Res Clin Pract*. 103:137-149.

Gutreuter, S., E. Igumbor, N. Wabiri, M. Desai, and L. Durand. 2019. Improving estimates of district HIV prevalence and burden in South Africa using small area estimation techniques. *PLoS One*. 14:e0212445.

Hamann, C., C. Goettsch, J. Mettelsiefen, V. Henkenjohann, M. Rauner, U. Hempel, R. Bernhardt, N. Fratzl-Zelman, P. Roschger, and S. Rammelt. 2011. Delayed bone regeneration and low bone mass in a rat model of insulin-resistant type 2 diabetes mellitus is due to impaired osteoblast function. *Am J Physiol Endocrinol Metab*. 301:E1220-E1228.

Harris, M., B. Nosyk, R. Harrigan, V.D. Lima, C. Cohen, and J. Montaner. 2012. Cost-effectiveness of antiretroviral therapy for multidrug-resistant HIV: past, present, and future. *AIDS Res Treatment*. 2012.

Hasegawa, H., S. Ozawa, K. Hashimoto, T. Takeichi, and T. Ogawa. 2008. Type 2 diabetes impairs implant osseointegration capacity in rats. *Int J Oral Maxillofac Implants*. 23:237-246.

He, H., R. Liu, T. Desta, C. Leone, L.C. Gerstenfeld, and D.T. Graves. 2004. Diabetes causes decreased osteoclastogenesis, reduced bone formation, and enhanced apoptosis of osteoblastic cells in bacteria stimulated bone loss. *Endocrinology*. 145:447-452.

Henneicke, H., S.J. Gasparini, T.C. Brennan-Speranza, H. Zhou, and M.J. Seibel. 2014. Glucocorticoids and bone: local effects and systemic implications. *Trends Endocrinol Metab*. 25:197-211.

Hill, H.S., J. Grams, R.G. Walton, J. Liu, D.R. Moellering, and W.T. Garvey. 2014. Carboxylated and uncarboxylated forms of osteocalcin directly modulate the glucose transport system and inflammation in adipocytes. *Horm Metab Res*. 46:341-347.

Hoang, Q.Q., F. Sicheri, A.J. Howard, and D.S. Yang. 2003. Bone recognition mechanism of porcine osteocalcin from crystal structure. *Nature*. 425:977-980.

Holt, R.I. 2004. Diagnosis, epidemiology and pathogenesis of diabetes mellitus: an update for psychiatrists. *Br J Psychiatry Suppl*. 47:S55-63.

Honnapurmath, V.K., and V.W. Patil. 2017. Antiretroviral Therapy-induced Insulin Resistance and Oxidative Deoxy Nucleic Acid Damage in Human Immunodeficiency Virus-1 Patients. *Indian J Endocrinol Metab*. 21:316-321.

Horbelt, D., A. Denkis, and P. Knaus. 2012. A portrait of transforming growth bactor beta superfamily signalling: background matters. *Int J Biochem Cell Biol*. 44:469-474.

Horberg, M.A., and D.B. Klein. 2010. An update on the use of Atripla in the treatment of HIV in the United States. *HIV AIDS (Auckl)*. 2:135-140.

Hsu, P.Y., M.T. Tsai, S.P. Wang, Y.J. Chen, J. Wu, and J.T. Hsu. 2016. Cortical bone morphological and trabecular bone microarchitectural changes in the mandible and femoral neck of ovariectomized rats. *PLoS One*. 11:e0154367.

Hu, F.B., J.E. Manson, M.J. Stampfer, G. Colditz, S. Liu, C.G. Solomon, and W.C. Willett. 2001. Diet, lifestyle, and the risk of type 2 diabetes mellitus in women. *N Engl J Med*. 345:790-797.

Huang, J., Y. Zhou, W. Xiao, P. Deng, Q. Wei, and W. Lu. 2022. Serum beta-catenin changes vary among different stages of osteonecrosis of the femoral head: an exploratory biomarker study. *BMC Musculoskelet Disord*. 23:434.

Ilich, J.Z., R.A. Brownbill, L. Tamborini, and Z. Crncevic-Orlic. 2002. To drink or not to drink: how are alcohol, caffeine and past smoking related to bone mineral density in elderly women? *J Am Coll Nutr*. 21:536-544.

kim, M.S., and R.D. Wilson. 2012. Experimentally induced rodent models of type 2 diabetes. *Methods Mol Biol*. 933:161-174.

Janssens, K., P. ten Dijke, S. Janssens, and W. Van Hul. 2005. Transforming growth factor-beta1 to the bone. *Endocr Rev*. 26:743-774.

Jepsen, K.J., M.J. Silva, D. Vashishth, X.E. Guo, and M.C. van der Meulen. 2015. Establishing biomechanical mechanisms in mouse models: practical guidelines for systematically evaluating phenotypic changes in the diaphyses of long bones. *J Bone Miner Res*. 30:951-966.

Jiang, G., H. Matsumoto, J. Yamane, N. Kuboyama, Y. Akimoto, and A. Fujii. 2004. Prevention of trabecular bone loss in the mandible of ovariectomized rats. *J Oral Sci*. 46:75-85.

Jindal, M., O. Lakhwani, K. Omkar, S. Agarwal, and G. Keerty. 2018. Bone density versus bone quality as a predictor of bone strength. *Orthop Rheumatol*. 12:21-31.

Johnson, J.T., M.A. Hussain, K.E. Cherian, N. Kapoor, and T.V. Paul. 2022. Chronic Alcohol Consumption and its Impact on Bone and Metabolic Health - A Narrative Review. *Indian J Endocrinol Metab*. 26:206-212.

Julg, B., and J.R. Bogner. 2008. Atriplatrade mark - HIV therapy in one pill. *Ther Clin Risk Manag*. 4:573-577.

Junqueira, L., and J. Carneiro. 2003. Basic Histology, 10th Edn, Lange Edition. McGraw Hill. 340 pp.

Kanazawa, I. 2015. Osteocalcin as a hormone regulating glucose metabolism. *World J Diabetes*. 6:1345.

Kao, W.H., I.B. Puddey, L.L. Boland, R.L. Watson, and F.L. Brancati. 2001. Alcohol consumption and the risk of type 2 diabetes mellitus: atherosclerosis risk in communities study. *Am J Epidemiol*. 154:748-757.

Karamanou, M., A. Protogerou, G. Tsoucalas, G. Androutsos, and E. Poulakou-Rebelakou. 2016. Milestones in the history of diabetes mellitus: the main contributors. *World J Diabetes*. 7:1-7.

Karsenty, G. 2017. Update on the biology of osteocalcin. *Endocr Pract*. 23:1270-1274.

Kaya, S., J. Basta-Pljakic, Z. Seref-Ferlengez, R.J. Majeska, L. Cardoso, T.G. Bromage, Q. Zhang, C.R. Flach, R. Mendelsohn, S. Yakar, S.P. Fritton, and M.B. Schaffler. 2017. Lactation-induced changes in the volume of osteocyte lacunar-canalicular space alter mechanical properties in cortical bone tissue. *J Bone Miner Res*. 32:688-697.

Ke, Y., H. Hu, J. Zhang, L. Yuan, T. Li, Y. Feng, Y. Wu, X. Fu, M. Wang, Y. Gao, W. Huo, Y. Chen, W. Zhang, L. Wang, X. Li, J. Pang, Z. Zheng, F. Hu, M. Zhang, L. Sun, Y. Zhao, J. Lu, and D. Hu. 2023. Alcohol Consumption and Risk of Fractures: A Systematic Review and Dose-Response Meta-Analysis of Prospective Cohort Studies. *Adv Nutr*. 14:599-611.

Keller, J., P. Catala-Lehnen, A.K. Huebner, A. Jeschke, T. Heckt, A. Lueth, M. Krause, T. Koehne, J. Albers, J. Schulze, S. Schilling, M. Haberland, H. Denninger, M. Neven, I. Hermans-Borgmeyer, T. Streichert, S. Breer, F. Barvencik, B. Levkau, B. Rathkolb, E. Wolf, J. Calzada-Wack, F. Neff, V. Gailus-Durner, H. Fuchs, M.H. de Angelis, S. Klutmann, E. Tsourdi, L.C. Hofbauer, B. Kleuser, J. Chun, T. Schinke, and M. Amling. 2014. Calcitonin controls bone formation by inhibiting the release of sphingosine 1-phosphate from osteoclasts. *Nat Commun*. 5:5215.

Khin, P.P., J.H. Lee, and H.-S. Jun. 2023. Pancreatic beta-cell dysfunction in type 2 tiabetes. *Euro J Inflamm*. 21:172.

Kierszenbaum, A.L., and L. Tres. 2015. Histology and cell ciology: an introduction to pathology Elsevier Health Sciences.

Kim, S.J., and D.J. Kim. 2012. Alcoholism and diabetes mellitus. *Diabetes Metab J*. 36:108-115.

Kim, Y.K., B.C. Lee, B.J. Ham, B.H. Yang, S. Roh, J. Choi, T.C. Kang, Y.G. Chai, and I.G. Choi. 2009. Increased transforming growth factor-beta1 in alcohol dependence. *J Korean Med Sci*. 24:941-944.

King, A., and J. Bowe. 2016. Animal models for diabetes: Understanding the pathogenesis and finding new treatments. *Biochem Pharmacol*. 99:1-10.

King, A.J. 2012. The use of animal models in diabetes research. *Br J Pharmacol*. 166:877-894.

Kinney, J.H., N.E. Lane, and D.L. Haupt. 1995. In vivo, three-dimensional microscopy of trabecular bone. *J Bone Miner Res*. 10:264-270.

Kleinert, M., C. Clemmensen, S.M. Hofmann, M.C. Moore, S. Renner, S.C. Woods, P. Huypens, J. Beckers, M.H. De Angelis, and A. Schürmann. 2018. Animal models of obesity and diabetes mellitus. *Nat Rev Endocrinol*. 14:140-162.

Klintstrom, E., B. Klintstrom, D. Pahr, T.B. Brismar, O. Smedby, and R. Moreno. 2018. Direct estimation of human trabecular bone stiffness using cone beam computed tomography. *Oral Surg Oral Med Oral Pathol Oral Radiol*. 126:72-82.

Kokabu, S., and V. Rosen. 2018. BMP3 expression by osteoblast lineage cells is regulated by canonical Wnt signaling. *FEBS Open Bio*. 8:168-176.

Kottaisamy, C.P.D., D.S. Raj, V. Prasanth Kumar, and U. Sankaran. 2021. Experimental animal models for diabetes and its related complications-a review. *Lab Anim Res*. 37:23.

Kousignian, I., A. Sautereau, C. Vigouroux, A. Cros, S. Kretz, J.P. Viard, and L. Slama. 2021. Diagnosis, risk factors and management of diabetes mellitus in HIV-infected persons in France: A real-life setting study. *PLoS One*. 16:e0250676.

Kufley, S., J.E. Scott, and G. Ramirez-Yanez. 2017. The effect of the physical consistency of the diet on the bone quality of the mandibular condyle in rats. *Arch Oral Biol*. 77:23-26.

Kum, J.J.Y., C.J. Howlett, and Z.A. Khan. 2022. Dysregulated transforming growth factor-beta mediates early bone marrow dysfunction in diabetes. *Communications Biology*. 5:1145.

Kumar, S.P., and A.M. Sandhya. 2018. A study on the glycemic, lipid and blood pressure control among the type 2 diabetes patients of north Kerala, India. *Indian Heart J*. 70:482-485.

Kusy, R.P., P.F. Hirsch, and T.C. Peng. 1989. Influence of ethanol on stiffness, toughness, and ductility of femurs of rats. *Alcohol Clin Exp Res*. 13:185-189.

Lakhtakia, R. 2013. The history of diabetes mellitus. *Sultan Qaboos Univ Med J*. 13:368-370.

Lauing, K., R. Himes, M. Rachwalski, P. Strotman, and J.J. Callaci. 2008. Binge alcohol treatment of adolescent rats followed by alcohol abstinence is associated with site-specific differences in bone loss and incomplete recovery of bone mass and strength. *Alcohol*. 42:649-656.

LeBoff, M.S., S.L. Greenspan, K.L. Insogna, E.M. Lewiecki, K.G. Saag, A.J. Singer, and E.S. Siris. 2022. The clinician's guide to prevention and treatment of osteoporosis. *Osteoporos Int*. 33:2049-2102.

Lee, N.K., H. Sowa, E. Hinoi, M. Ferron, J.D. Ahn, C. Confavreux, R. Dacquin, P.J. Mee, M.D. McKee, D.Y. Jung, Z. Zhang, J.K. Kim, F. Mauvais-Jarvis, P. Ducy, and G. Karsenty. 2007. Endocrine regulation of energy metabolism by the skeleton. *Cell*. 130:456-469.

Leppanen, O., H. Sievanen, J. Jokihaara, I. Pajamaki, and T.L. Jarvinen. 2006. Three-point bending of rat femur in the mediolateral direction: introduction and validation of a novel biomechanical testing protocol. *J Bone Miner Res*. 21:1231-1237.

Leung, K., K. Fung, A. Sher, C. Li, and K. Lee. 1993. Plasma bone-specific alkaline phosphatase as an indicator of osteoblastic activity. *J Bone Joint Surg Br*. 75:288-292.

Li, J., H. Zhang, C. Yang, Y. Li, and Z. Dai. 2016. An overview of osteocalcin progress. *J Bone Miner Metab*. 34:367-379.

Li, S., C. Moog, T. Zhang, and B. Su. 2022. HIV reservoir: antiviral immune responses and immune interventions for curing HIV infection. *Chin Med J (Engl)*. 135:2667-2676.

Lin, H.H., H.Y. Hsu, M.C. Tsai, L.Y. Hsu, K.L. Chien, and T.L. Yeh. 2021. Association between type 2 diabetes and osteoporosis risk: a representative cohort study in Taiwan. *PLoS One*. 16:e0254451.

Liu, J., Q. Xiao, J. Xiao, C. Niu, Y. Li, X. Zhang, Z. Zhou, G. Shu, and G. Yin. 2022. Wnt/beta-catenin signalling: function, biological mechanisms, and therapeutic opportunities. *Signal Transduct Target Ther*. 7:3.

Lunati, M.E., V. Grancini, C. Colombo, E. Palmieri, V. Resi, M. Perrino, E. Orsi, and L. Fugazzola. 2016. Basal and stimulated calcitonin levels in patients with type 2 diabetes did not change during 1 year of Liraglutide treatment. *Metabolism*. 65:1-6.

MacFarlane, I. 1990. Mathew Dobson of Liverpool (1735–1784) and the history of diabetes. *Pract Diabetes*. 7:246-248.

Mahmoud, A.A., and S.M. Elshazly. 2014. Ursodeoxycholic acid ameliorates fructose-induced metabolic syndrome in rats. *PLoS One*. 9:e106993.

Maki, K., T. Nishioka, E. Shioiri, T. Takahashi, and M. Kimura. 2002. Effects of dietary consistency on the mandible of rats at the growth stage: computed X-ray densitometric and cephalometric analysis. *Angle Orthod*. 72:468-475.

Manyema, M., J.L. Veerman, L. Chola, A. Tugendhaft, D. Labadarios, and K. Hofman. 2015. Decreasing the burden of type 2 diabetes in South Africa: the impact of taxing sugar-sweetened beverages. *PLoS One*. 10:e0143050.

Martin-Gonzalez, C., A.M. Godoy-Reyes, P. Abreu-Gonzalez, C.M. Fernandez-Rodriguez, E. Martin-Ponce, M.J. Sanchez-Perez, J.C. Alvisa-Negrin, M. Rodriguez-Gaspar, and E. Gonzalez-Reimers. 2023. Sclerostin, vascular risk factors, and brain atrophy in excessive drinkers. *Front Hum Neurosci*. 17:1084756.

Masi, L., and M.L. Brandi. 2007. Calcitonin and calcitonin receptors. *Clin Cases Miner Bone Metab*. 4:117-122.

Masiello, P., C. Broca, R. Gross, M. Roye, M. Manteghetti, D. Hillaire-Buys, M. Novelli, and G. Ribes. 1998. Experimental NIDDM: development of a new model in adult rats administered streptozotocin and nicotinamide. *Diabetes*. 47:224-229.

Maurel, D.B., N. Boisseau, C.-L. Benhamou, and C. Jaffré. 2012. Cortical bone is more sensitive to alcohol dose effects than trabecular bone in the rat. *Joint Bone Spine*. 79:492-499.

McCreadie, B.R., R.W. Goulet, L.A. Feldkamp, and S.A. Goldstein. 2001. Hierarchical structure of bone and micro-computed tomography. *Adv Exp Med Biol*. 496:67-83.

Mizokami, A., T. Kawakubo-Yasukochi, and M. Hirata. 2017. Osteocalcin and its endocrine functions. *Biochem Pharmacol*. 132:1-8.

Modarresi, R., Z. Xiang, M. Yin, and J. Laurence. 2009. WNT/beta-catenin signaling is involved in regulation of osteoclast differentiation by human immunodeficiency virus protease inhibitor ritonavir: relationship to human immunodeficiency virus-linked bone mineral loss. *Am J Pathol*. 174:123-135.

Mohamed, A.M. 2008. An overview of bone cells and their regulating factors of differentiation. *Malays J Med Sci*. 15:4-12.

Mohamed, J., A.H. Nazratun Nafizah, A.H. Zariyantey, and S.B. Budin. 2016. Mechanisms of diabetes-induced liver damage: the role of oxidative stress and inflammation. *Sultan Qaboos Univ Med J*. 16:e132-141.

Molina, P.E., G.J. Bagby, and S. Nelson. 2014. Biomedical consequences of alcohol use disorders in the HIV-infected host. *Curr HIV Res*. 12:265-275.

Morgan, E.F., and L.C. Gerstenfeld. 2021. The bone organ system: form and function. *In* Marcus and Feldman's osteoporosis. Elsevier. 15-35.

Mtshali, S., and O. Mahomed. 2020. Patient-level predictors of diabetes-related lower extremity amputations at a quaternary hospital in South Africa. *Plos one*. 15:e0240588.

Mutuli, L.A., P. Bukhala, and G. Nguka. 2020. Dietary Intake Patterns of Alcoholics; A Case Study of Selected Rehabilitation Centers in Kenya. *Int. J. Nutr.* 5:42-47.

Nakano, Y., S. Toyosawa, and Y. Takano. 2004. Eccentric localization of osteocytes expressing enzymatic activities, protein, and mRNA signals for type 5 tartrate-resistant acid phosphatase (TRAP). *J Histochem Cytochem*. 52:1475-1482.

Natukunda, E., A. Szubert, C. Otike, I. Namyalo, E. Nambi, A. Bamford, K. Doerholt, D.M. Gibb, V. Musiime, and P. Musoke. 2023. Bone mineral density among children living with HIV failing first-line anti-retroviral therapy in Uganda: a sub-study of the CHAPAS-4 trial. *PLoS One*. 18:e0288877.

Nkonge, K.M., D.K. Nkonge, and T.N. Nkonge. 2020. The epidemiology, molecular pathogenesis, diagnosis, and treatment of maturity-onset diabetes of the young (MODY). *Clin Diabetes Endocrinol*. 6:20.

Noubissi, E.C., J.C. Katte, and E. Sobngwi. 2018. Diabetes and HIV. *Curr Diab Rep*. 18:125.

Oei, L., M.C. Zillikens, A. Dehghan, G.H. Buitendijk, M.C. Castaño-Betancourt, K. Estrada, L. Stolk, E.H. Oei, J.B. van Meurs, and J.A. Janssen. 2013. High bone mineral density and fracture risk in type 2 diabetes as skeletal complications of inadequate glucose control: the Rotterdam Study. *Diabetes care*. 36:1619-1628.

Ofotokun, I., K. Titanji, A. Vunnava, S. Roser-Page, T. Vikulina, F. Villinger, K. Rogers, A.N. Sheth, C.D. Lahiri, J.L. Lennox, and M.N. Weitzmann. 2016. Antiretroviral therapy induces a rapid increase in bone resorption that is positively associated with the magnitude of immune reconstitution in HIV infection. *AIDS*. 30:405-414.

Oksztulska-Kolanek, E., B. Znorko, M. Michałowska, and K. Pawlak. 2016. The biomechanical testing for the assessment of bone quality in an experimental model of chronic kidney disease. *Nephron*. 132:51-58.

Osterhoff, G., E.F. Morgan, S.J. Shefelbine, L. Karim, L.M. McNamara, and P. Augat. 2016. Bone mechanical properties and changes with osteoporosis. *Injury*. 47 Suppl 2:S11-20.

Owembabazi, E., P. Nkomozepi, T. Calvey, and E.F. Mbajiorgu. 2023. Co-administration of alcohol and combination antiretroviral therapy (cART) in male Sprague Dawley rats: A study on testicular morphology, oxidative and cytokines perturbations. *Anat Cell Biol*. 56:236-251.

Parry, C.D. 2005. South Africa: alcohol today. *Addiction*. 100:426-429.

Paula, F.J., C.M. Lanna, T. Shuhama, and M.C. Foss. 2001. Effect of metabolic control on parathyroid hormone secretion in diabetic patients. *Braz J Med Biol Res*. 34:1139-1145.

Peterson, R.G., C.V. Jackson, K. Zimmerman, W. de Winter, N. Huebert, and M.K. Hansen. 2015. Characterization of the ZDSD rat: a translational model for the study of metabolic syndrome and type 2 diabetes. *J Diabetes Res*. 2015:487816.

Pheiffer, C., V. Pillay-van Wyk, J.D. Joubert, N. Levitt, M.D. Nglazi, and D. Bradshaw. 2018. The prevalence of type 2 diabetes in South Africa: a systematic review protocol. *BMJ Open*. 8:e021029.

Phimphilai, M., P. Pothacharoen, N. Chattipakorn, and P. Kongtawelert. 2023. The trajectory of osteoblast progenitor cells in patients with type 2 diabetes and the predictive model for their osteogenic differentiation ability. *Scientific Reports*. 13:2338.

Picke, A.K., G. Campbell, N. Napoli, L.C. Hofbauer, and M. Rauner. 2019. Update on the impact of type 2 diabetes mellitus on bone metabolism and material properties. *Endocr Connect*. 8:R55-R70.

Pierce, J.L., D.L. Begun, J.J. Westendorf, and M.E. McGee-Lawrence. 2019. Defining osteoblast and adipocyte lineages in the bone marrow. *Bone*. 118:2-7.

Polonsky, K.S. 2012. The past 200 years in diabetes. *N Engl J Med*. 367:1332-1340.

Pondel, M. 2000. Calcitonin and calcitonin receptors: bone and beyond. *Int J Exp Pathol*. 81:405-422.

Porter, J.A., and J.A. von Fraunhofer. 2005a. Success or failure of dental implants? A literature review with treatment considerations. *Gen Dent*. 53:423-432; quiz 433, 446.

Porter, J.A., and J.A. von Fraunhofer. 2005b. Success or failure of dental implants? A literature review with treatment considerations. *General Dentistry*. 53:423-446.

Qing, H., L. Ardeshirpour, P.D. Pajevic, V. Dusevich, K. Jahn, S. Kato, J. Wysolmerski, and L.F. Bonewald. 2012. Demonstration of osteocytic perilacunar/canalicular remodeling in mice during lactation. *J Bone Miner Res*. 27:1018-1029.

Rahman, M.S., K.S. Hossain, S. Das, S. Kundu, E.O. Adegoke, M.A. Rahman, M.A. Hannan, M.J. Uddin, and M.G. Pang. 2021. Role of insulin in health and disease: an update. *Int J Mol Sci*. 22:6403.

Ramlo-Halsted, B.A., and S.V. Edelman. 1999. The natural history of type 2 diabetes. Implications for clinical practice. *Prim Care*. 26:771-789.

Rebeiro, P.F., C.A. Jenkins, A. Bian, J.E. Lake, K. Bourgi, R.D. Moore, M.A. Horberg, W.C. Matthews, M.J. Silverberg, J. Thorne, A.M. Mayor, V.D. Lima, F.J. Palella, M.S. Saag, K.N. Althoff, M.J. Gill, C. Wong, M.B. Klein, H.M. Crane, V.C. Marconi, B.E. Shepherd, T.R. Sterling, and J.R. Koethe. 2021. Risk of incident diabetes mellitus, weight gain, and their relationships with integrase inhibitor-based initial antiretroviral therapy among persons with human immunodeficiency virus in the United States and Canada. *Clin Infect Dis*. 73:e2234-e2242.

Reed, M.J., K. Meszaros, L.J. Entes, M.D. Claypool, J.G. Pinkett, T.M. Gadbois, and G.M. Reaven. 2000. A new rat model of type 2 diabetes: the fat-fed, streptozotocin-treated rat. *Metabolism*. 49:1390-1394.

Reinwald, S., R.G. Peterson, M.R. Allen, and D.B. Burr. 2009. Skeletal changes associated with the onset of type 2 diabetes in the ZDF and ZDSD rodent models. *Am J Physiol Endocrinol Metab*. 296:E765-774.

Rharass, T., and S. Lucas. 2018. Mechanisms in endocrinology: Bone marrow adiposity and bone, a bad romance? *Eur J Endocrinol*. 179:R165-r182.

Riquelme-Gallego, B., L. García-Molina, N. Cano-Ibáñez, G. Sánchez-Delgado, F. Andújar-Vera, C. García-Fontana, S. González-Salvatierra, E. García-Recio, V. Martínez-Ruiz, and A. Bueno-Cavanillas. 2020. Circulating undercarboxylated osteocalcin as estimator of cardiovascular and type 2 diabetes risk in metabolic syndrome patients. *Scientific Reports*. 10:1840.

Ritter, N.M., M.C. Farach-Carson, and W.T. Butler. 2020. Evidence for the formation of a complex between osteopontin and osteocalcin. *J Bone Miner Res*. 7:877-885.

Romero-Díaz, C., D. Duarte-Montero, S.A. Gutiérrez-Romero, and C.O. Mendivil. 2021. Diabetes and Bone Fragility. *Diabetes Ther*. 12:71-86.

Rosen, C.J. 2009. Primer on the metabolic bone diseases and disorders of mineral metabolism. John Wiley & Sons.

Russell, J.W., K.A. Sullivan, A.J. Windebank, D.N. Herrmann, and E.L. Feldman. 1999. Neurons undergo apoptosis in animal and cell culture models of diabetes. *Neurobiol Dis*. 6:347-363.

Sadeghi, A., M. Beigy, S. Alizadeh, H. Mazloom, S. Vakili, S. Ahmadi, and R. Meshkani. 2017. Synergistic effects of ad-libitum low-dose fructose drinking and low-dose streptozotocin treatment in Wistar rats: a mild model of type 2 diabetes. *Acta Med Iran*. 55:304-310.

Saeedi, P., I. Petersohn, P. Salpea, B. Malanda, S. Karuranga, N. Unwin, S. Colagiuri, L. Guariguata, A.A. Motala, K. Ogurtsova, J.E. Shaw, D. Bright, R. Williams, and I.D.F.D.A. Committee. 2019. Global and regional diabetes prevalence estimates for 2019 and projections for 2030 and 2045: Results from the International Diabetes Federation Diabetes atlas, 9(th) edition. *Diabetes Res Clin Pract*. 157:107843.

Sakka, S., and P. Coulthard. 2009. Bone quality: a reality for the process of osseointegration. *Implant Dentistry*. 18:480-485.

Salam, R., S. Bajaj, N. Kapoor, B. Saboo, and A. Dasgupta. 2019. Diabetes and HIV. *J Soc Health Diab*. 7:45-49.

Sampson, H.W. 1998. Alcohol's harmful effects on bone. *Alcohol Health Res World*. 22:190-194.

Sass, M.R., N.J. Wewer Albrechtsen, J. Pedersen, K.J. Hare, N. Borbye-Lorenzen, K. Kiss, T. Vilsboll, F.K. Knop, S.S. Poulsen, N.R. Jorgensen, J.J. Holst, C. Orskov, and B. Hartmann. 2020. Secretion of parathyroid hormone may be coupled to insulin secretion in humans. *Endocr Connect*. 9:747-754.

Seibel, M.J. 2005. Biochemical markers of bone turnover: part I: biochemistry and variability. *Clin Biochem Rev*. 26:97-122.

Shah, S., and A. Hill. 2021. Risks of metabolic syndrome and diabetes with integrase inhibitor-based therapy. *Curr Opin Infect Dis*. 34.

Shankalala, P., C. Jacobs, S. Bosomprah, M. Vinikoor, P. Katayamoyo, and C. Michelo. 2017. Risk factors for impaired fasting glucose or diabetes among HIV infected patients on ART in the Copperbelt Province of Zambia. *J Diabetes Metab Disord* 16:1-8.

Sharifi, M., L. Ereifej, and E.M. Lewiecki. 2015. Sclerostin and skeletal health. *Rev Endocr Metab Disord*. 16:149-156.

Shaw, N., and W. Högler. 2012. Biochemical markers of bone metabolism. *In* Pediatric Bone. F.H. Glorieux, J.M. Pettifor, and H. Jüppner, editors. Academic Press, San Diego. 361-381.

Shuper, P.A., M. Neuman, F. Kanteres, D. Baliunas, N. Joharchi, and J. Rehm. 2010. Causal considerations on alcohol and HIV/AIDS--a systematic review. *Alcohol Alcohol*. 45:159-166.

Silverman, S.L. 2010. Sclerostin. *J Osteoporos*. 2010:941419.

Singh, L., S. Tyagi, D. Myers, and G. Duque. 2018. Good, bad, or ugly: the biological roles of bone marrow fat. *Curr Osteoporos Rep*. 16:130-137.

Singh, R., M. Gholipourmalekabadi, and S.H. Shafikhani. 2024. Animal models for type 1 and type 2 diabetes: advantages and limitations. *Front Endocrinol*. 15.

Starup-Linde, J., and P. Vestergaard. 2016. Biochemical bone turnover markers in diabetes mellitus - a systematic review. *Bone*. 82:69-78.

Stevenson, G.C., P.C. Riano, A.J. Moretti, C.M. Nichols, R.L. Engelmeier, and C.M. Flaitz. 2007. Short-term success of osseointegrated dental implants in HIV-positive individuals: a prospective study. *J Contemp Dent Pract*. 8:1-10.

Sun, H., P. Saeedi, S. Karuranga, M. Pinkepank, K. Ogurtsova, B.B. Duncan, C. Stein, A. Basit, J.C.N. Chan, J.C. Mbanya, M.E. Pavkov, A. Ramachandaran, S.H. Wild, S. James, W.H. Herman, P. Zhang, C. Bommer, S. Kuo, E.J. Boyko, and D.J. Magliano. 2022. IDF Diabetes Atlas: Global, regional and country-level diabetes prevalence estimates for 2021 and projections for 2045. *Diabetes Res Clin Pract*. 183:109119.

Sun, X., Q.H. Ren, L. Bai, and Q. Feng. 2015. Identification of molecular markers related to human alveolar bone cells and pathway analysis in diabetic patients. *Genet Mol Res*. 14:13476-13484.

Tang, Y., X. Wu, W. Lei, L. Pang, C. Wan, Z. Shi, L. Zhao, T.R. Nagy, X. Peng, J. Hu, X. Feng, W. Van Hul, M. Wan, and X. Cao. 2009. TGF-beta1-induced migration of bone mesenchymal stem cells couples bone resorption with formation. *Nat Med*. 15:757-765.

Tattersall, R.B., and D.R. Matthews. 2024. The history of diabetes mellitus. *Textbook of diabetes*:1-21.

Tchoubou, Z., B.B. Koubala, and D. Ndjonka. 2023. Antioxidant potential and improvement activities of sterculia setigera delile on insulin resistance in type 2 diabetic rats induced by high-fat diet and low dose of streptozotocin. *Dose Response*. 21:15593258231185460.

Thrailkill, K.M., C.K. Lumpkin Jr, R.C. Bunn, S.F. Kemp, and J.L. Fowlkes. 2005. Is insulin an anabolic agent in bone? Dissecting the diabetic bone for clues. *Am J Physiol Endocrinol Metab*. 289:E735-E745.

Totty, B.A. 2002. Mucins. In: Bancroft, J. D. (Ed.), The Theory and Practice of Histological Techniques. . Churchill Livingstone Edinburgh.

Tsai, C.Y., Y.M. Shyr, W.C. Chiu, and C.M. Lee. 2011. Bone changes in the mandible following botulinum neurotoxin injections. *Eur J Orthod*. 33:132-138.

Turner, C.H. 2006. Bone strength: current concepts. *Ann N Y Acad Sci*. 1068:429-446.

Vasiliadis, E.S., D.S. Evangelopoulos, A. Kaspiris, I.S. Benetos, C. Vlachos, and S.G. Pneumaticos. 2022. The Role of Sclerostin in Bone Diseases. *J Clin Med*. 11:806.

Vatandoust, N., F. Rami, A.R. Salehi, S. Khosravi, G. Dashti, G. Eslami, S. Momenzadeh, and R. Salehi. 2018. Novel high-fat diet formulation and streptozotocin treatment for induction of prediabetes and type 2 diabetes in rats. *Adv Biomed Res*. 7:107.

von Wilmowsky, C., P. Stockmann, I. Harsch, K. Amann, P. Metzler, R. Lutz, T. Moest, F.W. Neukam, and K.A. Schlegel. 2011. Diabetes mellitus negatively affects peri-implant bone formation in the diabetic domestic pig. *J Clin Periodontol*. 38:771-779.

Wang, A.N., J. Carlos, G.M. Fraser, and J.J. McGuire. 2022. Zucker Diabetic-Sprague Dawley (ZDSD) rat: type 2 diabetes translational research model. *Exp Physiol*. 107:265-282.

Watt, J., J. Schuon, J. Davis, T.F. Ferguson, D.A. Welsh, P.E. Molina, and M.J.J. Ronis. 2019. Reduced serum osteocalcin in high-risk alcohol using people living with HIV does not correlate with systemic oxidative stress or inflammation: data from the New Orleans alcohol use in HIV study. *Alcohol Clin Exp Res*. 43:2374-2383.

Wilson, R.D., and M.S. Islam. 2012. Fructose-fed streptozotocin-injected rat: an alternative model for type 2 diabetes. *Pharmacol Rep*. 64:129-139.

Wu, K.K., and Y. Huan. 2007. Diabetic atherosclerosis mouse models. *Atherosclerosis*. 191:241-249.

Wu, M., G. Chen, and Y.P. Li. 2016. TGF-beta and BMP signaling in osteoblast, skeletal development, and bone formation, homeostasis and disease. *Bone Res*. 4:16009.

Wu, P.H., G. Joseph, I. Saeed, A.M. Pirmoazen, K. Kenny, T.Y. Kim, A.L. Schafer, A.V. Schwartz, X. Li, T.M. Link, and G.J. Kazakia. 2023. Bone marrow adiposity alterations in type 2 diabetes are aex-specific and associated with serum lipid levels. *J Bone Miner Res*. 38:1877-1884.

Xu, C.Q., S.M. de la Monte, M. Tong, C.K. Huang, and M. Kim. 2015. Chronic Ethanol-Induced Impairment of Wnt/beta-Catenin Signaling is Attenuated by PPAR-delta Agonist. *Alcohol Clin Exp Res*. 39:969-979.

Yagihashi, S. 2023. Contribution of animal models to diabetes research: Its history, significance, and translation to humans. *J Diabetes Investig*. 14:1015-1037.

Yang, Y., N. Zhang, F. Lan, K. Van Crombruggen, L. Fang, G. Hu, S. Hong, and C. Bachert. 2014. Transforming growth factor-beta 1 pathways in inflammatory airway diseases. *Allergy*. 69:699-707.

Yarramsetty, G.V., B.M. Singiri, K.R. Vijay, V.C. Balaji, K. Anusha, and R.P. Thota. 2023. A Retrospective Analysis to Assess the Reasons for the Failure of Dental Implants. *J Pharm Bioallied Sci*. 15:S1119-s1122.

Yu, Z.J., E.P. Mosher, and N.N. Bumpus. 2021. Pharmacogenomics of antiretroviral drug metabolism and transport. *Annu Rev Pharmacol Toxicol*. 61:565-585.

Zaccardi, F., D.R. Webb, T. Yates, and M.J. Davies. 2016. Pathophysiology of type 1 and type 2 diabetes mellitus: a 90-year perspective. *Postgrad Med J*. 92:63-69.

Zajac, J., A. Shrestha, P. Patel, and L. Poretsky. 2010. The main events in the history of diabetes mellitus. Springer 3-16 pp.

Zakaria, Z.Z., M.N. Ahmad, and N.A. Qinna. 2021. Animal models in type 2 diabetes mellitus research: pros and cons. *Jordan J Agric Sci*. 17:425-440.

Zheng, Y., S.H. Ley, and F.B. Hu. 2018. Global aetiology and epidemiology of type 2 diabetes mellitus and its complications. *Nat Rev Endocrinol*. 14:88-98.

APPENDICES

APPENDIX A: ETHICAL CLEARANCE

STRICTLY CONFIDENTIAL

ANIMAL RESEARCH ETHICS COMMITTEE (AREC)

CLEARANCE CERTIFICATE NO. 2018/011/58/C

APPLICANT: Dr I Eguavoen

SCHOOL: Anatomical Sciences
DEPARTMENT:
LOCATION:

PROJECT TITLE: Characterization of Streptozontocin induced diabetic male Sprague-Dawley rats with chronic alcohol intake and antiretroviral therapy

Number and Species

120X 10 weeks/270-320g male Sprague-Dawley rats

Approval was given for the use of animals for the project described above at an AREC meeting held on 2018/11/27. This approval remains valid until 2021/02/13.
Unreported changes to the application may invalidate the clearance given by the AREC
An annual progress report must be provided

The use of these animals is subject to AREC guidelines for the use and care of animals, is limited to the procedures described in the application form and is subject to any additional conditions listed below:

Signed: _____ (Chairperson, AREC) Date: 23rd April 2019

I am satisfied that the persons listed in this application are competent to perform the procedures therein, in terms of Section 23 (1) (c) of the Veterinary and Para-Veterinary Professions Act (19 of 1982)

Signed: _____ (Registered Veterinarian) Date: 23 April 2019

cc: Supervisor: Prof E Mbajirogu and Dr R Ndou
Director: CAS

Works 2000/lain0015/AESCCert.wps

APPENDIX B1: FRUCTOSE DIET

High fructose diet preparation

Normal rodent chow was grounded into powder form

To make up 1 kilogram of high fructose diet, 800grams of ground normal rodent chow was mixed with 200 grams of fructose (granulated fruit sugar, Nature's choice).

Then, the powdered high fructose diet was combined and mixed with water to and placed in pellet food moulds before dehydration in in an incubator.

APPENDIX B2: CITRATE BUFFER AND STZ

Citrate buffer and STZ preparation (4mg/ml of 40mg/Kg BW)

Citrate buffer

- 3 parts 0.05M citrate acid
- 2 parts 0.05m sodium citrate
- Adjust pH to 4.5

STZ

- 4mg STZ--1 ml citrate buffer (CB)
- For a 40mg/Kg BW dose
- 40mg STZ in 10ml CB will be given to 1 Kg BW
- 10ml STZ in CB –1000g
- 1 ml STZ in CB - 100g
- Therefore, Xml STZ in CB = X g BW x 1/100ml

- Xml STZ in CB was administered to each animal according to their body weight

APPENDIX B3: Atripla®

Atripla® drug dose calculations

45kg body weight (BW) of average adolescent receives 1 tablet of Atripla per day and 1 tablet =1045mg active ingredients (AI) per day Atripla (efavirenz 600mg+ emtricitabine 200mg+ tenofovir 245mg).

Therefore, 1kg BW = 1045/45 = 23.22 mg AI per day and 1 gram BW= 0.0232 mg AI per day

One Atripla® tablet with 1045mg AI weighs 1612mg.

Therefore, 1mg tablet = 1X1045/1612 =0.648mg AI/mg tablet

If 1 gram BW requires 0.0232 mg AI per day

Then 200 g BW required = 200g x0.0232 mg AI per day/ 0.648mg AI/mg tablet =7.16 mg tablet per day (was administered to a rat weighing 200g)

APPENDIX B4: GELATINE CUBES

Gelatine cubes preparations

For each gelatine cube, 5ml l distilled water, 0.25g sugar, 2g gelatine and 0.1g beefy Bovril was used, minimising the entire content of each gelatine cube to one calorie to ensure that the gel administration does not contribute/ influence the diabetic condition.

The required amount of water was heated in a sterile vessel. The rest of the ingredients were added to the vessel while stirring with a mixer. When the mixture was cooled, the tablet Atripla was crushed and the required amount per cube added, and the mixture was aliquoted in gelatine tubes (5ml each) with a syringe. Atripla tablets were omitted in placebo gelatine cubes. The rats received a gelatin cube every day.